VERTICAL HYDRAULIC GRADIENTS AND GROUNDWATER-SURFACE WATER INTERACTION UNDER A PRE-RESTORATION PIEDMONT URBAN STREAM, CHARLOTTE NC

by

Derick Russell Haydin

A thesis submitted to the faculty of
The University of North Carolina at Charlotte
in partial fulfillment of the requirements
for the degree of Master of Science in
Earth Sciences

Charlotte

2017

Approved by:

_____
Dr. David Vinson

_____
Dr. Sandra Clinton

_____
Dr. Martha Cary Eppes

ABSTRACT

DERICK RUSSELL HAYDIN. Vertical hydraulic gradients and groundwater surface water interaction under a pre-restoration Piedmont urban stream, Charlotte, NC. (Under the direction of Dr. DAVID VINSON)

The hyporheic zone is a dynamic environment of physical and chemical gradients. These environmental gradients during groundwater-surface water interaction can be beneficial to aquatic life and water quality. Many urban streams have excess nutrient loading from sources such as development, agricultural runoff, and sewage. The hyporheic zone can be an area of mixing of groundwater and surface water, which can have distinct temperature and chemistry. Downwelling in the hyporheic zone increases hydrologic retention and can enhance biogeochemical processing (e.g. denitrification), with benefits for overall water quality. This research focuses on five short study reaches within Reedy Creek, a highly-incised urban forested stream in Charlotte, NC (watershed area 6.5 km^2). The objective of this research is to characterize hydrologic exchange between the stream and subsurface prior to restoration scheduled to occur in winter 2017.

From August 11, 2016 to February 3, 2017 groundwater-surface water interaction was examined in three ways at five stream cross-sections, 10 monitoring wells, and 87 piezometers in the Reedy Creek watershed. First, monitoring well water levels, stream water levels, and temperature have been measured since 2013. Second, vertical hydraulic gradient (VHG) measurements were taken at 25-75 cm deep piezometer nests (fall 2016-winter 2017) to quantify hyporheic exchange above and below geomorphic features in the streambed. Third, water quality samples were collected, and field measurements of pH, dissolved oxygen, and temperature were made in January-February 2017. To characterize groundwater that may discharge into the streams, slug testing was done on all piezometers and monitoring wells. Water samples were also collected from the monitoring wells located 5-60 meters from the stream channels.

Slug testing showed that ~half of the piezometers installed were in impermeable sediments. The majority of piezometers that were in impermeable sediments were in the deeper

sediments. Only two piezometer nests were hydrologically connected for all three piezometers. Slug testing data showed that the hyporheic zone in Reedy Creek is shallow within the sandy sediments that lay over impermeable clay and bedrock. The stream and well hydrographs indicate that riparian wells respond to precipitation and/or streamflow. VHG measurements suggest that a few piezometer nests had median downward VHGs at all depths. While downward VHGs (apparent downwelling) were detected at multiple locations, downward VHGs did not systematically occur where hypothesized (e.g. above debris features or above gravel bars). Other piezometer nests exhibited inconsistent VHGs with time and/or with depth (e.g. apparent downwelling at 25 cm and apparent upwelling at 50-75 cm). The data suggests these piezometers may have recorded stream flow variability interacting with subsurface heterogeneity. There are a few possibilities indicating from the VHG data. The stream could be perched on top of the impermeable sediments and bedrock, restricting any vertical exchange at these spots. Another possibility is that the groundwater at these spots is equilibrated with the streambed further downstream.

The five study reaches experienced similar VHGs even though each study reach had their own unique number of geomorphic features. The median reach-wide downwelling VHGs for the reaches were from -0.01 to -0.06 for all five study reaches. Two study reaches, C1 and P1, were the only reaches that had a date of median reach-wide apparent upwelling VHG. The geomorphic features varied greatly in the extent of their VHGs. Both above debris jam and below a debris jam features had the largest hyporheic flux out of all features.

Two of the five reaches had apparent perpendicular horizontal groundwater flow toward the stream while the three reaches apparently flowed away from the stream. Surface water and groundwater samples did not yield a great enough distinction between the two to be able to quantify the groundwater surface water interactions. Due to the high amounts of impermeable sediments and therefore low sub-streambed hydraulic conductivity, Reedy Creek has limited hyporheic exchange potential.

TABLE OF CONTENTS

LIST OF TABLES

LIST OF FIGURES

1 Introduction

1.1 Urban stream syndrome

Deforestation, soil erosion, and increased impervious surfaces, connected to urbanization, are a large contribution to the degradation of streams. Excess nutrient and pollutant concentrations and a lack of aquatic biota richness are characteristics of degraded water quality in urban streams (Cordy, 2001). This degradation is part of a condition popularized as "urban stream syndrome" by Walsh et al. (2005). Soil infiltration is reduced in areas of high impervious surface (Gagrani et al., 2010; Bell et al., 2016). The decrease in soil infiltration increases storm runoff that enters the stream channel. High concentration of impervious surface land use is typical of urban environments. The storm runoff comes into contact with urban contaminants that end up in the stream channel (O'Driscoll et al., 2010). This increase in runoff produces a "flashy" hydrograph that shows a sharp ascending and descending limb (Charlton, 2008). The increased discharge creates erosion of the stream banks. With time, continual erosion strips the stream banks of vegetation and sediment making it more susceptible to erosion and incision (Niezgoda and Johnson, 2005).

One measure to mitigate urban stream syndrome, and to re-establish some natural function, is stream restoration. Stream restoration is defined as the manipulation of the physical, chemical or biological characteristics of a stream with the goal of returning the reach to its natural *function* (Hough and Patterson, 2008; emphasis added). A variety of techniques are used depending on the goals of the restoration. Lowering the banks, adding large woody debris, and adding vegetation in the riparian zone are all examples of stream restoration techniques (Bernhardt and Palmer, 2007).

The hyporheic zone is an area of mixing of surface water and groundwater beneath and adjacent to the streams. Hyporheic flow is described as water flow that leaves the stream to the subsurface and returns to the stream (Triska et al., 1989). Groundwater and surface water

chemistry are influenced by hyporheic function. Geomorphic features such as gravel bars, large woody debris, riffle-pool sequences etc. have the potential to become "hot spots" for vertical hyporheic flux because of the changes in head they create across small intervals of stream length. Downward vertical hyporheic flux is key for the utilization of the hyporheic functions such as denitrification, which permanently removes nitrate from the system. This research focuses on a second-order stream, and its tributaries, at baseflow. Looking at the stream at baseflow allowed vertical hydraulic gradient measurements to be taken with more confidence that geomorphic features induce the hyporheic flux. Also, at baseflow, groundwater is a larger relative contribution to streamflow.

1.2 Physical hydrology of the hyporheic zone

1.2.1 Horizontal groundwater flow in riparian zones

Groundwater moves from high hydraulic head to low hydraulic head. From the stream to the upland, there is a sloping water table. Typically, the water table mirrors the topography of the upland sloping downward toward the stream. With the water table typically being higher at the upland the flow goes toward the stream. This means the stream would be gaining flow along its length (net gaining; Figure 1). In regions of low recharge, the water table may be lower at the upland than the stream. This would result in flow moving away from the stream, moving toward the upland (net losing; Figure 2). Horizontal groundwater flow often is dictated by topography. Areas of high elevation are typically areas of recharge to the aquifer. Areas of low elevation and low slopes are typically areas of discharge, like a stream (Daniel and Dahlen, 2002).

1.2.2 Vertical flows through the hyporheic zone

Transient storage is the temporary entrainment of stream water in recirculating flow in the stream channel (pools and backwater) and in the hyporheic zone (Figure 3; Jackson et al., 2012). Transient storage is an important function of the hyporheic zone as it regulates the exchange and storage of water and solutes. This process delays downstream transport. Solute movement is delayed for time scales longer than advection and dispersion (Bencala et al., 2010).

The steam catchment system is complex and more than a pipe that transports water and solutes with no interaction with the stream bed (Figure 4a). Water flows along the stream water is moving in and out of the stream through the hyporheic zone at multiple locations (Figure 4b; Bencala 1993).

In-stream geomorphic structures such as logjams, meander bends, and gravel bars occur naturally within stream systems, especially small shallow headwater streams where debris can accumulate with few floods large enough to remove it (Figure 5a). In addition, bedrock can influence stream channels in a variety of settings including small forest streams. These structures influence flow dynamics and induce hyporheic exchange. Hyporheic exchange can be induced by head gradients created by the stream's slope (change in hydraulic head). Downwelling occurs in a convex streambed profile and upwelling occurs in a concave profile (Vaux 1968). Head gradients induced by steps and riffles also create hyporheic exchange (Figure 5b, Figure 6; Hester and Doyle 2008). Hyporheic flux can also be induced from backwater collecting behind obstacles in the channel. Debris, log and boulder jams are examples (Hester and Doyle, 2008).

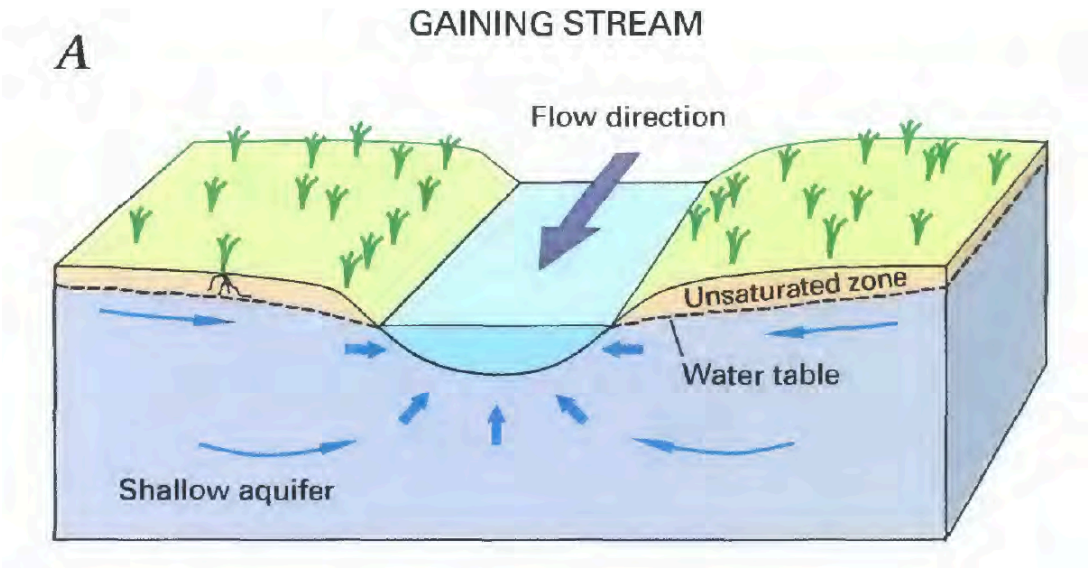

Figure 1. Cross-sectional view of a gaining stream. Groundwater movement is toward the stream resulting in a gaining stream (Winter et al., 1999).

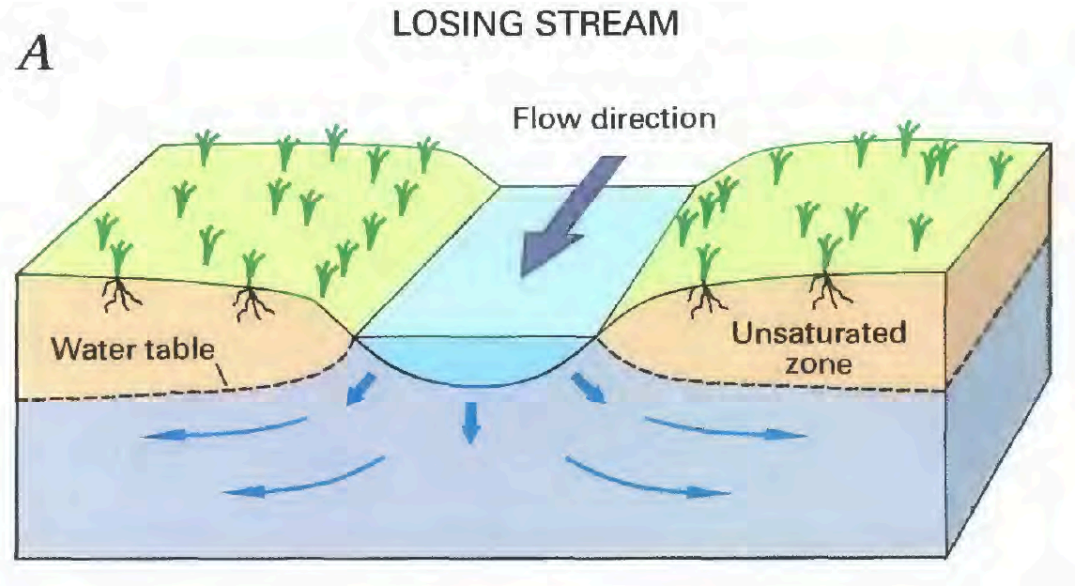

Figure 2. Cross-sectional view of a losing stream. Groundwater movement is toward the stream banks resulting in a losing stream (Winter et al., 1999).

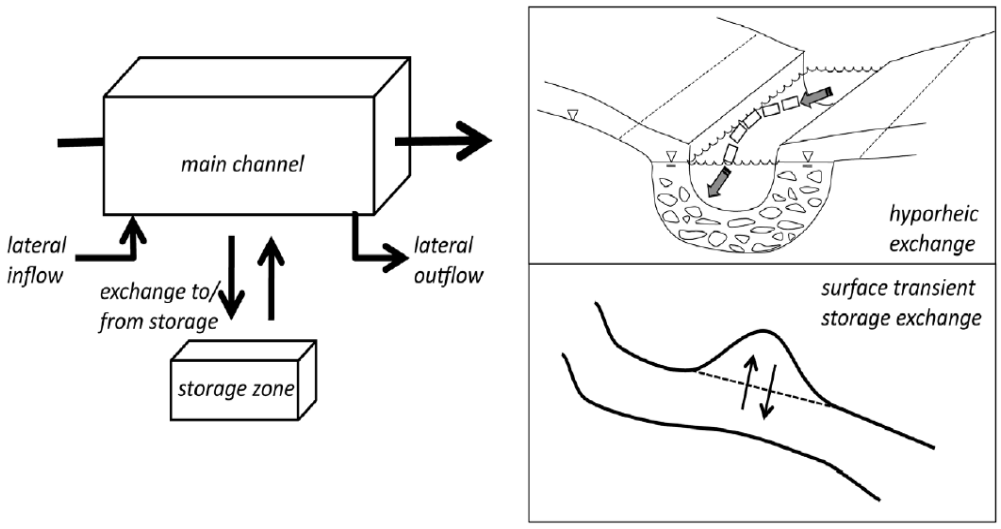

Figure 3. Transient storage takes place both in the subsurface and in the surface flow. Both diagrams show exchange from the channel to the hyporheic zone. The bottom right picture shows surface transient storage exchange in pools and eddies (Bencala et al 2010).

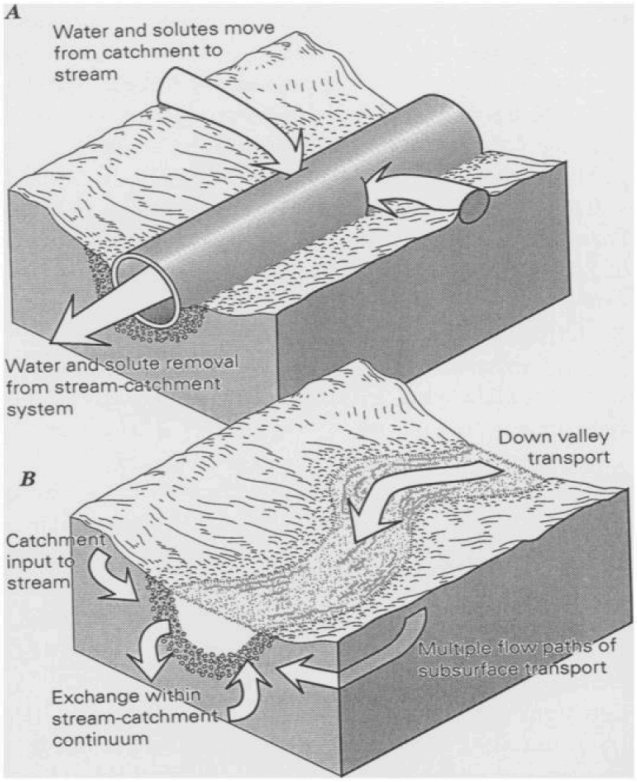

Figure 4. A, shows the stream-catchment system as a simple system that merely moves water and solute downstream with no interaction from the hyporheic zone. B, shows a complex stream system that has the stream interacting with the hyporheic zone as it moves along its length (Bencala 1993).

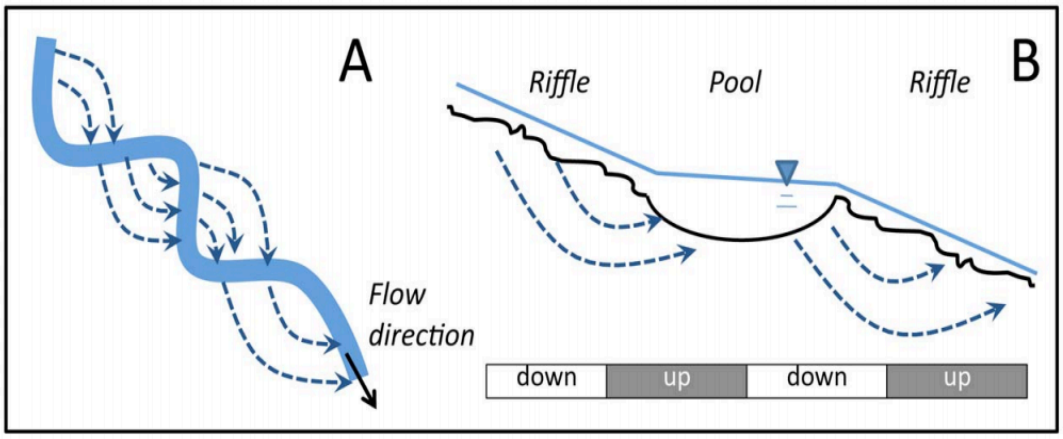

Figure 5. Left diagram (map view) shows hyporheic exchange through meander bends. Right diagram (cross-section view) shows geomorphic features inducing vertical hyporheic exchange. Pools induce a downward pressure pushing the water down; riffles have less pressure, which induces the water to return to the surface (Bencala et al., 2010)

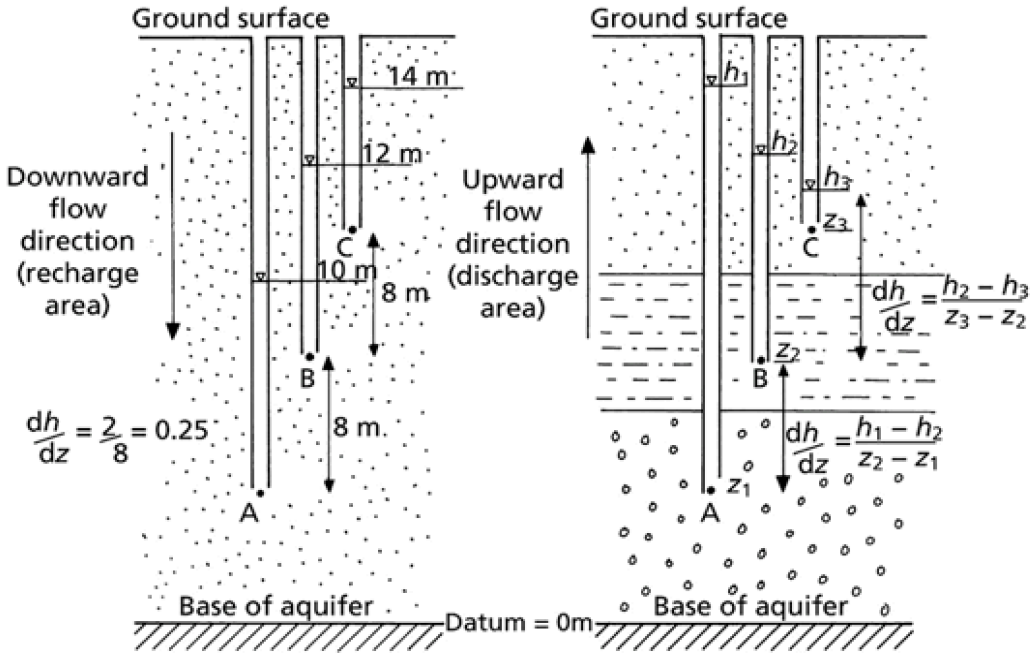

Figure 6. Left shows downward VHG (recharge or downwelling) and the right shows upward VHG (discharge or upwelling) using the water levels in nested piezometers. Vertical hydraulic gradient is defined by the difference in hydraulic head between two piezometers relative to their depth (Hiscock and Bense, 2014).

1.2.3 Ecological function of the hyporheic zone

The hyporheic zone regulates surface water temperature. Stream water temperature is variable under direct sunlight (the main control on stream water temperature), but groundwater has a more consistent temperature and groundwater inputs to streams can moderate stream water temperatures. The ability to moderate stream water temperatures is an important driver of habitat heterogeneity in streams. It is crucial for macroinvertebrate and fish species' survival ability during low flow. The ability to moderate stream water temperatures can be an important influence on the thermodynamic constraints of biogeochemical reactions (Hester and Gooseff, 2010).

Biologists have identified organisms that spend some to most of their life span within the hyporheic zone or use it for critical phases of life. These organisms are often referred to as hyporheos (Wood et al. 2010). Some fish species, such as Chinook salmon and bull trout, use the hyporheic zone as a preferred spot to lay eggs. In areas of downwelling, these fish take advantage of the hyporheic zone's consistent water temperature and high dissolved oxygen levels (Hester

and Gooseff 2010). Amphibians, such as salamanders, use the hyporheic zone to forage, escape predators and nest in the hyporheic zone (Feral et al., 2004).

The hyporheic zone has been known to be a habitat for invertebrates. Hyporheic invertebrates are classified by the amount of time spent in the hyporheic zone and by size. Streams are highly disturbance-dependent ecosystems. Flooding and drying out are examples. Invertebrate distributions are affected by stream disturbance frequency and extent (Ward 1998). The hyporheic zone can act as a refuge for invertebrates from the turbulence of high discharge events (Hester and Gooseff 2010). The hyporheic fauna provide services and can alter the state of the hyporheic zone. Boring and mixing of the hyporheic sediments (bioturbation) can increase pore space and increase hyporheic flux (Boulton 2007). They excrete and produce fecal pellets which generates labile dissolved organic carbon and other nutrients that promote microbial growth (Marshall and Hall 2004). Microorganisms also are found in the hyporheic zone. Their main contribution is the biogeochemical transformations that happen within the hyporheic zone. Depending on the different levels of oxygen, different chemical transformations will happen. Microorganisms need organic carbon to transform other chemicals. The hyporheic zone is often known to be a heterotrophic environment, in that more carbon is being depleted than produced (Lawrence et al., 2013).

Water storage in the surface or subsurface increases hydrologic residence time and a variety of microbes can perform biogeochemical transformations. Therefore, downwelling of water slows the velocity of nutrient spiraling, which refers to the transport and cycling of nutrients as they travel downstream (Ensign and Doyle 2006).

1.2.4 Water quality

The hyporheic zone has been known to be a “hot spot” for biogeochemical transformations. This is due to the hyporheic zone typically having high oxygen in the shallow strata and lower oxygen in the deeper sediments (Lawrence et al., 2013). The hyporheic zone can be anoxic, typically in deeper sediments. Anoxia is operationally defined as dissolved oxygen

levels below 0.5 mg/L O_2. Hyporheic nutrient transformations include N mineralization, nitrification, denitrification, and ammonification (Figure 7). Nitrogen mineralization is the process of organic N converting to plant-available inorganic forms. Nitrification is the biological oxidation of ammonia or ammonium to nitrite followed by the oxidation of the nitrite to nitrate. Denitrification is the process of nitrate being reduced into atmospheric nitrogen (N_2). Denitrification is often sought after in terms of restoration because it removes nitrate, a common urban contaminant.

The anoxic conditions of the hyporheic zone are reliant on the residence time of the downwelling water and contact with organic matter, which provides the electron source for chemical reduction. Oxygen entering the subsurface via downwelling is depleted due to microbial aerobic respiration. Once oxygen is consumed the microbes use a ladder of different electron acceptors based on thermodynamic favorability. NO_3^- is the first electron acceptor on the ladder (after DO) to be used as an electron acceptor (denitrification; Baker et al. 1994). The nitrate ion is reduced to nitrous oxide (N_2O), nitrogen (N_2), or ammonia (NH_3; Figure 8). If nitrate is reduced to atmospheric nitrogen the nitrogen may leave the system into the atmosphere. Denitrification to N_2 is one of the only ways to permanently remove nitrogen from the stream system because N_2 has a gas phase that escapes to the atmosphere. This is different from instream metabolism. Biomass that forms instream inevitably dies and those nutrients within the biomass are released back into the stream system (Charlton 2008). Therefore, the recipe for riparian denitrification includes several physical and chemical ingredients: sufficient permeability, downward VHG, organic matter, and sufficient residence time to become anoxic.

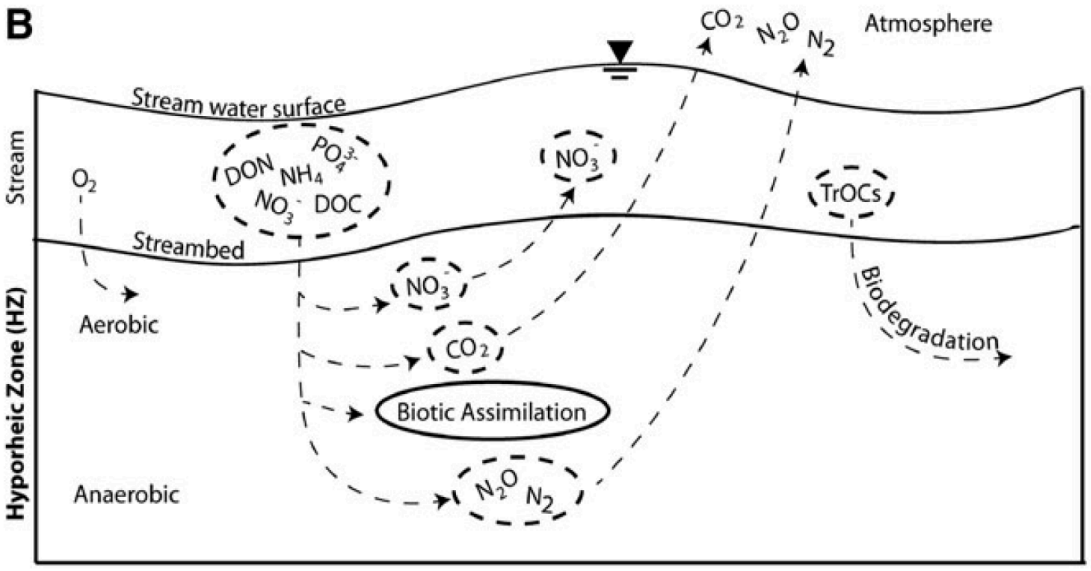

Figure 7. Cross-section of the stream, streambed, and hyporheic zone showing different N and P (nutrient) compounds and their transformations as they move through the hyporheic zone (Lawrence et al., 2013).

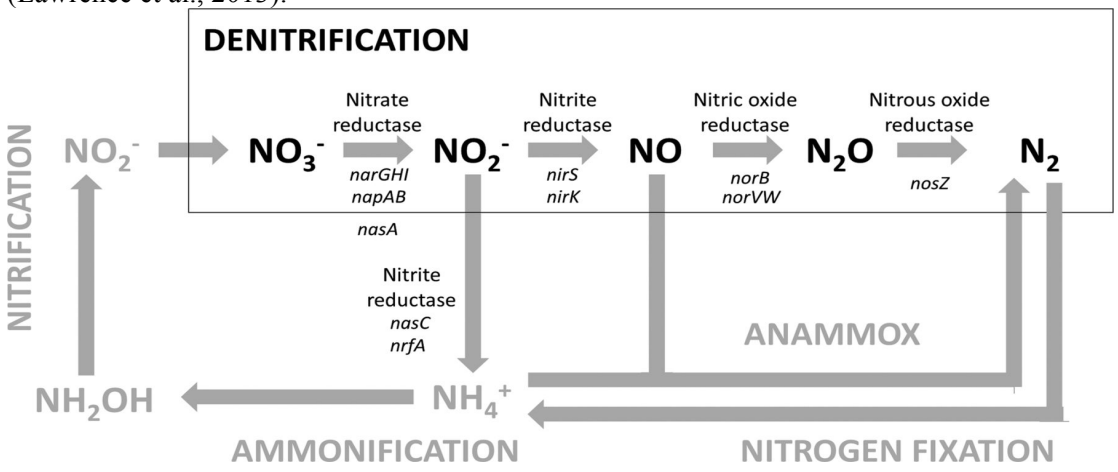

Figure 8. Nitrogen cycling through an oxic/anoxic zone (Alvarez et al., 2013).

1.2.5 Urban impairment of the hyporheic zone

Human activities both directly and indirectly affect the hyporheic zone. Pollution, metal, and nutrient runoff harm the hyporheos. Urban and industrial particulates disrupt the connection between the surface water and groundwater and as a result decreases stream bed hydraulic conductivity (Boulton et al., 2000; Dent et al., 2000). Construction and mining runoff can change salinity of the hyporheic waters that can harm the hyporheos. Pesticide and metal pollution from

industrial and urban sources can also harm the hyporheos. Construction and highway runoff can lead to siltation in the hyporheic sediments reducing porosity. Channelization of the stream removes meander bends, which result in faster flow and reduces downwelling. Channelization also can disconnect the stream from the floodplain (Hancock 2002). With reduced floodplain inundation frequency, transient storage and hydrologic retention would decrease.

1.2.6 The hyporheic zone in stream restoration

Stream restoration can be a tool to remediate the hyporheic zone and increase hyporheic exchange and storage retention. Techniques such as adding large woody debris, riffle-pool sequences, sediment coarsening, gravel cleaning and riparian planting are used to increase the health and function of the hyporheic zone (Bernhardt and Palmer, 2007; Meyer et al. 2008). Large woody debris and other geomorphic features induce pressure gradients that increase hyporheic exchange. Sediment coarsening is a technique used to increase porosity within the streambed, in turn increasing hyporheic exchange. Adding riparian plants increases bank stability and adds an organic material source to the stream and streambed. This carbon source is critical to some hyporheic functions, such as denitrification, which requires certain levels of organic carbon as electron donors to fuel the biogeochemical process (Hester and Gooseff, 2010). It has been shown that restored reaches, using cross-vanes, can significantly increase downwelling directly adjacent to the cross-vane. Cross-vanes are engineered structures that concentrate the stream flow and create repeating bedforms (Daniluk et al., 2013).

Considering the many priorities of stream restoration and the frequent need to use stable bed material, it is common for the hyporheic zone to be overlooked in the design and construction of stream restoration (Hester and Gooseff, 2013). Even with recent research, our understanding of hyporheic processes and controls remains fragmented (Ward, 2015). Examining temporal and spatial variation of hyporheic flux is needed to help advance our understanding of the hyporheic zone. This research focuses on the pre-restoration vertical hydraulic gradients in an incised urban

stream. The results of this research will be used as a benchmark to assess restoration effects on the hyporheic zone.

1.3 Objectives

The primary objective of this study was to determine the pre-restoration vertical hydraulic gradients (upwelling and downwelling) beneath the channels in a forested urban stream and selected tributaries. Because downwelling water into the hyporheic zone can promote processing, this study will provide a benchmark for evaluating the future success of restoration at meeting water quality objectives. Geomorphic structures are known to induce groundwater surface water interactions and will be examined as potential hyporheic flux hot spots. The vertical hydraulic gradient indicates the direction of movement in the z-orientation. If the water is moving from the groundwater to the stream water (upwelling) or moving from the stream to the subsurface (downwelling). Factors influencing hyporheic exchange are the permeability of the sediment, bedform shape, and the geomorphic structure. Figure 9 shows the difference between a natural channel and an urbanized channel, and the hydrographs of both.

This research has examined the pre-restoration groundwater surface water interactions of an incised urban-forested stream in the Piedmont region of North Carolina. In this study, physical and chemical data were gathered pertaining to groundwater-surface water interactions in the pre-restoration period. This research has been supplemented with data collected by the Reedy Creek Restoration Study. The Reedy Creek Restoration Study has collected hydrologic data from wells and streams in the Reedy Creek watershed since 2013.

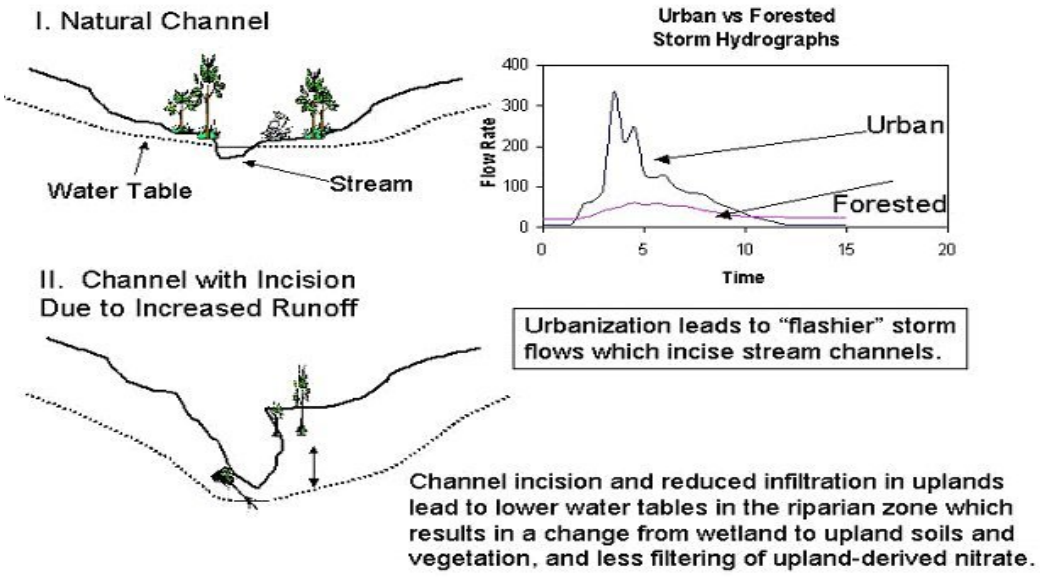

Figure 9. Urbanized channels result in steep banks and lowered water tables compared to natural channels (Groffman et al., 2003) The figure on the right shows the difference between an urban and forested hydrograph. The urban hydrograph shows a sharp spike in both rising and falling limbs. These sharp spikes characterize the high fluctuations in discharge.

1.4 Study Reach

The headwaters section of Reedy Creek is a second-order stream with a drainage area of 6.5 km^2. The USGS gauging station marks the end of the study reach. The stream originates on soil-covered hillsides typical of the Piedmont with scattered outcrops of meta-quartz diorite and residual saprolite. Saprolite is chemically weathered rock that can range in permeability (White et al., 2001). The stream flows over and cuts into a subhorizontal geomorphic surface roughly equivalent to a floodplain, especially in the lower reaches.

Reedy Creek is a forested urban stream and shows some attributes of urban stream syndrome, including flashy hydrograph, heavy sediment loads, and low macroinvertebrate counts and diversity (Figure 10). The fluctuation of discharge has stripped the banks of its vegetation and has been incised. The incised stream flows over a sand and gravel streambed in places, and saprolite and bedrock in others. The RC upper watershed (RCW) has been selected for restoration based on its current state, especially the deep bank incision that extends downward to saprolite

and bedrock in many places (Figure 11). Some incision might have been a result of prior agricultural land use, when streams in the Charlotte region were apparently straightened and dredged. These levees are assumed to be artificially made. It is likely that these tall levee-like structures represent sediment removed from straightening the stream.

In the original Reedy Creek Restoration Project monitoring program in place since mid-2013 (McMillan and Clinton, 2013), RCW was sub-divided into 5 sub-watersheds based on land use: pond-influenced (P), control/underdeveloped (C), agriculture (A), development (D), and lower Reedy Creek (R) below the confluence of D, P, and C (Figure 12). Reach C2 lacks incision and is underdeveloped making it the control reach for Reedy Creek. C2 will not be restored.

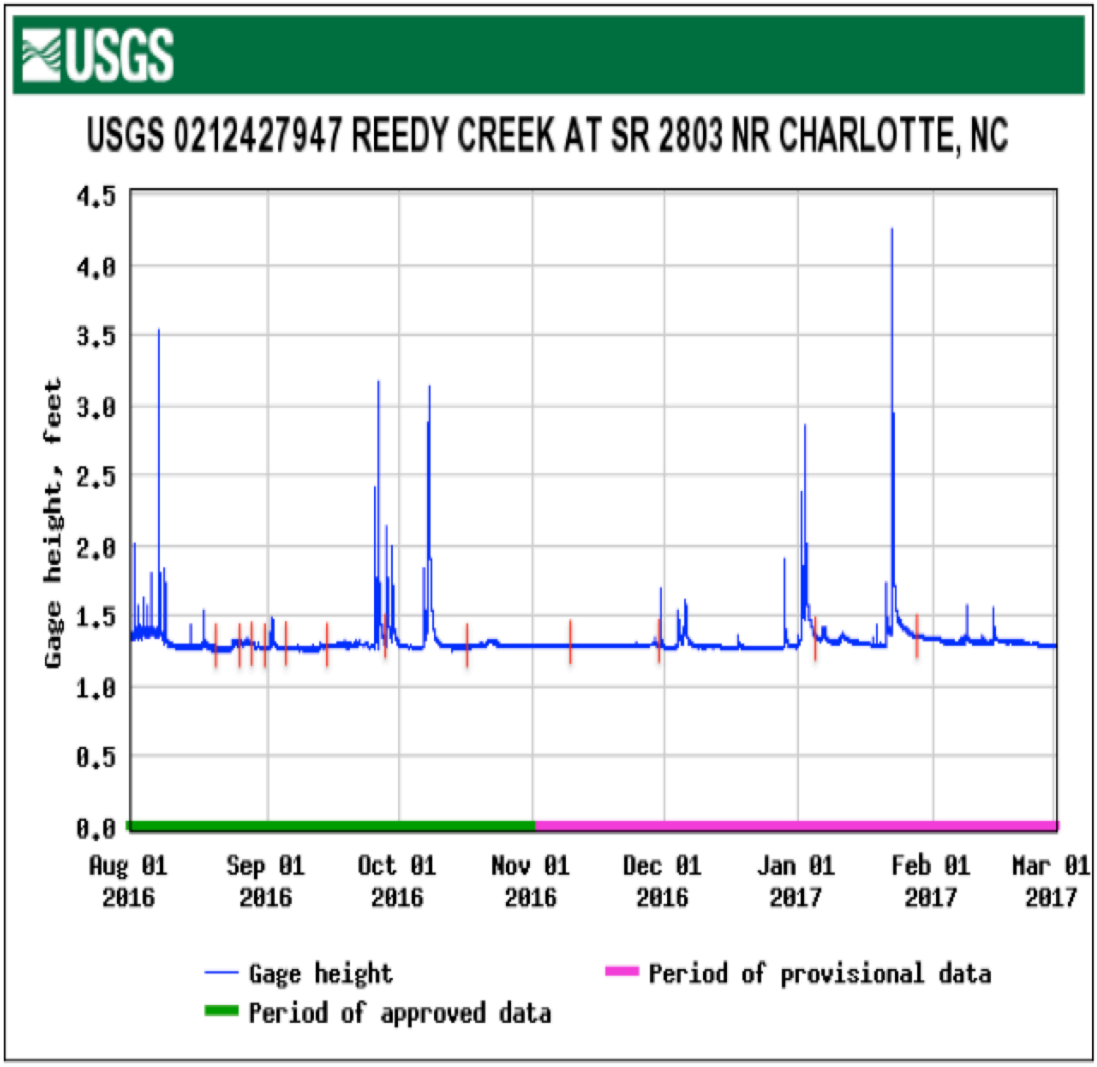

Figure 10. Hydrograph of Reedy Creek at reach R1, the main watershed outlet, during the period of the study (Aug 1, 2016 – March 1, 2017). Red vertical lines signify dates of VHG measurements. During the period of the study the amount of precipitation was typical for the study area (USGS 351540080430045 CRN-16 at waterdata.usgs.gov).

Figure 11. The D1 study reach showing the ~10’ deep incision.

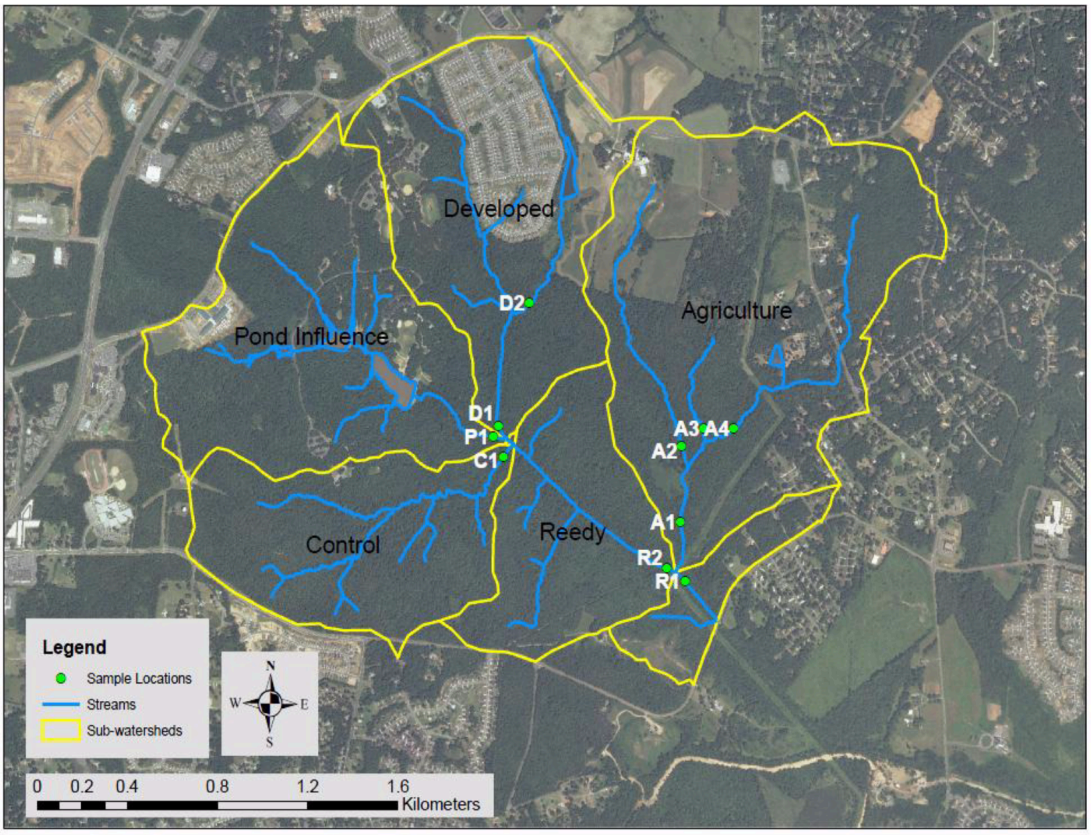

Figure 12. Map of Reedy Creek, sub-watersheds, and sampling locations (McMillan and Clinton, 2013).

2 Hypotheses

It was hypothesized that the study reaches will be overall *net* upwelling in the pre-restoration condition.

It was further hypothesized that geomorphic structures will act as hyporheic exchange hotspots and may show localized downwelling at predicted reaches in the pre-restoration condition:

- Upwelling will take place at the bottom of a meander bend.
- Upwelling will take place downstream of a debris jam.
- Upwelling will take place downstream of a gravel bed.
- Downwelling will take place at the top of a meander bend.
- Downwelling will take place upstream of a debris jam.

- Downwelling will take place upstream of a gravel bed.
- Downwelling will take place within pools.
- Downwelling will take place downstream of a bedrock formation.

3 Methods

3.1 Reach infrastructure

This study used five transects established at Reedy Creek Nature Preserve. Each surveyed transect contained 2 monitoring wells and a location for high-frequency (weekly) surface water sampling. Monitoring wells were screened approximately 12-20 feet below the surface, which is generally below the water table during most conditions at most reaches.

3.2 Horizontal hydraulic gradients

All five study reaches' monitoring wells and piezometers were surveyed as part of participation in the GEOL 5145 Hydrogeology course. A Topcon total station was used for surveying. Each reach had one to three survey stations, which had a clear view of the monitoring wells and piezometers. Once the survey data were collected at the different survey stations, the x distance was made relative to the riparian well. The relative z elevations were given absolute elevations based on the monitoring well top of casing elevation previously surveyed by the city of Charlotte.

Horizontal hydraulic gradients were measured between upland and riparian settings using relative water levels in the wells and piezometers and a survey of horizontal distances.

$$\text{Horizontal hydraulic gradient} = \frac{dh}{dx} = \frac{(difference\ of\ hydraulic\ head\ between\ upland\ and\ riparian)}{(distance\ between\ upland\ and\ riparian)} \quad (1)$$

3.3 Vertical hydraulic gradients

Piezometer nests were used to measure vertical hydraulic gradients in the hyporheic zone beneath Reedy Creek and its tributaries approximately weekly at baseflow. Piezometers were installed at selected in-stream structures that were hypothesized to be possible locations of hot spots for hyporheic flux (downwelling and upwelling). The piezometer nests were constructed

within 50 meters upstream or downstream from the transect at each reach. To construct these nests, 1" diameter PVC pipes, each 5 ft long were inserted at three different depths, typically 30, 50 and 75cm below the streambed (where depth to bedrock allowed; Figure 13). The piezometers were perforated across a ~15 cm open interval at the bottom of the tube. These three depths were used to quantify upwelling or downwelling relative to the water levels in the stream and in the other piezometers at that nest. The sign of *dh/dz* indicates which vertical direction the groundwater could flow if flow occurred. A positive *dh/dz* indicates an upward direction of flow (upwelling) and a negative *dh/dz* indicates a downward direction of flow (downwelling; Figure 14).

$$\frac{dh}{dz} = \frac{(water\ level\ in\ stream - water\ level\ in\ piezometer)}{(depth\ of\ piezometer\ below\ stream)} \quad (2)$$

also as,

$$\frac{dh}{dz} = \frac{(hs - hp)}{(depth\ of\ piezometer\ below\ stream)} \quad (3)$$

h_s is the water level in stream and h_p is the water level in the piezometer.

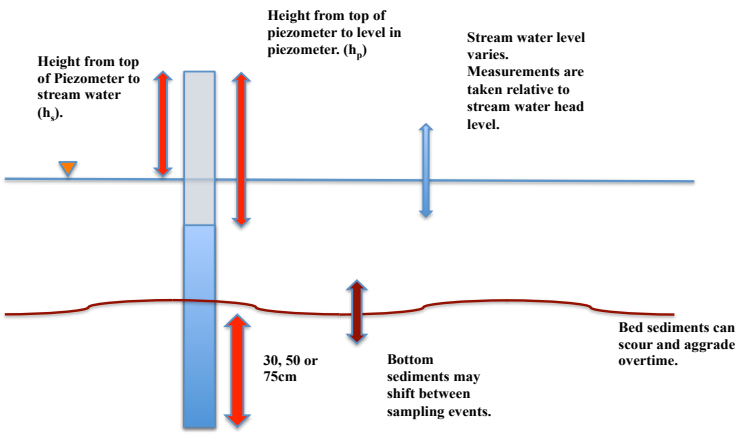

Figure 13. Piezometer measurements taken to calculate a vertical hydraulic gradient. The height from the top of piezometer to the stream water (h_s) and the height from the top of piezometer to the water level in the piezometer (h_p). The depth of the piezometer below the bed also must be known to calculate VHG.

Vertical hydraulic gradients, *dh*/*dz*, were calculated between each piezometer and the stream water level on each date. Piezometers were initially read weekly to monitor the response of new piezometers and to watch them stabilize. Once the piezometer recharge rates were analyzed, readings became less frequent by the end of the study (biweekly to monthly).

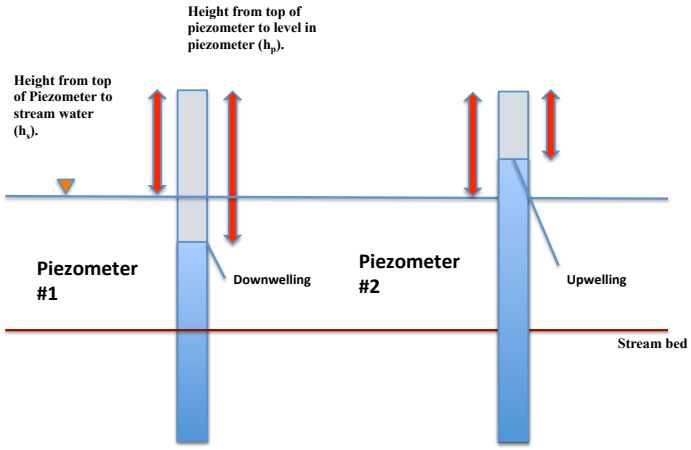

Figure 14. An example of piezometers showing downwelling in piezometer #1 and upwelling in piezometer #2, relative to the stream. *dh*/*dz* is defined with the sign convention that a positive value of *dh*/*dz* represents upward hydraulic gradient.

3.4 Water sampling and analysis

Piezometer nests, stream water, and the monitoring wells were sampled at baseflow. The water sampling procedure was: (1) measure h_p, distance from top of tube to water level inside piezometer and h_s, the distance from top of piezometer to water level in stream (Figure 13). (2) A bailer was then used to remove stagnant water from piezometers. (3) Once bailed, a wait time was administered to allow piezometers to recharge partially or fully. (4) Stream water and piezometers samples were then collected using grab sampling, hand pump, or peristaltic pump. (5) The samples were then filtered in the lab using 0.2 micron polyethersulfone (PES) filters.

Monitoring well samples were collected using a similar protocol after purging stagnant water. Stream samples were taken the same day as piezometer and well samples. Temperature, pH, specific conductivity, and dissolved oxygen were measured in the field using YSI Professional Plus multiparameter meter.

Water samples were analyzed for alkalinity, anions, cations, nutrients (nitrate, nitrite, and phosphate), and water isotopes (oxygen and hydrogen). Upon return to the laboratory, water samples were refrigerated and the cation samples were preserved with a few drops of high-purity nitric acid to a final acidity of 0.5%. Alkalinity concentrations were measured by Gran titration using a Metrohm digital titrator with 0.1M hydrochloric acid. Cations (sodium, potassium, magnesium, calcium) were analyzed using a Dionex DX-500 ion chromatograph with AS14A and AG14 analytical columns. Anions (fluoride, chloride, nitrate, sulfate) were analyzed using a Dionex DX-500 ion chromatograph with C-12 analytical column. Isotope samples were wrapped in parafilm to reduce any evaporation prior to analysis. Water isotopes ($\delta^{18}O$ and $\delta^{2}H$) were analyzed using a Los Gatos Research (LGR) DLT-100 liquid water isotope analyzer (LWIA).

In addition, radon samples were collected during the months of May and June 2017 to fingerprint groundwater inputs to surface water at baseflow. I collected large-volume (2 liter), unfiltered water samples from the stream and monitoring wells, and two piezometer samples (where piezometer would yield enough water) resulting in five water samples from five study transects. Due to the slow throughput of radon analysis, each transect was sampled once during the project, on staggered dates. Not all study transects had piezometers with high enough *K* to yield the required recharge for sample collection. A total of 19 radon samples were collected. The large-volume water samples were analyzed immediately upon return to the lab using a Durridge RAD7 radon analyzer because of the short half-life of radon (3.8 days).

3.5 Data analysis

To examine the reach-to-reach correlation between geomorphic setting and upwelling/downwelling, vertical hydraulic gradients were compiled by hydrologic setting and then compared using Student's t-test. The Student's T-test was set up by comparing geomorphic features of hypothesized downwelling reaches against geomorphic features of hypothesized upwelling. For example: "Above meander bend" with "above debris jam" (hypothesized

downwelling reaches) against "below meander bend" with "below wood jam" (hypothesized upwelling reaches).

3.6 Slug Testing using Hvorslev Method

The Hvorslev method was used to determine hydraulic conductivity (*K*), performing slug tests. The Hvorslev method is based on the observation that water level returns to the static water level at an exponential rate and the recovery time depends on the *K* of the porous material (Hiscock and Bense, 2014). Using the Hvorslev method, a semi-logarithmic plot of the ratio of h/h_0 over time was made.

The Hvorslev method assumes a homogeneous, isotropic material in an unconfined aquifer. It is assumed the substrate is homogeneous and isotropic because the piezometer openings at each depth are at a small increment rather than covering the entire thickness of the aquifer. It is assumed that the length of the piezometer, *L*, is more than eight times the radius of the screened interval, *R*. This was the case for the piezometers, which were 5 feet in length, with a radius of 0.5 inches and the case for the wells that range from 12 feet to 21 feet deep and have a radius of 1 inch.

$$K = \frac{(r^2 \ln\frac{L}{r})}{(2Lt_{37})} \quad (4)$$

In Equation 4, *K* is hydraulic conductivity, *r* is radius of the piezometer, *L* is length of the open interval of the piezometer, and t_{37} is the time lag for the water level to rise or fall to 37% of the initial change induced by the perturbation (Hiscock and Bense 2014).

3.7 Vertical and horizontal specific discharge

Vertical and horizontal specific discharge, (q_z and q_x respectively) are the hydraulic conductivity of the sediment multiplied by the hydraulic gradient (Eq. 5, Eq.6). Vertical specific discharge uses the hydraulic gradient in the z direction while horizontal uses it in the x direction. Vertical specific discharge represents the vertical component of the hyporheic flow velocity (upward or downward). Horizontal specific discharge was used to find the horizontal component

of groundwater flow velocity from the upland and riparian wells in each transect to the piezometers. The equation for horizontal specific discharge (q_x) is:

$$qx = \frac{dh}{dL}K \quad (5)$$

The equation for vertical specific discharge (q_z) is:

$$qz = \frac{dh}{dz}K \quad (6)$$

3.8 Radon Analysis

Radon samples were taken at baseflow for all five reaches. The purpose of this sampling was to differentiate the piezometer samples to find which water was dominant. Radon-222 is not naturally found in precipitation and is created by water-rock interaction within the subsurface. The only way for the radon to be in the stream water is for upwelling of the groundwater to the surface water.

The Durridge RAD7 radon counter detects the alpha decay energy of radon's radioactive decay. It is used in conjunction with the RADH2O, a closed-loop water aerator. Sample volumes were 2000 mL for surface water and 250 mL for groundwater/piezometers. Samples were decay corrected to the time of collection.

4 Results

4.1 Vertical hydraulic gradients

The VHGs reported in this section were calculated using equation 2. VHG averages were calculated but not used for interpretation. The VHG averages were skewed due to isolated high VHG results and did not accurately represent the reaches/piezometers.

4.1.1 VHGs at the five study reaches on each date

These VHG results are for each individual date at each of the five study reaches. Each median is for one date only.

4.1.1.1 R2

Study reach R2 had a median VHG apparent downwelling signature -0.01 to -0.02. The largest reach-wide median apparent downwelling was seen on 10/17/16, 11/8/16, and 1/5/17. There was no median reach-wide apparent upwelling for any of the sampling dates. Two dates had a median VHG of zero, 8/11/16 and 8/30/16. Maximum VHG ranged from 0.07 to 1.28. Minimum VHG was -0.03 to -0.85. Study reach R2 had a range of VHG from 0.15 to 1.80 (Figure 15, Figure 20, Table 1).

4.1.1.2 A1

Study reach A1 had a median VHG apparent downwelling signature of >-0.01 to -0.05. The largest reach-wide median apparent downwelling happened on 10/17/16. There is no reach-wide median apparent upwelling for any date. On 1/20/17 the reach had a median VHG of zero. Maximum VHG ranged from 0.01 to 0.31. Minimum VHG was from 0.00 to -0.38. The range of VHGs were 0.01 to 0.66 (Figure 16, Figure 21, Table 2).

4.1.1.3 C1

Study reach C1 had median VHG apparent downwelling signature of -0.01 to -0.07. The largest median reach-wide apparent downwelling happened on 9/14/16. The median VHG apparent upwelling signature was 0.02 to 0.09. Only two dates had a reach-wide median apparent upwelling, dates 11/30/16 and 1/5/17. The largest apparent upwelling happened on 1/5/17. Maximum VHG was 0.00 to 0.63. Minimum VHG was from -0.05 to -0.55. Range of VHGs was 0.15 to 0.97 (Figure 17, Figure 22, Table 3).

4.1.1.4 D1

Study reach D1 had a reach-wide median VHG apparent downwelling signature of >-0.01 to -0.02. The largest reach-wide median apparent downwelling happened on 8/31/16 and 10/19/16. There was no reach-wide median VHG apparent upwelling signature for any dates. Dates 9/7/16, 9/14/16, 9/28/16 and 11/9/16 had a median VHG of zero. Maximum VHG was 0.01

to 0.30. Minimum VHG ranged from -0.01 to -0.08. The range of VHGs were 0.02 to 0.32 (Figure 18, Figure 23, Table 4).

4.1.1.5 P1

Study reach P1 had reach-wide median VHG apparent downwelling signature of -0.01 to -0.06. The largest median apparent downwelling happened on 8/31/16. The reach-wide median VHG apparent upwelling signature was <0.01. Only one date had an apparent upwelling signature (2/3/17). 11/9/16 had a median VHG of zero. Maximum VHG was 0.03 to 0.63. Minimum VHG was -1.24 to -0.01. The range of VHGs were 0.04 to 1.40 (Figure 19, Figure 24, Table 5).

4.1.2 VHGs at the five study reaches across all measurement dates

The VHG results are shown by each individual piezometer and producing a median for all dates of the study. This shows a median of all the measurements that all the piezometers have had. For example, if a reach had a median apparent upwelling signature range of 0.13 to 0.42, one of the piezometers had the lowest median apparent upwelling of 0.13 and another piezometer had the highest median apparent upwelling of 0.42 across all the measurement dates.

4.1.2.1 R2

Study reach R2 had a median VHG apparent downwelling signature of >-0.01 to -0.78, encompassing 14 of the total 18 piezometers. The piezometer with the largest apparent downwelling was “BDJ#1 75cm.” The median VHG apparent upwelling signature was 0.04 to 0.50, encompassing four of the total 18 piezometers. The piezometer with the largest apparent upwelling was “ADJ#2 30cm” (Table 6).

4.1.2.2 A1

Study reach A1 had a median VHG apparent downwelling signature of >-0.01 to -0.09, encompassing 13 of the total 18 piezometers. The piezometer with the largest apparent downwelling was “BDJ#2 75cm.” The median VHG apparent upwelling signature was 0.01 to 0.05, encompassing five of the 18 piezometers. The piezometer with the largest apparent upwelling was “BOM 50cm” (Table 7).

4.1.2.3 C1

Study reach C1 had a median VHG apparent downwelling signature of -0.01 to -0.14, encompassing six of the total 11 piezometers. The piezometer with the largest apparent downwelling was “AGB 70cm.” The median VHG apparent upwelling signature was 0.08 to 0.25, encompassing four piezometers of the total 11. The piezometer with the largest median apparent upwelling was “Pool #2 30cm.” One piezometer had a median VHG of 0.00 and showed no flux, “BGB#1 45cm” (Table 8).

4.1.2.4 D1

Study reach D1 had a median VHG apparent downwelling signature of >-0.01 to -0.03, encompassing 15 of the total 20 piezometers. The piezometer with the largest median apparent downwelling “BGB#1 20cm.” The median VHG apparent upwelling signature was 0.01 to 0.17, encompassing five of the total 20 piezometers. “Pool#1 75cm” had the largest median apparent upwelling (Table 9).

4.1.2.5 P1

Study reach P1 had a median VHG apparent downwelling signature of -0.01 to -0.23, encompassing 14 of 20 piezometers. The piezometer with the largest median apparent downwelling was “ADJ#1 25cm.” The median VHG apparent upwelling signature was <0.01 to 0.14, encompassing five of the 20 piezometers. The piezometer with the largest apparent upwelling was “ADJ#2 50cm.” One piezometer had a median VHG of 0.00 and showed no flux, “BOM 50cm” (Table 10).

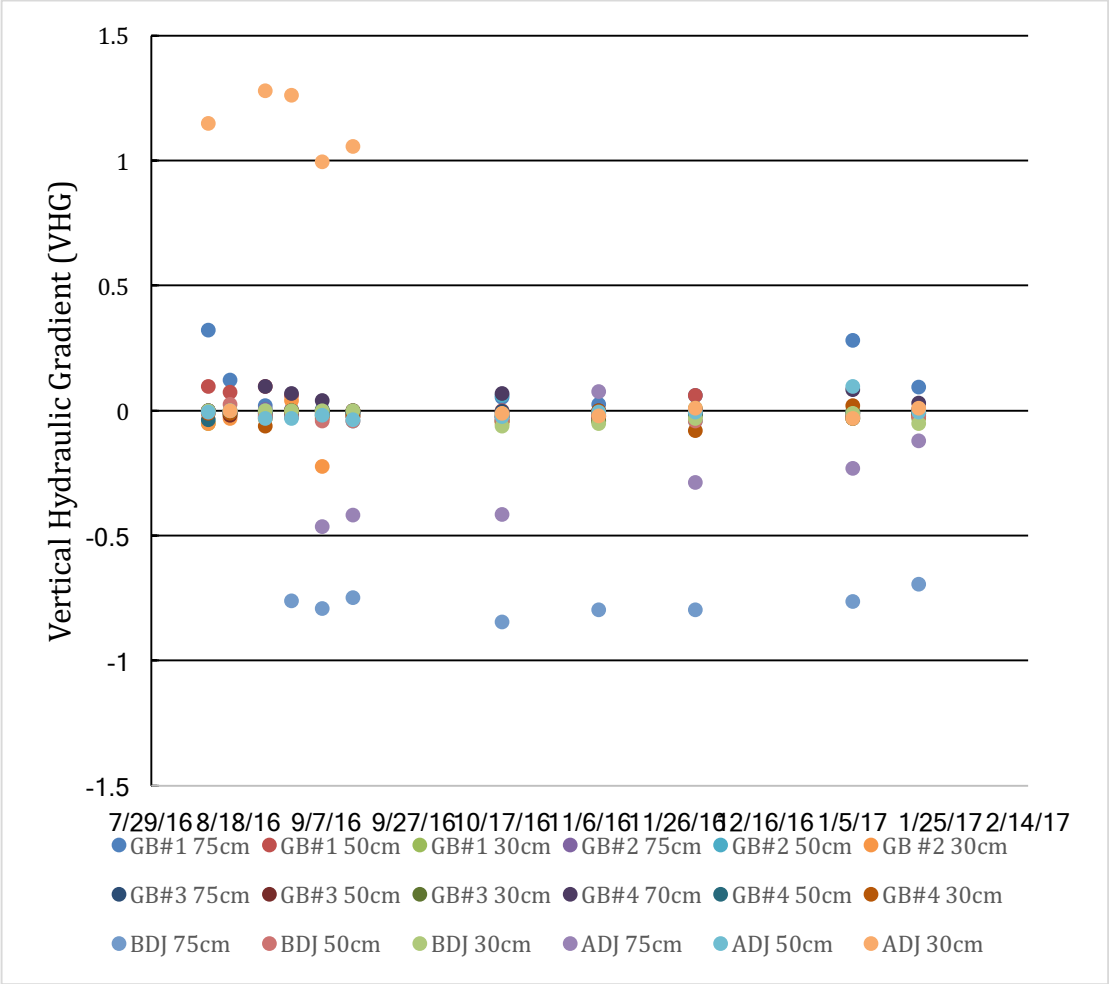

Figure 15. Reach R2 VHG measurements (all piezometers) from 8/11/16 to 1/20/17.

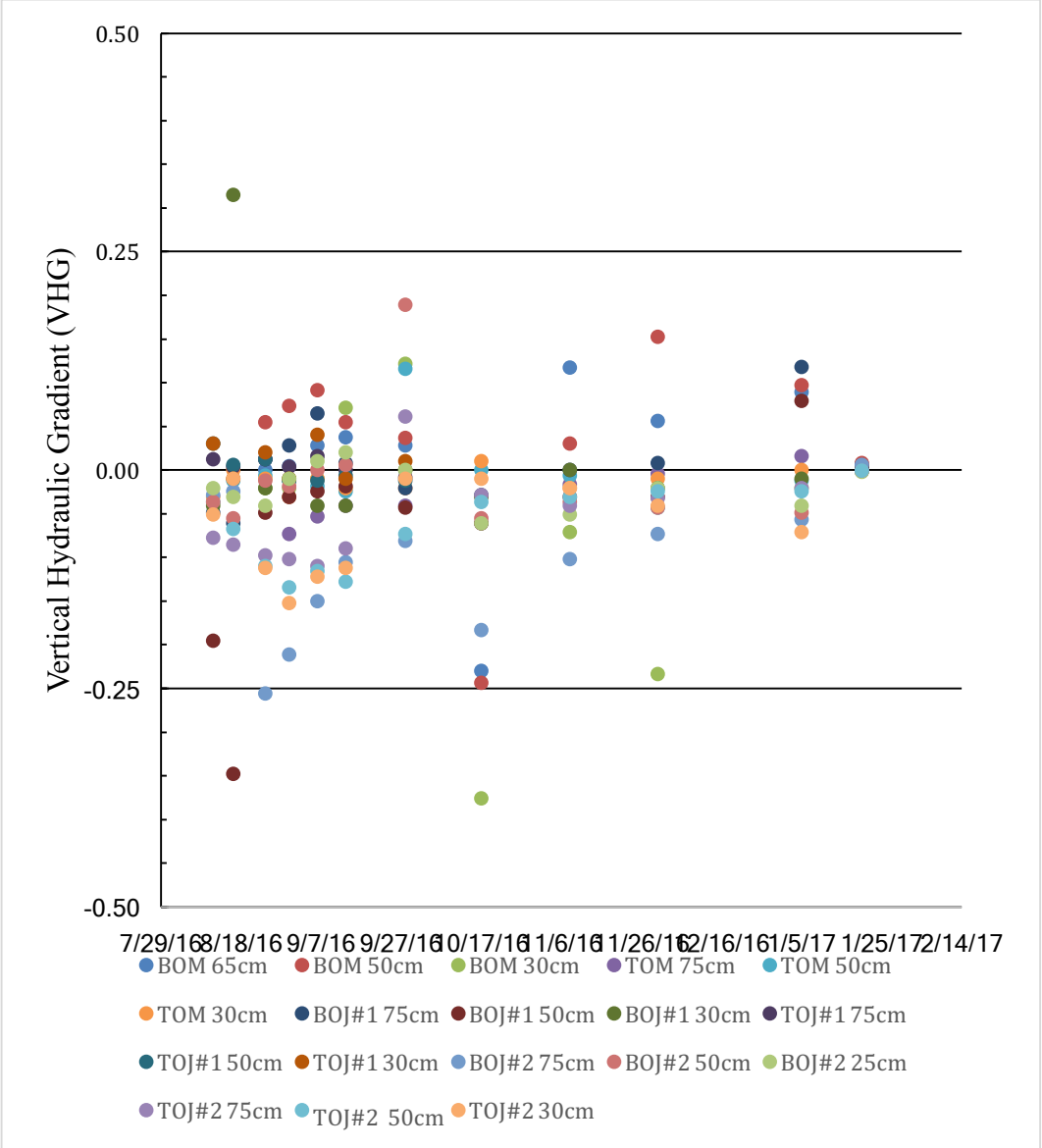

Figure 16. Reach A1 VHG measurements (all piezometers) from 8/11/16 to 1/20/17.

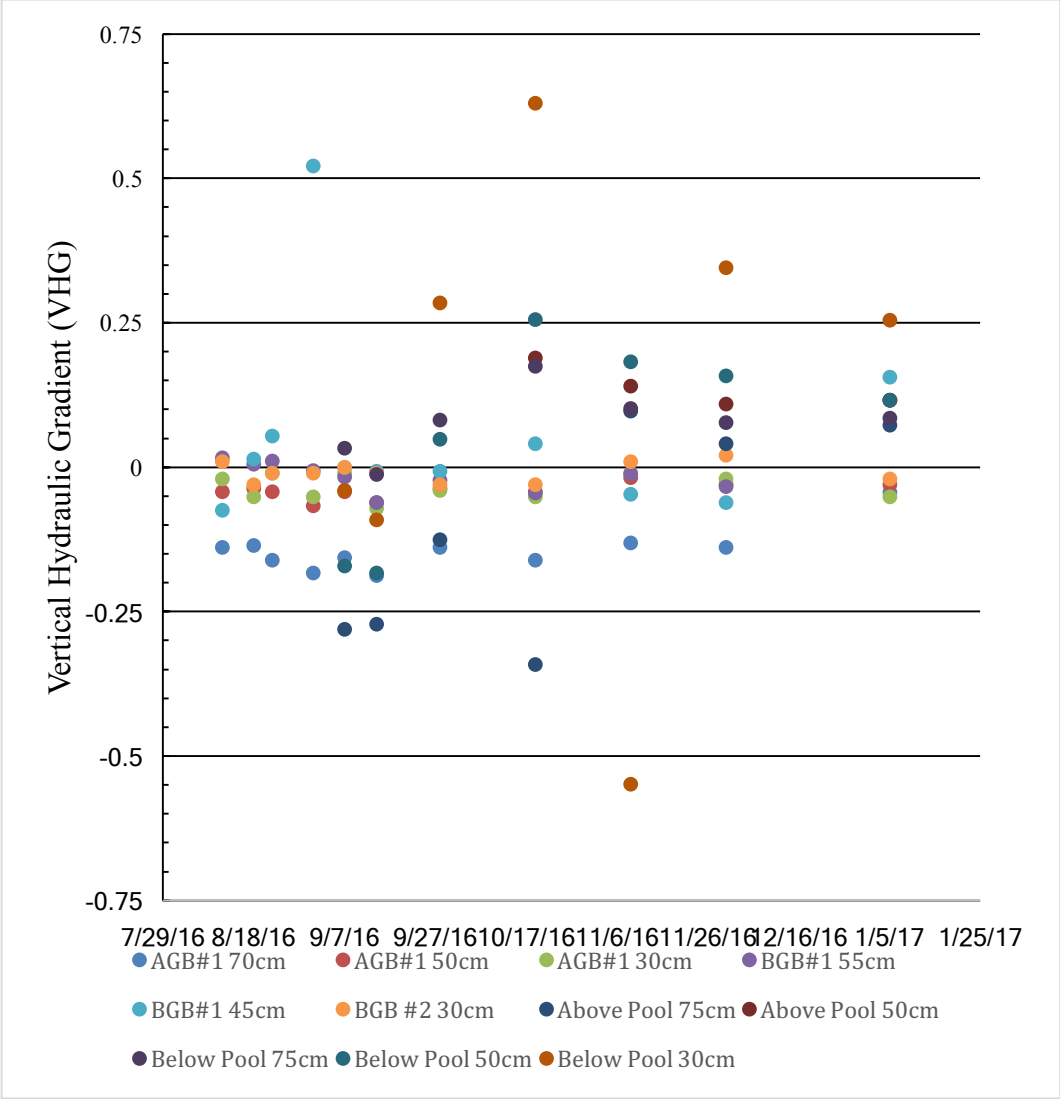

Figure 17. Reach C1 VHG measurements (all piezometers) from 8/11/16 to 1/5/17.

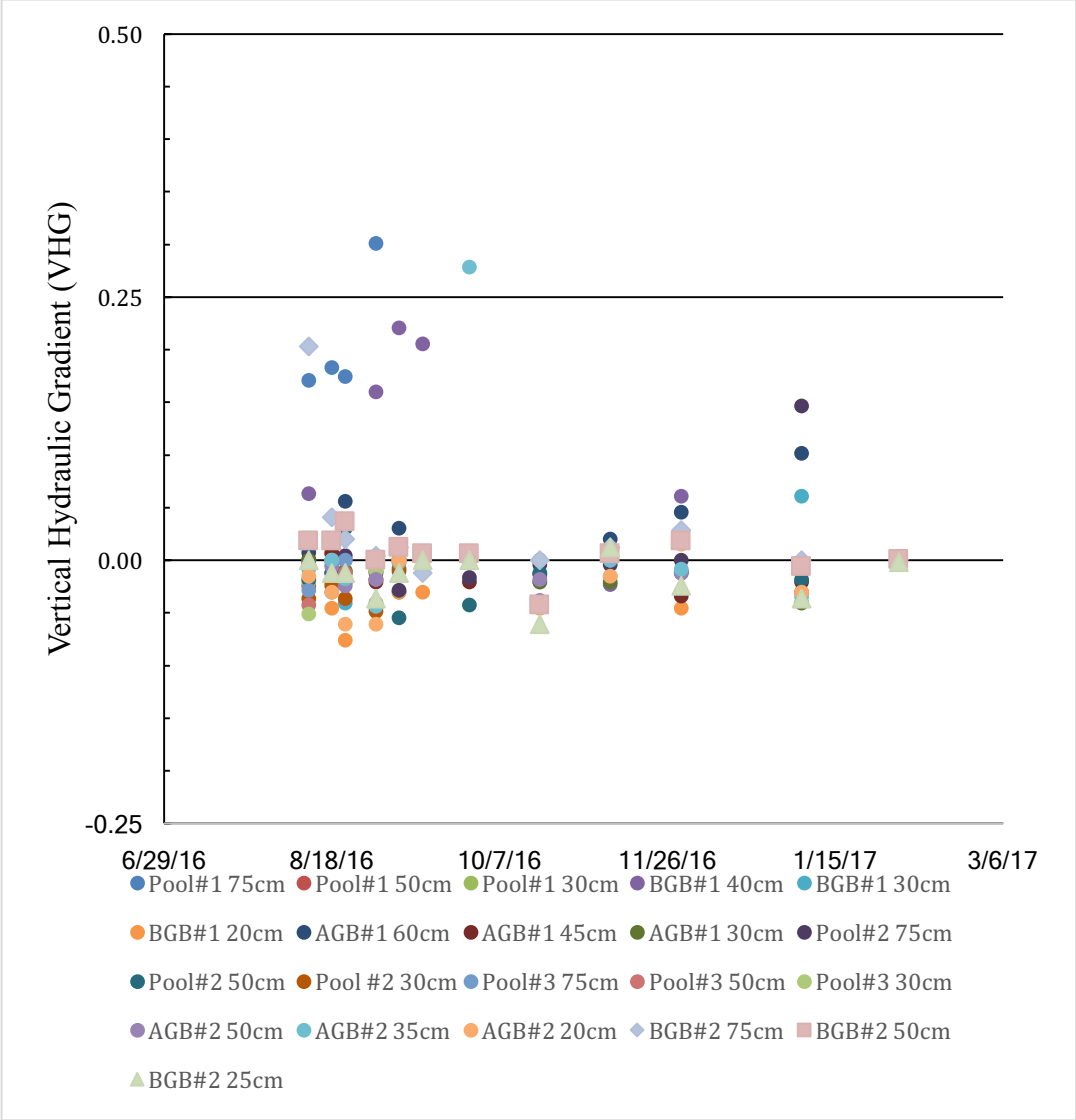

Figure 18. Reach D1 VHG measurements (all piezometers) from 8/11/16 to 2/3/17.

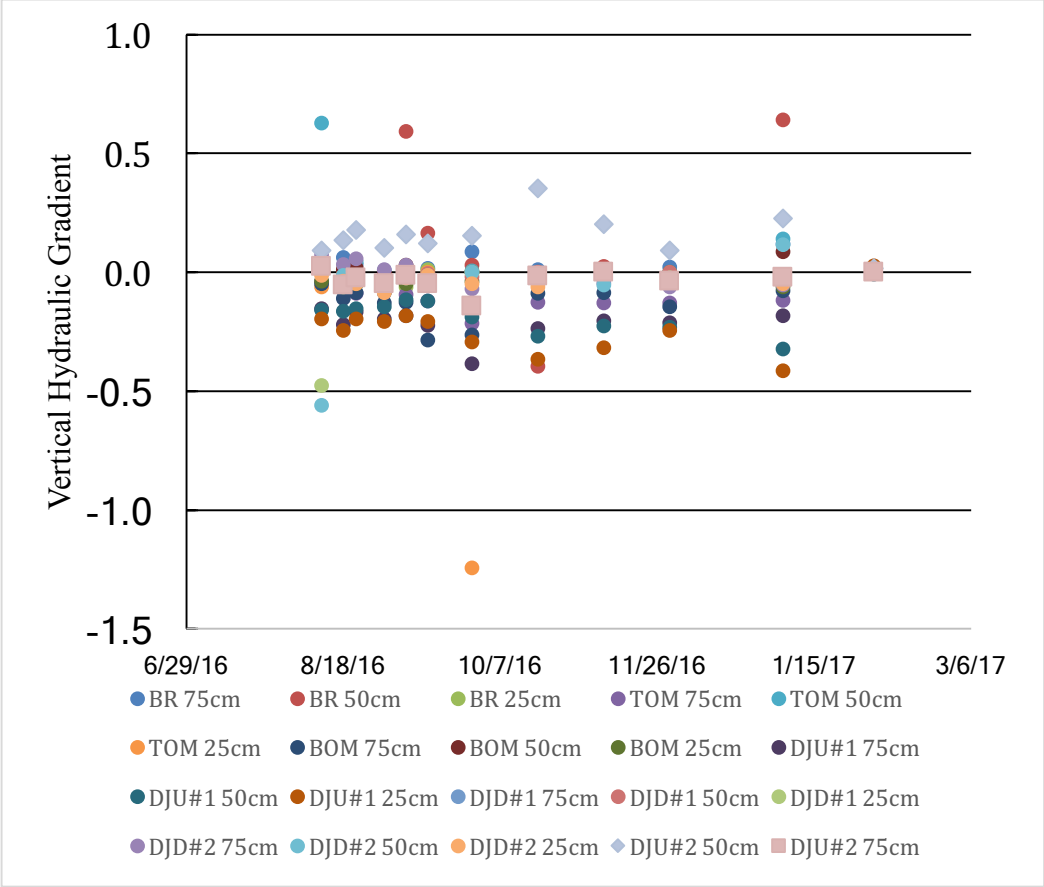

Figure 19. Reach P1 VHG measurements (all piezometers) from 8/11/16 to 2/3/17.

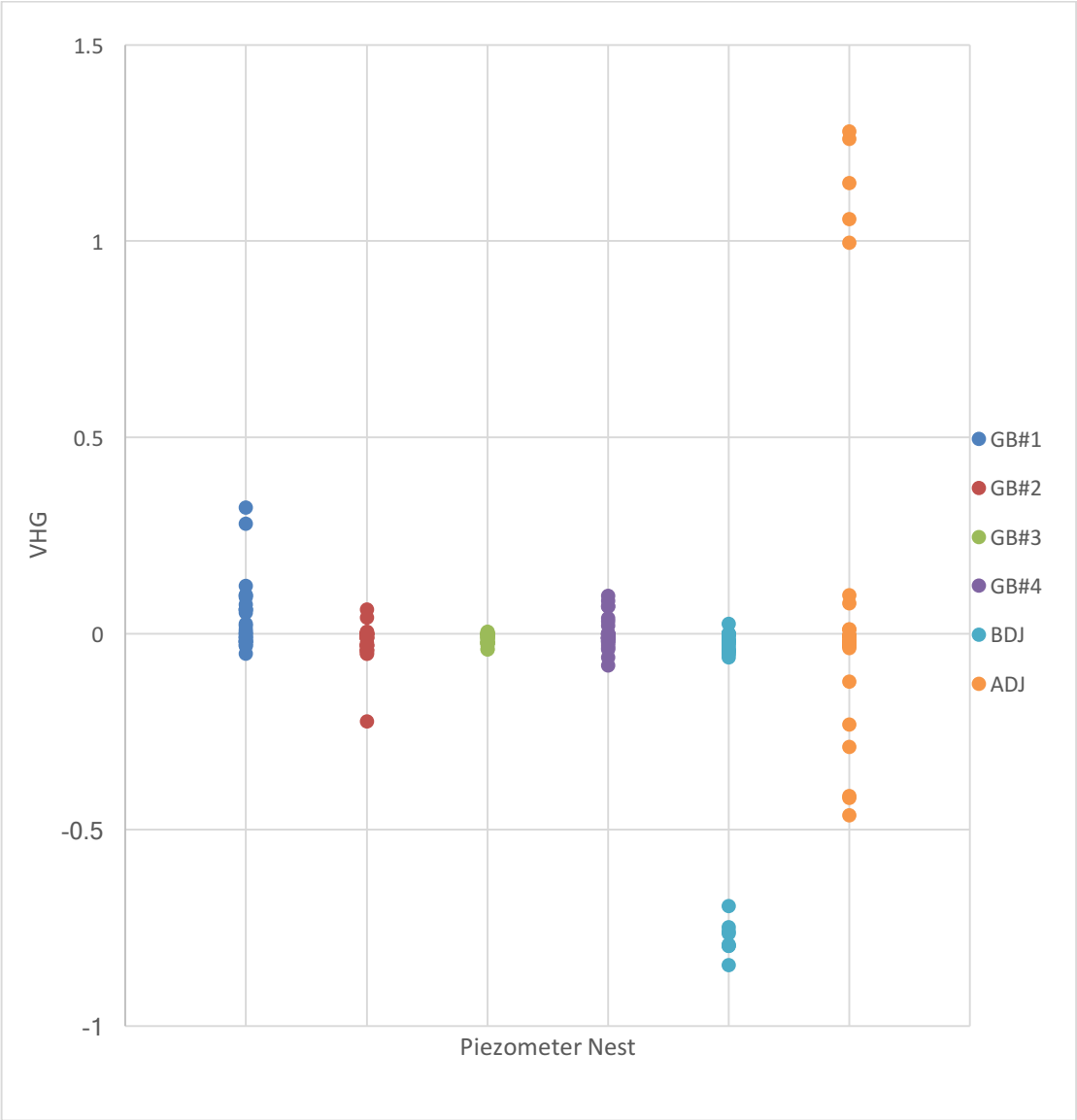

Figure 20. VHGs of each piezometer nest at reach R2.

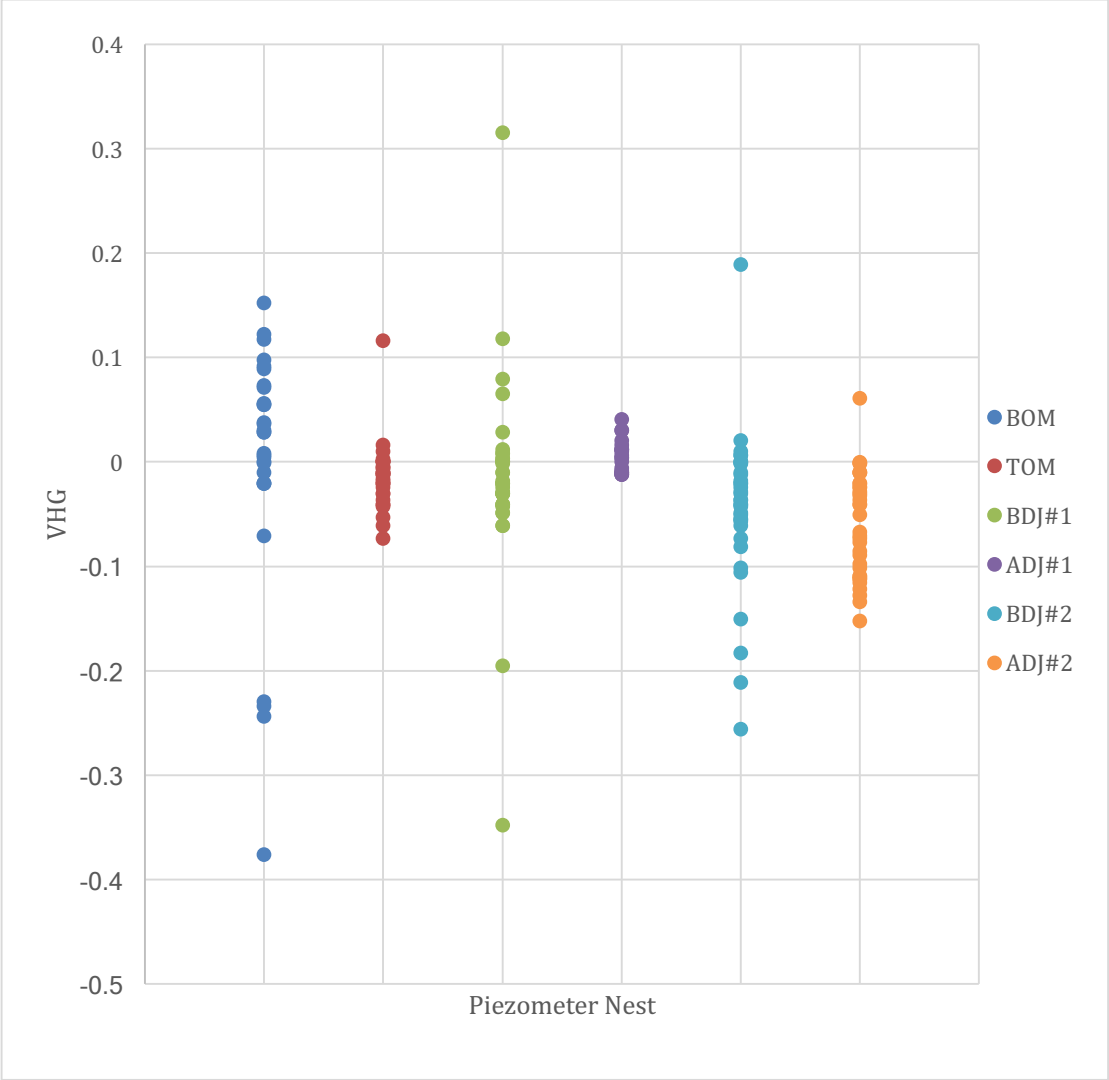

Figure 21. VHGs of each piezometer nest at reach A1.

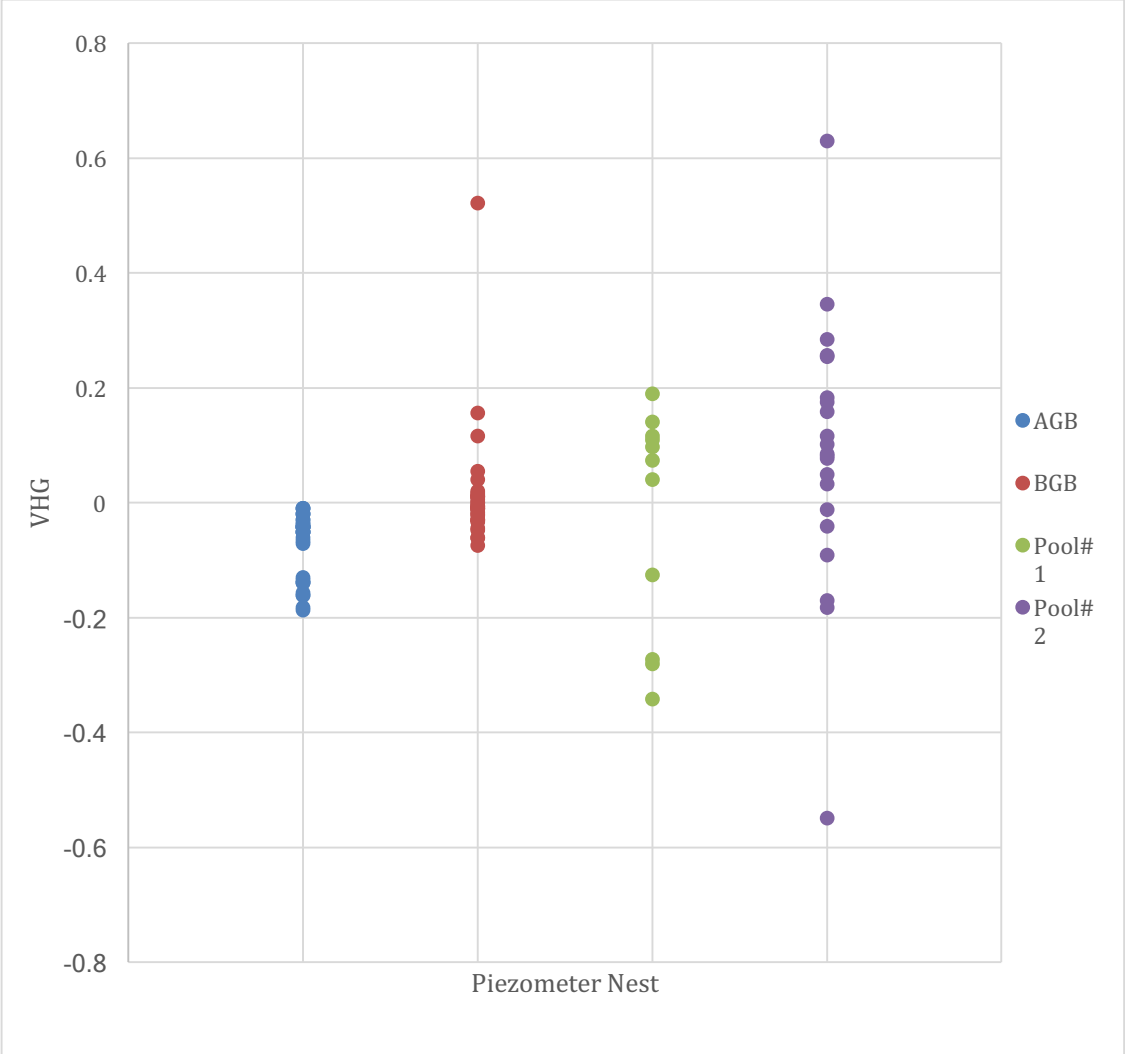

Figure 22. VHGs of each piezometer nest at reach C1.

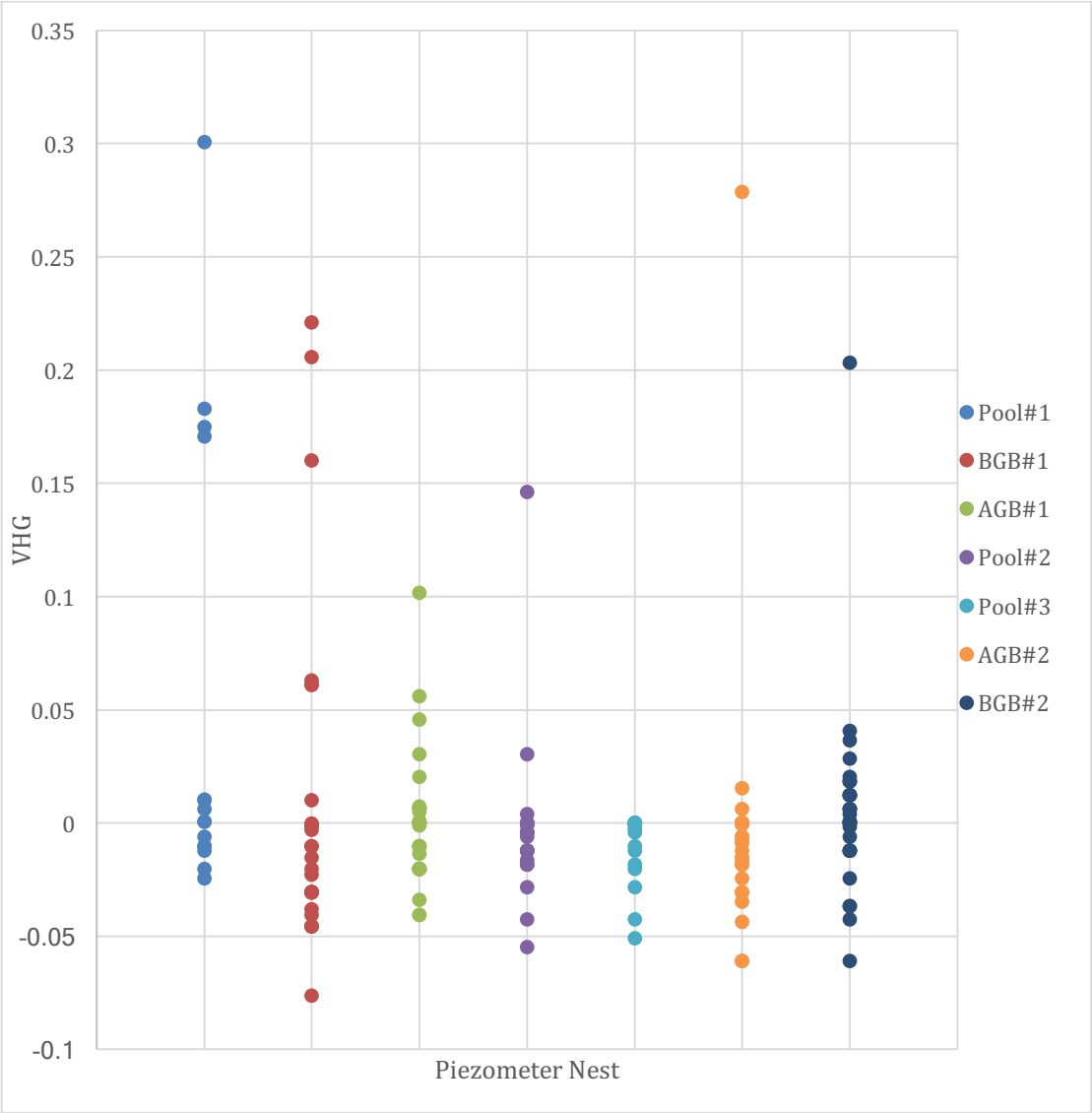

Figure 23. VHGs of each piezometer at reach D1.

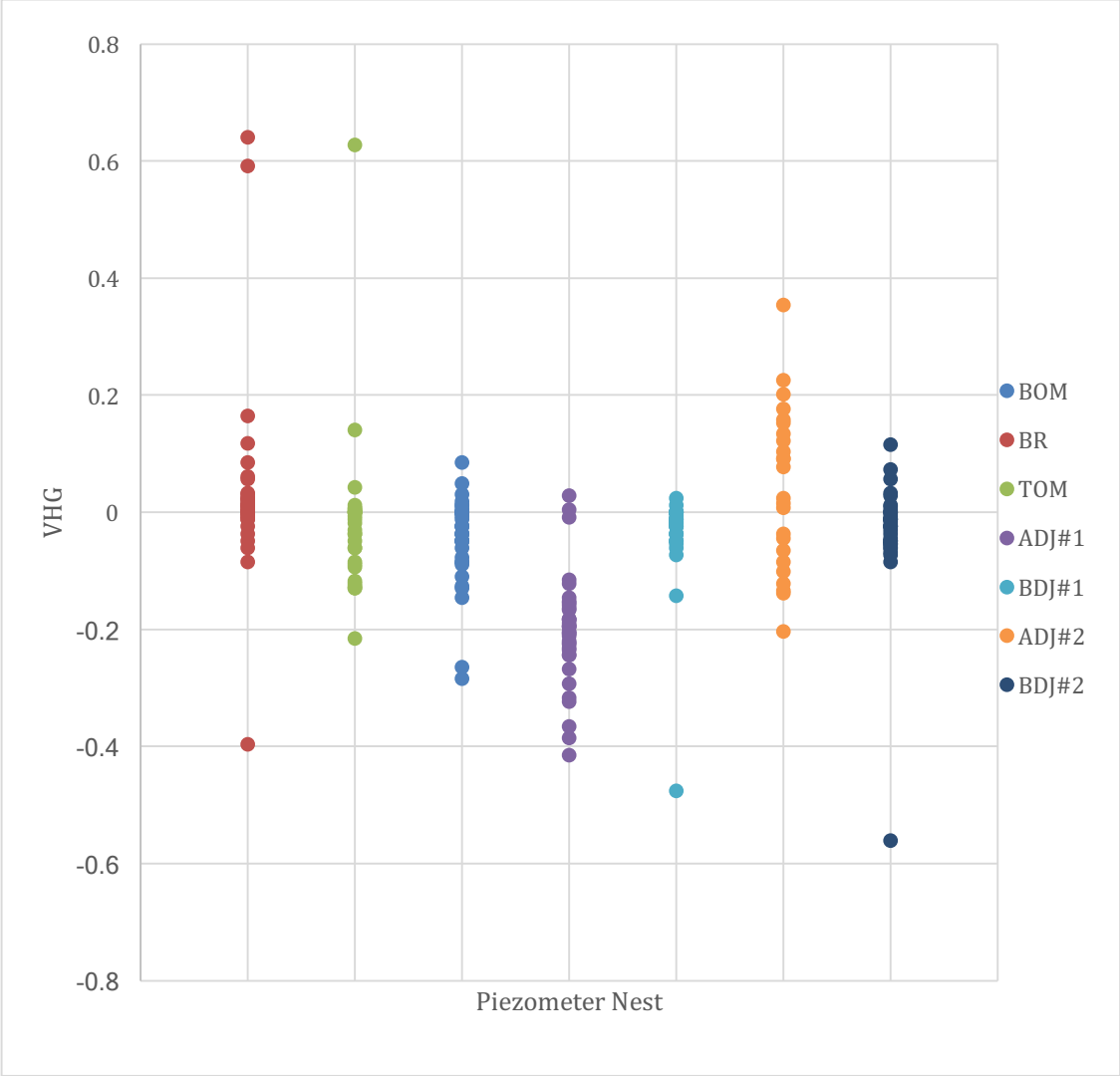

Figure 24. VHGs of each piezometer nest at reach P1.

Table 1. Reach R2 median, average, maximum, minimum and range of VHG on each date VHG measurements were taken.

R2	8/11/16	8/16/16	8/24/16	8/30/16	9/6/16	9/13/16	10/17/16	11/8/16	11/30/16	1/5/17	1/20/17
	VHG	VHG	VHG	VHG	VHG	VHG	VHG	VHG	VHG	VHG	VHG
Reach-wide Median	0.00	-0.01	-0.01	0.00	-0.01	-0.01	-0.02	-0.02	-0.01	-0.02	-0.01
Reach-wide Average	0.10	0.00	0.09	0.04	-0.03	-0.01	-0.08	-0.06	-0.07	-0.04	-0.05
Reach-wide Max	1.15	0.12	1.28	1.26	1.00	1.06	0.07	0.08	0.06	0.28	0.09
Reach-wide Min	-0.05	-0.03	-0.06	-0.76	-0.79	-0.75	-0.85	-0.80	-0.80	-0.76	-0.69
Reach-wide Range	1.20	0.15	1.34	2.02	1.79	1.80	0.91	0.87	0.86	1.04	0.79

Table 2. Reach A1 median, average, maximum, minimum, and range of VHG on each date VHG measurements were taken.

A1	8/11/16	8/16/16	8/24/16	8/30/16	9/6/16	9/13/16	9/28/16	10/17/16	11/8/16	11/30/16	1/5/17	1/20/17
	VHG	VHG	VHG	VHG	VHG	VHG	VHG	VHG	VHG	VHG	VHG	VHG
Reach-wide Median	-0.04	-0.02	-0.01	-0.02	-0.01	-0.01	0.00	-0.05	-0.02	-0.02	-0.01	0.00
Reach-wide Average	-0.04	-0.03	-0.04	-0.04	-0.02	-0.02	0.01	-0.09	-0.02	-0.02	0.01	0.00
Reach-wide Max	0.03	0.31	0.05	0.07	0.09	0.07	0.19	0.01	0.12	0.15	0.12	0.01
Reach-wide Min	-0.20	-0.35	-0.26	-0.21	-0.15	-0.13	-0.08	-0.38	-0.10	-0.23	-0.07	0.00
Reach-wide Range	0.23	0.66	0.31	0.28	0.24	0.20	0.27	0.39	0.22	0.39	0.19	0.01

Table 3. Reach C1 median, average, maximum, minimum and range values on each date VHG measurements were taken.

C1	8/11/16	8/18/16	8/22/16	8/31/16	9/7/16	9/14/16	9/28/16	10/19/16	11/9/16	11/30/16	1/5/17
	VHG	VHG	VHG	VHG	VHG	VHG	VHG	VHG	VHG	VHG	VHG
Reach-wide Median	-0.03	-0.03	-0.01	-0.03	-0.02	-0.06	-0.02	-0.03	-0.01	0.01	0.08
Reach-wide Average	-0.04	-0.04	-0.03	0.03	-0.04	-0.07	-0.05	-0.05	-0.03	-0.04	0.02
Reach-wide Max	0.02	0.01	0.05	0.52	0.03	0.00	0.28	0.63	0.18	0.35	0.25
Reach-wide Min	-0.14	-0.13	-0.16	-0.18	-0.28	-0.27	-0.14	-0.34	-0.55	-0.14	-0.05
Reach-wide Range	0.16	0.15	0.22	0.70	0.31	0.27	0.42	0.97	0.73	0.48	0.30

Table 4. Reach D1 median, average, maximum, minimum and range values on each date VHG measurements were taken.

D1	8/11/16	8/18/16	8/22/16	8/31/16	9/7/16	9/14/16	9/28/16	10/19/16	11/9/16	11/30/16	1/5/17	2/3/17
	VHG	VHG	VHG	VHG	VHG	VHG	VHG	VHG	VHG	VHG	VHG	VHG
Reach-wide Median	0.00	-0.01	-0.01	-0.02	0.00	0.00	0.00	-0.02	0.00	-0.01	-0.01	0.00
Reach-wide Average	0.02	-0.01	-0.01	-0.01	0.01	0.01	0.03	-0.02	0.01	0.00	0.01	0.00
Reach-wide Max	0.20	0.04	0.06	0.16	0.22	0.21	0.28	0.17	0.18	0.17	0.30	0.01
Reach-wide Min	-0.02	-0.05	-0.08	-0.06	-0.05	-0.03	-0.04	-0.06	-0.02	-0.05	-0.05	-0.01
Reach-wide Range	0.22	0.09	0.13	0.22	0.28	0.24	0.32	0.23	0.21	0.22	0.35	0.02

Table 5. Reach P1 median, average, maximum, minimum and range values on each date VHG measurements were taken.

P1	8/11/16	8/18/16	8/22/16	8/31/16	9/7/16	9/14/16	9/28/16	10/19/16	11/9/16	11/30/16	1/5/17	2/3/17
	VHG	VHG	VHG	VHG	VHG	VHG	VHG	VHG	VHG	VHG	VHG	VHG
Reach-wide Median	-0.01	-0.03	-0.03	-0.06	-0.02	-0.02	-0.04	-0.03	0.00	-0.02	-0.02	0.00
Reach-wide Average	-0.04	-0.04	-0.04	-0.07	-0.01	-0.05	-0.08	-0.07	-0.04	-0.06	0.00	0.00
Reach-wide Max	0.63	0.13	0.18	0.10	0.59	0.16	0.15	0.35	0.20	0.09	0.64	0.03
Reach-wide Min	-0.56	-0.24	-0.20	-0.21	-0.18	-0.28	-0.39	-0.40	-0.32	-0.24	-0.41	-0.01
Reach-wide Range	1.19	0.38	0.37	0.31	0.77	0.45	0.54	0.75	0.52	0.34	1.05	0.04

Table 6. VHG data for each piezometer at each date for reach R2. A blank cell means either that the piezometer data could not be collected or early data was not accurate due to slow recharge in the piezometer.

R2		8/11/16	8/16/16	8/24/16	8/30/16	9/6/16	9/13/16	10/17/16	11/8/16	11/30/16	1/5/17	1/20/17	
Piezometer	**Depth**	**VHG**	**VHG**	**VHG**	**VHG**	**VHG**	**VHG**	**VHG**	**VHG**	**VHG**	**VHG**	**VHG**	**Median for all dates**
GB #1	**75**	0.32	0.12	0.02	0.00	0.00	-0.01	0.05	0.02	0.06	0.28	0.09	0.05
GB #1	**50**			0.10	0.07	0.10	0.06				-0.02	0.06	0.07
GB #1	**30**	-0.05	-0.02	-0.03	-0.02	-0.02	-0.01	-0.02	-0.01	0.01	0.00	-0.03	-0.02
GB #2	**75**	0.00	0.00	0.00	0.00	0.00	-0.01	-0.03	-0.02	0.00	-0.01	-0.01	0.00
GB #2	**50**	0.00		0.00	0.00	0.00	-0.04	0.06	-0.04	-0.04	-0.03	-0.01	-0.01
GB #2	**30**	-0.05	-0.03	-0.03	0.04	-0.22	0.00	-0.05	-0.04	-0.01	-0.03	-0.01	-0.03
GB #3	**75**	0.00	-0.01	-0.01	0.00	0.00	0.00	0.00	-0.02	0.00	-0.01	0.00	0.00
GB #3	**50**	0.00	-0.02	-0.02	-0.02	-0.01	-0.02	-0.02	-0.02	-0.01	-0.02	-0.01	-0.02
GB #3	**30**				0.00	0.00	0.00	-0.04	-0.04	-0.02	-0.03	-0.01	-0.02
GB#4	**70**			0.10	0.07	0.04	0.00	0.07	0.00	0.00	0.08	0.03	0.04
GB#4	**50**	-0.04	-0.01	-0.01	-0.02	-0.02	-0.01	-0.01	-0.01	-0.01	-0.01	-0.01	-0.01
GB#4	**30**	-0.01	-0.01	-0.06		-0.03	-0.02	-0.04	0.00	-0.08	0.02	-0.02	-0.02
BDJ#1	**75**				-0.76	-0.79	-0.75	-0.85	-0.80	-0.80	-0.76	-0.69	-0.78
BDJ#1	**50**	-0.01	0.02	-0.02	-0.02	-0.04	-0.04	-0.04	-0.02	-0.04	-0.02	-0.02	-0.02
BDJ#1	**30**	0.00	0.00		0.00	0.00	0.00	-0.06	-0.05	-0.03	-0.01	-0.05	-0.01
ADJ#2	**75**					-0.46	-0.42	-0.41	0.08	-0.29	-0.23	-0.12	-0.29
ADJ#2	**50**	-0.01		-0.03	-0.03	-0.02	-0.04	-0.02	-0.01	-0.01	0.10	-0.01	-0.01
ADJ#2	**30**	1.15		1.28	1.26	1.00	1.06	-0.01	-0.02	0.01	-0.03	0.01	0.50

Table 7. VHG data for each piezometer at each date for reach A1. A blank cell means either that the piezometer data could not be collected or early data was not accurate due to slow recharge in the piezometer.

A1		8/11/16	8/16/16	8/24/16	8/30/16	9/6/16	9/13/16	9/28/16	10/17/16	11/8/16	11/30/16	1/5/17	1/20/17	
Piezometer	Depth (cm)	VHG	VHG	VHG	VHG	VHG	VHG	VHG	VHG	VHG	VHG	VHG	VHG	Median for all dates
BOM	65			0.00	0.00	0.03	0.04	0.03	-0.23	0.12	0.06	0.09	0.01	0.03
BOM	50			0.05	0.07	0.09	0.05	0.04	-0.24	0.03	0.15	0.10	0.01	0.05
BOM	30			-0.02	-0.02	-0.01	0.07	0.12	-0.38	-0.07	-0.23	-0.02	0.00	-0.02
TOM	75				-0.07	-0.05	-0.04	-0.04	-0.06	-0.02	0.00	0.02	0.00	-0.04
TOM	50	-0.04	-0.01	-0.01	-0.01	-0.02	-0.02	0.12	0.00	-0.01	-0.04	-0.01	0.00	-0.01
TOM	30	-0.03	0.00	-0.01	-0.03	-0.01	-0.02	-0.02	0.01	-0.02	-0.01	0.00	0.00	-0.01
BDJ#1	75	-0.05	-0.06	0.01	0.03	0.07	0.01	-0.02	-0.03	0.00	0.01	0.12	0.00	0.01
BDJ#1	50	-0.20	-0.35	-0.05	-0.03	-0.02	-0.02	-0.04	-0.06	-0.03	-0.03	0.08	0.00	-0.03
BDJ#1	30	-0.04	0.31	-0.02	-0.01	-0.04	-0.04	0.00	-0.03	0.00	-0.02	-0.01	0.00	-0.02
ADJ#1	75	0.01	0.00	0.01	0.00	0.02	0.00	-0.01			0.00			0.00
ADJ#1	50	0.03	0.01	0.01	-0.01	-0.01	-0.01	-0.01			0.00			0.00
ADJ#1	30	0.03	-0.01	0.02	-0.01	0.04	-0.01	0.01			0.00			0.01
BDJ#2	75	-0.03	-0.02	-0.26	-0.21	-0.15	-0.11	-0.08	-0.18	-0.10	-0.07	-0.06	0.01	-0.09
BDJ#2	50	-0.04	-0.05	-0.01	-0.02	0.00	0.01	0.19	-0.05	-0.04	-0.04	-0.05	0.00	-0.03
BDJ#2	30	-0.02	-0.03	-0.04	-0.01	0.01	0.02	0.00	-0.06	-0.05	-0.02	-0.04	0.00	-0.02
ADJ#2	75	-0.08	-0.09	-0.10	-0.10	-0.11	-0.09	0.06	-0.03	-0.04	-0.03	-0.02	0.00	-0.06
ADJ#2	50		-0.07	-0.11	-0.13	-0.12	-0.13	-0.07	-0.04	-0.03	-0.02	-0.02	0.00	-0.07
ADJ#2	30	-0.05	-0.01	-0.11	-0.15	-0.12	-0.11	-0.01	-0.01	-0.02	-0.04	-0.07	0.00	-0.05

Table 8. VHG data for each piezometer at each date for reach C1. A blank cell means either that the piezometer data could not be collected or early data was not accurate due to slow recharge in the piezometer.

C1		8/11/16	8/18/16	8/22/16	8/31/16	9/7/16	9/14/16	9/28/16	10/19/16	11/9/16	11/30/16	1/5/17	
Piezometer	**Depth (cm)**	**VHG**	**VHG**	**VHG**	**VHG**	**VHG**	**VHG**	**VHG**	**VHG**	**VHG**	**VHG**	**VHG**	**Median for all dates**
AGB#1	**70**	-0.14	-0.13	-0.16	-0.18	-0.16	-0.19	-0.14	-0.16	-0.13	-0.14	-0.04	-0.14
AGB#1	**50**	-0.04	-0.04	-0.04	-0.07	-0.04	-0.06	-0.04	-0.04	-0.02	-0.03	-0.03	-0.04
AGB#1	**30**	-0.02	-0.05	-0.01	-0.05	-0.01	-0.07	-0.04	-0.05	-0.01	-0.02	-0.05	-0.04
BGB#1	**55**	0.02	0.01	0.01	-0.01	-0.02	-0.06	-0.02	-0.04	-0.01	-0.03	0.12	-0.01
BGB#1	**45**	-0.07	0.01	0.05	0.52	0.00	-0.01	-0.01	0.04	-0.05	-0.06	0.16	0.00
BGB#1	**30**	0.01	-0.03	-0.01	-0.01	0.00	-0.01	-0.03	-0.03	0.01	0.02	-0.02	-0.01
Pool #1	**75**					-0.28	-0.27	-0.13	-0.34	0.10	0.04	0.07	-0.13
Pool #1	**50**								0.19	0.14	0.11	0.12	0.13
Pool #2	**75**					0.03	-0.01	0.08	0.17	0.10	0.08	0.09	0.08
Pool #2	**50**					-0.17	-0.18	0.05	0.26	0.18	0.16	0.12	0.12
Pool #2	**30**					-0.04	-0.09	0.28	0.63	-0.55	0.35	0.25	0.25

Table 9. VHG data for each piezometer at each date for reach D1. A blank cell means either that the piezometer data could not be collected or early data was not accurate due to slow recharge in the piezometer.

D1		8/11/16	8/18/16	8/22/16	8/31/16	9/7/16	9/14/16	9/28/16	10/19/16	11/9/16	11/30/16	1/5/17	2/3/17	
Cluster	Depth (cm)	VHG	VHG	VHG	VHG	VHG	VHG	VHG	VHG	VHG	VHG	VHG	VHG	Median for all dates
Pool #1	75								0.17	0.18	0.17	0.30	0.01	0.17
Pool #1	50								-0.02	0.01	-0.01	-0.01	0.00	-0.01
Pool #1	30								-0.02	0.01	-0.01	-0.01	0.00	-0.01
BGB#1	40	0.06			0.16	0.22	0.21		-0.04	-0.02	0.06	-0.03	0.00	0.06
BGB#1	30	0.00	-0.03	-0.04	-0.01	-0.03	-0.01		-0.02	0.01	-0.03	0.06	0.00	-0.01
BGB#1	20	0.00	-0.05	-0.08	-0.05	-0.03	-0.03		-0.05	-0.02	-0.05	-0.03	0.00	-0.03
AGB#1	60	0.01		0.06	0.00	0.03	0.01		0.00	0.02	0.05	0.10	0.01	0.01
AGB#1	45	0.00	0.01	-0.02	-0.02	0.01	0.00	-0.02	-0.01	0.01	-0.03	-0.02	0.00	-0.01
AGB#1	30	0.00	-0.02	-0.01	-0.04	-0.01	-0.01	0.00	-0.02	-0.02	-0.01	-0.04	0.00	-0.01
Pool #2	75	0.00	-0.01	0.00	-0.01	-0.03	0.00	-0.02	0.00	0.00	0.00	0.15	0.00	0.00
Pool #2	50	-0.02	-0.01	0.03	-0.02	-0.05	-0.01	-0.04	-0.01	0.00	-0.01	-0.02	0.00	-0.01
Pool #3	75								-0.03	0.00	0.00	0.00	0.00	0.00
Pool #3	50								-0.04	0.00	-0.01	-0.02	0.00	-0.01
Pool #3	30								-0.05	0.00	-0.02	-0.01	0.00	-0.01
AGB#2	50	-0.01	-0.01	-0.02	-0.02	0.00	-0.01	0.01	-0.02	0.00	-0.01	-0.01	0.00	-0.01
AGB#2	35	-0.01	0.00	-0.02	-0.04	0.00	0.00	0.28	0.00	0.00	-0.01	-0.03	0.00	0.00
AGB#2	20	-0.02	-0.03	-0.06	-0.06	0.00	0.00	0.00	0.00	-0.02	0.02	-0.03	0.00	-0.01
BGB#2	75	0.20	0.04	0.02	0.00	0.01	-0.01			0.01	0.03	0.00	0.00	0.01
BGB#2	50	0.02	0.02	0.04	0.00	0.01	0.01	0.01	-0.04	0.01	0.02	-0.01	0.00	0.01
BGB#2	25	0.00	-0.01	-0.01	-0.04	-0.01	0.00		-0.06	0.01	-0.02	-0.04	0.00	-0.01

Table 10. VHG data for each piezometer at each date for reach P1. A blank cell means either that the piezometer data could not be collected or early data was not accurate due to slow recharge in the piezometer.

P1		8/11/16	8/18/16	8/22/16	8/31/16	9/7/16	9/14/16	9/28/16	10/19/16	11/9/16	11/30/16	1/5/17	2/3/17	
Piezometer	Depth (cm)	VHG	VHG	VHG	VHG	VHG	VHG	VHG	VHG	VHG	VHG	VHG	VHG	Median for all dates
BR	75	0.06	0.06	0.03	0.01	0.02	0.02	0.09	0.01	0.00	0.02	0.12	0.00	0.02
BR	50	0.00	0.01	-0.02	-0.01	0.59	0.16	0.03	-0.40	0.02	-0.01	0.64	0.00	0.00
BR	25	0.00	0.01	-0.05	-0.09	-0.06	0.01	0.00	-0.04	0.00	-0.01	-0.01	0.00	-0.01
TOM	75	-0.04	-0.06	-0.09	-0.09	-0.09	-0.12	-0.22	-0.13	-0.13	-0.13	-0.12	0.00	-0.11
TOM	50	0.63	-0.02	0.04	-0.03	0.01	-0.01	0.01	0.00	0.00	0.00	0.14	0.00	0.00
TOM	25	-0.06	0.01	-0.04	-0.05	-0.01	0.00		-0.01	0.00	-0.02	-0.02	0.00	-0.01
BOM	75	-0.05	-0.11	-0.09	-0.13	-0.13	-0.28	-0.26	-0.09	-0.09	-0.15	-0.08	0.01	-0.10
BOM	50	0.05	0.01	0.02	-0.01	0.03	-0.05	0.00	0.00	0.00	-0.02	0.09	0.00	0.00
BOM	25	-0.04	-0.04	-0.05	-0.02	-0.05	-0.02	-0.04	-0.01	0.01	0.00	-0.06	0.00	-0.03
ADJ#1	75	-0.15	-0.22	-0.17	-0.20	-0.18	-0.22	-0.39	-0.24	-0.20	-0.21	-0.18	0.00	-0.20
ADJ#1	50	-0.16	-0.16	-0.15	-0.15	-0.12	-0.12	-0.19	-0.27	-0.23	-0.23	-0.32	-0.01	-0.16
ADJ#1	25	-0.20	-0.24	-0.20	-0.21	-0.18	-0.21	-0.29	-0.37	-0.32	-0.24	-0.41	0.03	-0.23
BDJ#1	75	0.02	-0.05	-0.02	-0.05	-0.01	-0.05	-0.14	-0.02	0.00	-0.04	-0.02	0.00	-0.02
BDJ#1	50	0.00	-0.02	-0.02	-0.05	-0.01	-0.01	-0.02	0.00	0.00	0.00	-0.01	0.00	-0.01
BDJ#1	25	-0.48	-0.06	-0.02	-0.07	-0.01	-0.01	0.00	-0.04	0.01	-0.02	-0.04	0.00	-0.02
ADJ#2	75	0.02	-0.10	-0.09	-0.13	-0.12	-0.14	-0.20	-0.04	-0.04	-0.07	0.08	0.01	-0.08
ADJ#2	50	0.09	0.13	0.18	0.10	0.16	0.12	0.15	0.35	0.20	0.09	0.23	0.02	0.14
BDJ#2	75	0.07	0.03	0.06	0.01	0.03	-0.02	-0.07	-0.01	-0.04	-0.06	-0.05	0.01	0.00
BDJ#2	50	-0.56	-0.01	-0.01	-0.07	-0.02	-0.05	0.00	-0.03	-0.05	-0.02	0.12	0.00	-0.02
BDJ#2	25	-0.01	-0.04	-0.05	-0.09	-0.02	-0.01	-0.05	-0.06	0.00	-0.02	-0.05	0.00	-0.03

4.1.3 VHG by geomorphic feature

4.1.3.1 Bedrock

Only one location was suitable for a downstream of bedrock piezometer nest (study reach P1). One piezometer in this nest had a median apparent downwelling signature of -0.01 across all dates. Two piezometers in this nest had a median apparent upwelling signature of <0.01 across all dates. The piezometer with the largest apparent downwelling was "BR 25cm". The piezometer with the largest apparent upwelling was "BR 75cm" (Table 11).

4.1.3.2 Pool

Two study reaches contained the "Pool" feature, reach D1 and C1, encompassing five nests containing a total of 14 piezometers. Nine piezometers exhibited a median apparent downwelling signature from -0.01 to -0.13 across all sampling dates. Five piezometers exhibited a median apparent upwelling signature from 0.08 to 0.25 across all sampling dates. The piezometer with the largest apparent downwelling was in C1 "Pool#1 75cm." The piezometer with the largest apparent upwelling was in C1 "Pool#2 30cm" (Table 12).

4.1.3.3 Above debris jam

Three different study reaches contained the "above debris jam" feature (A1, R2, P1) encompassing five nests containing a total of 14 piezometers. Reach A1 contained two nests, R2 contained one nest, and P1 contained two nests. 10 piezometers exhibited a median apparent downwelling signature from -0.01 to -0.29 for all sampling dates. Four piezometers exhibited a median apparent upwelling signature from 0.01 to 0.50 for all sampling dates. The piezometer with the largest apparent downwelling was at reach R2 "ADJ#2 75cm". The piezometer with the largest apparent upwelling was at reach R2 "ADJ#2 30cm" (Table 13).

4.1.3.4 Below debris jam

Three different study reaches contained the "below debris jam" feature (A1, R2, P1), encompassing five nests containing a total of 15 piezometers. Reach A1 contained two nests, R2

contained one nest, and P1 contained two nests. 13 piezometers exhibited a median apparent downwelling signature of -0.01 to -0.78 for all sampling dates. The piezometer with the largest median apparent downwelling was at reach R2 piezometer "BDJ#1 75cm." Two piezometers exhibited a median apparent upwelling signature of <0.01 and 0.01. The piezometer with the largest apparent upwelling was at reach A1 "BDJ#1 75cm" (Table 14).

4.1.3.5 Top of meander bend

Study reaches A1 and P1 are the only reaches with the "top of meander bend" feature, encompassing two nests containing a total six piezometers. Five piezometers contain a median apparent downwelling signature of -0.01 to -0.11 for all sampling dates. The piezometer with the largest median apparent downwelling was at reach P1 piezometer "TOM 75cm." One piezometer exhibited a median apparent upwelling signature of <0.01 for all sampling dates, at reach P1 "TOM 50cm" (Table 15).

4.1.3.6 Bottom of meander bend

Study reaches A1 and P1 are the only reaches with the "bottom of meander bend" feature, encompassing two nests containing a total six piezometers. Three piezometers exhibited a median apparent downwelling signature of -0.02 to -0.10 for all sampling dates. The piezometer with the largest median apparent downwelling was at reach P1 "BOM 75cm." Two piezometers exhibited a median apparent upwelling signature of 0.03 to 0.05 for all sampling dates. The piezometer with the largest median apparent upwelling was at reach A1 piezometer "BOM 50cm." One piezometer exhibited a median VHG value of zero across all sampling dates, at reach P1 "BOM 50cm" (Table 16).

4.1.3.7 Above gravel bed

Reach D1 is the only reach with the "above gravel bed" feature, encompassing two nests containing a total six piezometers for this feature. Five piezometers showed a median apparent downwelling signature of >-0.01 to -0.01 for all sampling dates. Four of the apparent downwelling piezometers had the same VHG of -0.01. The one apparent downwelling piezometer

with the >-0.01 VHG was “AGB#2 35cm.” One piezometer exhibited a median apparent upwelling signature of 0.01 for all sampling dates. This piezometer was “AGB#1 60cm” (Table 17).

4.1.3.8 Between gravel bed

Reach R2 is the only reach with the “between gravel bed” feature, encompassing four nests containing a total 12 piezometers. Nine piezometers exhibited a median apparent downwelling signature of >-0.01 to -0.03 for all sampling dates. The piezometer with the largest median apparent downwelling was “GB#2 30cm.” Three piezometers exhibited a median apparent upwelling signature of 0.04 to 0.07 for all sampling dates. The piezometer with the largest median apparent upwelling was “GB#1 50cm” (Table 18).

4.1.3.9 Below gravel bed

Reach D1 is the only reach with the “below gravel bed” feature, encompassing two nests and six piezometers were assigned to this feature. Three piezometers exhibited a median apparent downwelling signature of -0.01 to -0.03 for all sampling dates. The piezometer with the largest median apparent downwelling was “BGB#1 20cm.” Three piezometers exhibited a median apparent upwelling signature of 0.01 to 0.06. The piezometer with the largest median apparent upwelling was “BGB#1 40cm” (Table 19).

Table 11. VHG data for the piezometer with the “below bedrock” geomorphic feature for all sampling dates.

Depth (cm)	Reach	Nest	8/11/16 VHG	8/18/16 VHG	8/22/16 VHG	8/31/16 VHG	9/7/16 VHG	9/14/16 VHG	9/28/16 VHG	10/19/16 VHG	11/9/16 VHG	11/30/16 VHG	1/5/17 VHG	2/3/17 VHG	Median all dates VHG
75	P1	BR	0.06	0.06	0.03	0.01	0.02	0.02	0.09	0.01	0.00	0.02	0.12	0.00	0.02
50	P1	BR	0.00	0.01	-0.02	-0.01	0.59	0.16	0.03	-0.40	0.02	-0.01	0.64	0.00	0.00
25	P1	BR	0.00	0.01	-0.05	-0.09	-0.06	0.01	0.00	-0.04	0.00	-0.01	-0.01	0.00	-0.01

Table 12. VHG data for each piezometer with the "pool" geomorphic feature for all sampling dates.

Depth (cm)	Nest	Reach	8/11/16 VHG	8/18/16 VHG	8/22/16 VHG	8/31/16 VHG	9/7/16 VHG	9/14/16 VHG	9/28/16 VHG	10/19/16 VHG	11/9/16 VHG	11/30/16 VHG	1/5/17 VHG	2/3/17 VHG	Median all dates
75	Pool#1	D1								0.17	0.18	0.17	0.30	0.01	0.17
50	Pool#1	D1								-0.02	0.01	-0.01	-0.01	0.00	-0.01
30	Pool#1	D1								-0.02	0.01	-0.01	-0.01	0.00	-0.01
75	Pool#2	D1	0.00	-0.01	0.00	-0.01	-0.03	0.00	-0.02	0.00	0.00	0.00	0.15	0.00	0.00
50	Pool#2	D1	-0.02	-0.01	0.03	-0.02	-0.05	-0.01	-0.04	-0.01	0.00	-0.01	-0.02	0.00	-0.01
25	Pool#2	D1								-0.04	-0.02	-0.04	-0.05	-0.01	-0.04
75	Pool#3	D1								-0.03	0.00	0.00	0.00	0.00	0.00
50	Pool#3	D1								-0.04	0.00	-0.01	-0.02	0.00	-0.01
30	Pool#3	D1								-0.05	0.00	-0.02	-0.01	0.00	-0.01
75	Pool#1	C1					-0.28	-0.27	-0.13	-0.34	0.10	0.04	0.07		-0.13
50	Pool#1	C1								0.19	0.14	0.11	0.12		0.13
75	Pool#2	C1					0.03	-0.01	0.08	0.17	0.10	0.08	0.09		0.08
50	Pool#2	C1					-0.17	-0.18	0.05	0.26	0.18	0.16	0.12		0.12
30	Pool#2	C1					-0.04	-0.09	0.28	0.63	-0.55	0.35	0.25		0.25

Table 13. VHG data for each piezometer with the "above debris jam" geomorphic feature for all sampling dates. A blank cell means either that the piezometer data could not be collected or early data was not accurate due to slow recharge in the piezometer.

Depth (cm)	Nest	Reach	8/11/16 VHG	8/18/16 VHG	8/22/16 VHG	8/31/16 VHG	9/7/16 VHG	9/14/16 VHG	9/28/16 VHG	10/19/16 VHG	11/9/16 VHG	11/30/16 VHG	1/5/17 VHG	2/3/17 VHG	Median all dates
75	ADJ#1	P1	-0.15	-0.22	-0.17	-0.20	-0.18	-0.22	-0.39	-0.24	-0.20	-0.21	-0.18	0.00	-0.20
50	ADJ#1	P1	-0.16	-0.16	-0.15	-0.15	-0.12	-0.12	-0.19	-0.27	-0.23	-0.23	-0.32	-0.01	-0.16
25	ADJ#1	P1	-0.20	-0.24	-0.20	-0.21	-0.18	-0.21	-0.29	-0.37	-0.32	-0.24	-0.41	0.03	-0.23
75	ADJ#2	P1	0.02	-0.10	-0.09	-0.13	-0.12	-0.14	-0.20	-0.04	-0.04	-0.07	0.08	0.01	-0.08
50	ADJ#2	P1	0.09	0.13	0.18	0.10	0.16	0.12	0.15	0.35	0.20	0.09	0.23	0.02	0.14
75	ADJ#1	A1	0.01	0.00	0.01	0.00	0.02	0.00	-0.01						0.00
50	ADJ#1	A1	0.03	0.01	0.01	-0.01	-0.01	-0.01	-0.01						-0.01
30	ADJ#1	A1	0.03	-0.01	0.02	-0.01	0.04	-0.01	0.01						0.01
75	ADJ#2	A1	-0.08	-0.09	-0.10	-0.10	-0.11	-0.09	0.06	-0.03	-0.04	-0.03	-0.02	0.00	-0.06
50	ADJ#2	A1		-0.07	-0.11	-0.13	-0.12	-0.13	-0.07	-0.04	-0.03	-0.02	-0.02	0.00	-0.07
30	ADJ#2	A1	-0.05	-0.01	-0.11	-0.15	-0.12	-0.11	-0.01	-0.01	-0.02	-0.04	-0.07	0.00	-0.05
75	ADJ#2	R2					-0.46	-0.42	-0.41	0.08	-0.29	-0.23	-0.12		-0.29
50	ADJ#2	R2	-0.01		-0.03	-0.03	-0.02	-0.04	-0.02	-0.01	-0.01	0.10	-0.01		-0.01
30	ADJ#2	R2	1.15		1.28	1.26	1.00	1.06	-0.01	-0.02	0.01	-0.03	0.01		0.50

Table 14. Averages and medians of VHG data for each piezometer with the "below debris jam" geomorphic feature for all sampling dates. A blank cell means either that the piezometer data could not be collected or early data was not accurate due to slow recharge in the piezometer.

Depth (cm)	Nest	Reach	8/11/16 VHG	8/16/16 VHG	8/24/16 VHG	8/30/16 VHG	9/6/16 VHG	9/13/16 VHG	10/17/16 VHG	11/8/16 VHG	11/30/16 VHG	1/5/17 VHG	1/20/17 VHG	2/3/17 VHG	Median all dates
75	BDJ#1	R2				-0.76	-0.79	-0.75	-0.85	-0.80	-0.80	-0.76	-0.69		-0.78
50	BDJ#1	R2	-0.01	0.02	-0.02	-0.02	-0.04	-0.04	-0.04	-0.02	-0.04	-0.02	-0.02		-0.02
30	BDJ#1	R2	0.00	0.00		0.00	0.00	0.00	-0.06	-0.05	-0.03	-0.01	-0.05		-0.01
75	BDJ#1	A1	-0.05	-0.06	0.01	0.03	0.07	0.01	-0.02	-0.03	0.00	0.01	0.12	0.00	0.01
50	BDJ#1	A1	-0.20	-0.35	-0.05	-0.03	-0.02	-0.02	-0.04	-0.06	-0.03	-0.03	0.08	0.00	-0.03
30	BDJ#1	A1	-0.04	0.31	-0.02	-0.01	-0.04	-0.04	0.00	-0.03	0.00	-0.02	-0.01	0.00	-0.02
75	BDJ#2	A1	-0.03	-0.02	-0.26	-0.21	-0.15	-0.11	-0.08	-0.18	-0.10	-0.07	-0.06	0.01	-0.09
50	BDJ#2	A1	-0.04	-0.05	-0.01	-0.02	0.00	0.01	0.19	-0.05	-0.04	-0.04	-0.05	0.00	-0.03
30	BDJ#2	A1	-0.02	-0.03	-0.04	-0.01	0.01	0.02	0.00	-0.06	-0.05	-0.02	-0.04	0.00	-0.02
75	BDJ#1	P1	0.02	-0.05	-0.02	-0.05	-0.01	-0.05	-0.14	-0.02	0.00	-0.04	-0.02	0.00	-0.02
50	BDJ#1	P1	0.00	-0.02	-0.02	-0.05	-0.01	-0.01	-0.02	0.00	0.00	0.00	-0.01	0.00	-0.01
25	BDJ#1	P1	-0.48	-0.06	-0.02	-0.07	-0.01	-0.01	0.00	-0.04	0.01	-0.02	-0.04	0.00	-0.02
75	BDJ#2	P1	0.07	0.03	0.06	0.01	0.03	-0.02	-0.07	-0.01	-0.04	-0.06	-0.05	0.01	0.00
50	BDJ#2	P1	-0.56	-0.01	-0.01	-0.07	-0.02	-0.05	0.00	-0.03	-0.05	-0.02	0.12	0.00	-0.02
25	BDJ#2	P1	-0.01	-0.04	-0.05	-0.09	-0.02	-0.01	-0.05	-0.06	0.00	-0.02	-0.05	0.00	-0.03

Table 15. Averages and medians of VHG data for each piezometer with the "top of meander bend" geomorphic feature for all sampling dates. A blank cell means either that the piezometer data could not be collected or early data was not accurate due to slow recharge in the piezometer.

Depth (cm)	Cluster	Site	8/11/16 VHG	8/16/16 VHG	8/24/16 VHG	8/30/16 VHG	9/6/16 VHG	9/13/16 VHG	10/17/16 VHG	11/8/16 VHG	11/30/16 VHG	1/5/17 VHG	1/20/17 VHG	2/3/17 VHG	Median all dates
75	TOM	P1	-0.04	-0.06	-0.09	-0.09	-0.09	-0.12	-0.22	-0.13	-0.13	-0.13	-0.12	0.00	-0.11
50	TOM	P1	0.63	-0.02	0.04	-0.03	0.01	-0.01	0.01	0.00	0.00	0.00	0.14	0.00	0.00
25	TOM	P1	-0.06	0.01	-0.04	-0.05	-0.01	0.00		-0.01	0.00	-0.02	-0.02	0.00	-0.01
75	TOM	A1					-0.07	-0.05	-0.04	-0.04	-0.06	-0.02	0.00	0.02	0.00	-0.04
50	TOM	A1	-0.04	-0.01	-0.01	-0.01	-0.02	-0.02	0.12	0.00	-0.01	-0.04	-0.01	0.00	-0.01
30	TOM	A1	-0.03	0.00	-0.01	-0.03	-0.01	-0.02	-0.02	0.01	-0.02	-0.01	0.00	0.00	-0.01

Table 16. Averages and medians of VHG data for each piezometer with the "bottom of meander bend" geomorphic feature for all sampling dates. A blank cell means either that the piezometer data could not be collected or early data was not accurate due to slow recharge in the piezometer.

Depth (cm)	Nest	Reach	8/11/16 VHG	8/16/16 VHG	8/24/16 VHG	8/30/16 VHG	9/6/16 VHG	9/13/16 VHG	10/17/16 VHG	11/8/16 VHG	11/30/16 VHG	1/5/17 VHG	1/20/17 VHG	2/3/17 VHG	Median of all dates
75	BOM	P1	-0.05	-0.11	-0.09	-0.13	-0.13	-0.28	-0.26	-0.09	-0.09	-0.15	-0.08	0.01	-0.10
50	BOM	P1	0.05	0.01	0.02	-0.01	0.03	-0.05	0.00	0.00	0.00	-0.02	0.09	0.00	0.00
25	BOM	P1	-0.04	-0.04	-0.05	-0.02	-0.05	-0.02	-0.04	-0.01	0.01	0.00	-0.06	0.00	-0.03
75	BOM	A1			0.00	0.00	0.03	0.04	0.03	-0.23	0.12	0.06	0.09	0.01	0.03
50	BOM	A1			0.05	0.07	0.09	0.05	0.04	-0.24	0.03	0.15	0.10	0.01	0.05
25	BOM	A1			-0.02	-0.02	-0.01	0.07	0.12	-0.38	-0.07	-0.23	-0.02	0.00	-0.02

Table 17. Averages and medians of VHG data for each piezometer with the "above gravel bed" geomorphic feature for all sampling dates. A blank cell means either that the piezometer data could not be collected or early data was not accurate due to slow recharge in the piezometer.

Depth (cm)	Nest	Reach	8/11/16 VHG	8/16/16 VHG	8/24/16 VHG	8/30/16 VHG	9/6/16 VHG	9/13/16 VHG	10/17/16 VHG	11/8/16 VHG	11/30/16 VHG	1/5/17 VHG	1/20/17 VHG	2/3/17 VHG	Median of all dates
60	AGB#1	D1	0.01		0.06	0.00	0.03	0.01		0.00	0.02	0.05	0.10	0.01	0.01
45	AGB#1	D1	0.00	0.01	-0.02	-0.02	0.01	0.00	-0.02	-0.01	0.01	-0.03	-0.02	0.00	-0.01
30	AGB#1	D1	0.00	-0.02	-0.01	-0.04	-0.01	-0.01	0.00	-0.02	-0.02	-0.01	-0.04	0.00	-0.01
50	AGB#2	D1	-0.01	-0.01	-0.02	-0.02	0.00	-0.01	0.01	-0.02	0.00	-0.01	-0.01	0.00	-0.01
35	AGB#2	D1	-0.01	0.00	-0.02	-0.04	0.00	0.00	0.28	0.00	0.00	-0.01	-0.03	0.00	0.00
20	AGB#2	D1	-0.02	-0.03	-0.06	-0.06	0.00	0.00	0.00	0.00	-0.02	0.02	-0.03	0.00	-0.01

Table 18. Averages and medians of VHG data for each piezometer with the "between gravel bed" geomorphic feature for all sampling dates. A blank cell means either that the piezometer data could not be collected or early data was not accurate due to slow recharge in the piezometer.

Depth (cm)	Nest	Reach	8/11/16 VHG	8/16/16 VHG	8/24/16 VHG	8/30/16 VHG	9/6/16 VHG	9/13/16 VHG	10/17/16 VHG	11/8/16 VHG	11/30/16 VHG	1/5/17 VHG	1/20/17 VHG	Median all dates
75	GB#1	R2	0.32	0.12	0.02	0.00	0.00	-0.01	0.05	0.02	0.06	0.28	0.09	0.05
50	GB#1	R2			0.10	0.07	0.10	0.06				-0.02	0.06	0.07
30	GB#1	R2	-0.05	-0.02	-0.03	-0.02	-0.02	-0.01	-0.02	-0.01	0.01	0.00	-0.03	-0.02
75	GB#2	R2	0.00	0.00	0.00	0.00	0.00	-0.01	-0.03	-0.02	0.00	-0.01	-0.01	0.00
50	GB#2	R2	0.00		0.00	0.00	0.00	-0.04	0.06	-0.04	-0.04	-0.03	-0.01	-0.01
30	GB#2	R2	-0.05	-0.03	-0.03	0.04	-0.22	0.00	-0.05	-0.04	-0.01	-0.03	-0.01	-0.03
75	GB#3	R2	0.00	-0.01	-0.01	0.00	0.00	0.00	0.00	-0.02	0.00	-0.01	0.00	0.00
50	GB#3	R2	0.00	-0.02	-0.02	-0.02	-0.01	-0.02	-0.02	-0.02	-0.01	-0.02	-0.01	-0.02
30	GB#3	R2				0.00	0.00	0.00	-0.04	-0.04	-0.02	-0.03	-0.01	-0.02
75	GB#4	R2			0.10	0.07	0.04	0.00	0.07	0.00	0.00	0.08	0.03	0.04
50	GB#4	R2	-0.04	-0.01	-0.01	-0.02	-0.02	-0.01	-0.01	-0.01	-0.01	-0.01	-0.01	-0.01
30	GB#4	R2	-0.01	-0.01	-0.06		-0.03	-0.02	-0.04	0.00	-0.08	0.02	-0.02	-0.02

Table 19. Averages and medians of VHG data for each piezometer with the "below gravel bed" geomorphic feature for all sampling dates. A blank cell means either that the piezometer data could not be collected or early data was not accurate due to slow recharge in the piezometer.

Depth (cm)	Nest	Reach	8/11/16 VHG	8/16/16 VHG	8/24/16 VHG	8/30/16 VHG	9/6/16 VHG	9/13/16 VHG	10/17/16 VHG	11/8/16 VHG	11/30/16 VHG	1/5/17 VHG	1/20/17 VHG	2/3/17 VHG	Median of all dates
40	BGB#1	D1	0.06			0.16	0.22	0.21		-0.04	-0.02	0.06	-0.03	0.00	0.06
30	BGB#1	D1	0.00	-0.03	-0.04	-0.01	-0.03	-0.01		-0.02	0.01	-0.03	0.06	0.00	-0.01
20	BGB#1	D1	0.00	-0.05	-0.08	-0.05	-0.03	-0.03		-0.05	-0.02	-0.05	-0.03	0.00	-0.03
75	BGB#2	D1	0.20	0.04	0.02	0.00	0.01	-0.01			0.01	0.03	0.00	0.00	0.01
50	BGB#2	D1	0.02	0.02	0.04	0.00	0.01	0.01	0.01	-0.04	0.01	0.02	-0.01	0.00	0.01
25	BGB#2	D1	0.00	-0.01	-0.01	-0.04	-0.01	0.00		-0.06	0.01	-0.02	-0.04	0.00	-0.01

4.2 Hydraulic conductivity

Over 100 slug tests were performed on piezometers and monitoring wells in five study reaches within Reedy Creek. While slug tests were performed for every piezometer and well, the t_{37} data could not be obtained for every piezometer and well. Only the upland well at study reach D1 could not be recorded. The well did not respond as expected during slug testing and a t_{37} could not be reported. Table 25 displays the number of piezometers within each reach that recovered too slowly to acquire t_{37} data. Overall, the reach with the largest number of responsive piezometers was R2, with four piezometers out of 18 that could not be used to determine t_{37}. The largest number of piezometers that had tests too slow to obtain the t_{37} data were in the P1 reach, with 13 unresponsive piezometers out of 21 total piezometers. The slug testing results showed a vertical trend for *K*. The shallow sediments exhibited a higher *K* than the deeper sediments. The piezometers' *K* estimates fall within the range of fluvial deposits (silt, sand and gravel; Hiscock and Bense, 2014).

4.2.1 R2

Overall the piezometers' *K* ranges over two orders of magnitude. The piezometers that had a t_{37} exhibited a median *K* of 1.56 m/day. The riparian well of R2 exhibited a *K* of 1.34 m/day, while the upland well exhibited a *K* of 36.46 m/day (Table 20).

4.2.2 A1

Overall the piezometers' *K* ranges over two orders of magnitude. *K* ranges from the order of 10^{-1} m/day to 10^{1} m/day. The median *K* for the piezometers is 7.65 m/day The A1 upland well exhibited a *K* of 1.05 m/day. The A1 riparian well exhibited a *K* of 9.07 m/day (Table 21).

4.2.3 C1

Piezometers located within C1 exhibited *K* that ranged from 7.65 to 11.49 m/day. The upland well had a *K* of 72.75 m/day and the riparian well had a *K* 203.90 m/day (Table 22).

4.2.4 D1

The piezometers show a median *K* of 10.54 m/day and the *K* ranges over two orders of magnitude from 0.18 to 38.19 m/day. The riparian well exhibited a *K* of 0.02 m/day (Table 23).

4.2.5 P1

The piezometers' *K* spans a range of three orders of magnitude from 0.26 m/day to 114.91 m/day. The median *K* for the piezometers was 1.56 m/day. The P1 upland well exhibited a *K* of 6.14 m/day. The P1 riparian well exhibited a *K* of 1.90 m/day (Table 24). P1 exhibited the largest *K* range of all the study reaches, showing diversity among grain sizes.

4.3 Radon

Overall, stream water exhibited the lowest radon-222 with a range of 12-37 pCi/L across all five study reaches. Well water exhibited the highest radon-222 (excluding one piezometer sample) with a range of 170-647 pCi/L. Piezometer water covered a larger range than either stream water or well water, with a range of 29-707 pCi/L.

4.3.1 R2

The stream concentration of Rn-222 was 19 pCi/L. The upland well concentration was 647 pCi/L. The riparian well concentration was 288 pCi/L. Only one piezometer was sampled in R2 due to lack of rapid recharge in other piezometers. The piezometer "GB#3 25cm" exhibited a concentration of 272 pCi/L. Rn-222 sampling took place on 6/22/17 (Table 20).

4.3.2 A1

The stream concentration of Rn-222 was 12 pCi/L. The upland well concentration was 194 pCi/L. The riparian well concentration was 248 pCi/L. None of the available piezometers were able to recharge rapidly enough to produce a radon sample. Rn-222 sampling took place on 6/22/17 (Table 21).

4.3.3 C1

The stream concentration of Rn-222 was 37 pCi/L. The upland concentration was 248 pCi/L. Two piezometers were used for radon sampling. Piezometer "AGB 25cm" had a

concentration of 707 pCi/L. Piezometer “BGB 25cm” had a concentration of 126 pCi/L Rn-222 sampling took place on 6/8/17 (Table 22).

4.3.4 D1

The stream concentration of Rn-222 was 25 pCi/L. The upland concentration was 208 pCi/L. Two piezometers were sampled. Piezometer “BGB#2 25cm” had a concentration of 30 pCi/L. Piezometer “AGB#2 25cm” had a concentration of 118 pCi/L. Rn-222 sampling took place on 6/1/17 (Table 23).

4.3.5 P1

The stream concentration of Rn-222 was 34 pCi/L. The upland concentration was 170 pCi/L. Two piezometers were sampled. Piezometer “ADJ#1 25cm” had a concentration of 38 pCi/L. Piezometer “ADJ#1 50cm” had a concentration of 29 pCi/L. Rn-222 sampling took place on 5/18/17 (Table 24).

Table 20. Reach R2 Hvorslev Calculations and Horizontal Specific Discharge. n/a represents values in which the equation was not applicable for the cell. Slug tests were performed 3/30/17. Rn-222 sampling took place 6/22/17. A positive *dh/dz* and q_x means that the groundwater is flowing toward the stream. Cell "*dh/dx* upland well to piezometer" and "q_x upland to piezometers" refers to the direction of flow.

Piezometer or well	Depth (cm)	t_{37} (s)	*K* (m/d)	Water level *(m above sea level)*	*dh/dx* upland well to piezometer	*dh/dx* riparian well to piezometer	q_x Upland to piezometer (m/day)	q_x Riparian to piezometer (m/day)	Rn-222 (pCi/L)
R2GB#1	25	180	0.64	195.69	0.02	0.02	0.01	0.01	
R2GB#2	25	75	1.53	195.69	0.02	0.02	0.04	0.03	
R2GB#2	50	400	0.29	195.73	0.02	0.02	0.01	0.01	
R2GB#3	25	1300	0.09	195.64	0.03	0.03	0.00	0.01	272
R2GB#3	50	13	8.81	195.65	0.03	0.03	0.23	0.66	
R2GB#3	75	10	11.49	195.60	0.03	0.03	0.31	0.32	
R2GB#4	25	310	0.37	195.73	0.02	0.05	0.01	0.02	
R2GB#4	50	1.5	76.46	195.74	0.02	0.05	1.77	12.27	
R2BDJ	25	72	1.59	195.94	0.01	0.01	0.02	0.01	
R2ADJ	25	41	2.80	195.69	0.02	0.01	0.05	0.03	
R2 Riparian Well		815	1.34	196.20			n/a		647
R2 Upland Well		30	36.46	196.66	0.01		0.39	n/a	288
Average of R2 piezometers			10.37				0.24	1.33	
Range of R2 piezometers			76.38				1.77	12.27	
Stream									19

Table 21. Reach A1 Hvorslev Calculations and Horizontal Specific Discharge. n/a represents values in which the equation was not applicable for the cell. Slug tests were performed 3/30/17. Rn-222 sampling took place 6/22/17. A positive *dh/dz* and q_x means that the groundwater is flowing toward the stream. Cell "*dh/dx* upland well to piezometer" and "q_x upland to piezometers" refers to the direction of flow.

Piezometer or well	Depth (cm)	t_{37} (s)	*K* (m/day)	Water level *(m above sea level)*	*dh/dx* upland well to piezometer	*dh/dx* riparian well to piezometer	q_x Riparian to piezometer (m/day)	q_x Upland to piezometer (m/day)	Rn-222 (pCi/L)
A1 BDJ#2	25	15	7.65	195.81	0.02	0.02	0.17	0.12	
A1 BDJ#2	50	13	8.81	195.84	0.01	0.02	0.17	0.13	
A1 ADJ #2	25	8	14.34	195.81	0.01	0.01	0.13	0.13	
A1 TOM	25	660	0.17	195.64	0.03	0.14	0.02	0.00	
A1 TOM	50	121	0.95	195.66	0.03	0.14	0.13	0.02	
A1 Upland well		850	1.05	196.71	0.06				194
A1 Riparian well		98	9.07	196.40		-0.06		n/a	248
Average of A1 piezometers			6.00				0.12	0.08	
Range of A1 piezometers			14.17				1.82	0.13	
Stream									12

Table 22. Reach C1 Hvorslev Calculations and Horizontal Specific Discharge. n/a represents values in which the equation was not applicable for the cell. Slug tests were performed 3/23/17. Rn-222 sampling took place 6/8/17. A positive *dh/dz* and q_x means that the groundwater is flowing toward the stream. Cell "*dh/dx* upland well to piezometer" and "q_x upland to piezometers" refers to the direction of flow.

Piezometer or well	**Depth (cm)**	t_{37} **(s)**	***K*** **m/day**	**Water level *(m above sea level)***	***dh/dx*** **upland well to piezometer**	***dh/dx*** **riparian well to piezometer**	q_x **Upland to piezometers (m/day)**	q_x **Riparian to piezometers (m/day)**	**Rn-222 (pCi/L)**
AGB	25	15	7.65	200.48	-0.013	-0.05	-0.10	-0.37	707
BGB	25	10	11.49	200.00	-0.003	-0.06	-0.04	-0.66	126
Riparian well		5	203.90	199.35			n/a		
Upland well		14	72.75	200.00	0.02		1.75	n/a	248
Average of C1 piezometers			9.59				-0.07	-0.51	
Range of C1 piezometers			3.84				0.06	0.29	
Stream									37

Table 23. Reach D1 Hvorslev Calculations and Horizontal Specific Discharge. n/a represents values in which the equation was not applicable for the cell. Slug tests were performed 3/6/17. Rn-222 sampling took place 6/1/17. A positive *dh/dz* and q_x means that the groundwater is flowing toward the stream. Cell "*dh/dx* upland well to piezometer" and "q_x upland to piezometers" refers to the direction of flow.

Piezometer or well	**Depth (cm)**	**t_{37} (s)**	***K* (m/day)**	***Water level (m above sea level)***	***dh/dx* upland well to piezometer**	***dh/dx* riparian well to piezometer**	**q_x Upland to piezometer (m/day)**	**q_x Riparian to piezometers (m/day)**	**Rn-222 (pCi/L)**
Pool #1	25	3	38.19	199.21	0.01	0.01	0.56	0.39	
Pool #1	50	9	12.70	199.20	0.01	0.01	0.19	0.13	
BGB #1	75	625	0.18	199.72	0	0	0.00	0.00	
AGB #1	25	41	2.80	199.84	0	-0.01	0.00	-0.02	
Pool #2	25	31	3.70	200.07	-0.01	-0.02	-0.04	-0.06	
Pool #2	50	3	38.19	200.10	-0.01	-0.02	-0.46	-0.71	
Pool #2	75	8	14.34	200.07	-0.01	-0.02	-0.15	-0.25	
Pool #3	25	7	16.42	199.62	0.01	0	0.10	-0.01	
Pool #3	50	4	28.68	199.71	0	0	0.07	-0.12	
Pool #3	75	16	7.17	199.69	0	0	0.03	-0.02	
BGB #2	25	12	9.59	200.10	-0.02	-0.03	-0.16	-0.25	30
AGB #2	25	10	11.49	200.42	-0.03	-0.04	-0.38	-0.49	118
AGB #2	50	12	9.59	200.09	-0.02	-0.03	-0.16	-0.24	
AGB #2	75	40	2.87	200.06	-0.01	-0.02	-0.04	-0.07	
D1 Riparian Well		2150	0.02	199.61			n/a		
D1 Upland Well		n/a	n/a	199.77	0.01		n/a	n/a	208
Average of D1 Piezometers			14.00				-0.03	-0.12	
Range of D1 Piezometers			38.02				1.02	1.10	
Stream									25

Table 24. Reach P1 Hvorslev Calculations and Horizontal Specific Discharge. n/a represents values in which the equation was not applicable for the cell. Slug tests were performed 3/16/17. Rn-222 sampling took place 5/18/17. A positive *dh/dz* and q_x means that the groundwater is flowing toward the stream. Cell "*dh/dx* upland well to piezometer" and "q_x upland to piezometers" refers to the direction of flow.

Piezometer or well	Depth (cm)	t_{37} (s)	*K* m/day	Water level *(m above sea level)*	*dh/dx* upland well to piezometer	*dh/dx* riparian well to piezometer	q_x Upland to piezometers (m/day)	q_x Riparian to piezometers (m/day)	Rn-222 (pCi/L)
TOM	25	1	114.91	200.68	-0.02	-0.01	-2.26	-1.24	
ADJ#1	25	64	1.79	200.63	-0.02	-0.02	-0.04	-0.03	38
ADJ#1	50	86	1.33	200.57	-0.02	-0.01	-0.03	-0.02	29
BDJ#1	25	143	0.80	200.47	-0.01	-0.01	-0.01	-0.01	
BDJ#1	75	445	0.26	200.51	-0.02	-0.01	0.00	0.00	
DJD#2	25	8	14.34	200.69	-0.02	-0.02	-0.30	-0.29	
Riparian well		535	1.90	200.34			n/a		
Upland well		178	6.14	199.73	-0.02		-0.11		170
Average of P1 piezometers			22.20				-0.44	-0.27	
Range of P1 piezometers			114.91				2.26	1.24	
Stream									34

Table 25. Numbers of piezometers that responded too slowly for Hvorslev method and for which t_{37}, K, and q_x and q_z are not reported.

Reach	**Total**	**25cm**	**50cm**	**75cm**
A1	7	1	2	4
R2	4	0	1	3
P1	13	1	6	6
C1	9	2	4	3
D1	6	0	3	3
All	39	4	16	19

4.4 Vertical component of specific discharge (q_z)

In terms of vertical specific discharge (q_z), a positive value indicates vertical movement in the up direction. A negative q_z indicates vertical movement in the down direction. The data found the q_z averages were greatly skewed and did not accurately represent the reaches/piezometers.

4.4.1 Specific discharge (q_z) at the five study reaches for each individual reading date

4.4.1.1 Reach R2

There were 10 piezometers with high *K,* encompassing a total of 18 piezometers. The reach-wide median upward q_z ranged from <0.00 to -0.03 m/day. The day of the largest median apparent downwelling was 11/8/16. There was no reach-wide median upward q_z on any dates. Dates that had zero flux were 8/11/16 and 8/30/16. The reach-wide maximum q_z ranged from 0.00 to 3.58 m/day. The minimum reach-wide q_z ranged from -0.47 to -2.80 m/day. R2 had a reach-wide range of q_z from 0.47 to 6.01 m/day (Figure 25,Table 26).

4.4.1.2 Reach A1

Five piezometers exhibited high *K,* encompassing a total of 18 piezometers. The reach-wide median q_z ranged from <0.00 to -0.31 m/day. The day of the largest reach-wide median apparent downwelling was 11/8/16. There was no reach-wide median upward q_z on any dates. The reach-wide maximum q_z ranged from 0.01 to 1.67 m/day. The reach-wide minimum q_z ranged from -0.15 to -2.19 m/day. A1 had a reach-wide range of q_z from 0.38 to 2.18 m/day (Figure 26, Table 27).

4.4.1.3 Reach C1

Two piezometers exhibited high *K,* encompassing a total of 11 piezometers. The reach-wide median q_z ranged from -0.02 to -0.37 m/day in the downward direction. The date with the largest downward rate was 10/19/16. The reach-wide median upward q_z was 0.02 to 0.04 m/day. The date with the largest reach-wide median upward q_z was 11/30/16. The reach-wide maximum

q_z ranged from 0.12 to 0.23 m/day. The reach-wide minimum q_z ranged from -0.08 to-0.54 m/day. C1 had a reach-wide q_z range from 0.04 to 0.43 m/day, (Figure 27, Table 28).

4.4.1.4 Reach D1

14 piezometers exhibited high *K,* encompassing a total of 20 piezometers. The reach-wide median q_z ranged from <0.00 to -0.26 m/day in the downward direction. The date with the largest median downward rate was 8/31/16. There was no reach-wide median q_z in the upward direction on any dates. The reach-wide maximum q_z ranged from 0.00 to 2.67 m/day. The reach-wide minimum q_z ranged from -0.04 to -2.10 m/day. The reach-wide range for q_z was 0.17 to 4.30 m/day, (Figure 28, Table 29).

4.4.1.5 Reach P1

Seven piezometers exhibited high *K,* encompassing a total of 20 piezometers. The reach-wide median q_z ranged from <0.00 to -0.43 m/day in the downward direction. The date with the largest reach-wide median downward rate was on 1/5/17. There was one date that had a reach-wide median q_z upward rate. This date was on 2/3/17 with a q_z of <0.01. The reach-wide maximum q_z was 0.01 to 6.76 m/day. The reach-wide minimum q_z was -7.01 to -0.37 m/day. The reach-wide q_z range was 0.58 to 10.27 m/day, (Figure 29, Table 30).

4.4.2 Specific discharge (q_z) at the five study reaches for all reading dates

4.4.2.1 Reach R2

10 piezometers exhibited high *K,* encompassing a total of 18 piezometers. The median q_z in the downward direction was >-0.01 to -0.93 m/day. The piezometer with the largest median q_z in the downward direction was "GB#4 50cm." There was only one piezometer with a median q_z in the upward direction. That piezometer is "ADJ 30cm" with a q_z of 1.41 m/day (Table 31).

4.4.2.2 Reach A1

Five piezometers exhibited high *K*, encompassing a total of 18 piezometers. The median q_z in the downward direction was >-0.01 to -0.66 m/day. The piezometer with the largest median

q_z in the downward direction was "ADJ #2 30cm." There were no piezometers with a median q_z in the upward direction (Table 32).

4.4.2.3 Reach C1

Two piezometers exhibited high *K*, encompassing a total of 11 piezometers. The median q_z in the downward direction was -0.12 to -0.31 m/day. The piezometer with the largest median q_z in the downward direction was "AGB 30cm." There were no piezometers with a median q_z in the upward direction (Table 33).

4.4.2.4 Reach D1

14 piezometers exhibited high *K*, encompassing a total of 20 piezometers. The median q_z in the downward direction was >-0.01 to -0.47 m/day. The piezometer with the largest median q_z in the downward direction was "Pool #2 50cm." The median q_z in the upward direction was 0.01 to 2.22 m/day. The piezometer with the largest median q_z in the upward direction was "Pool#1 75cm" (Table 34).

4.4.2.5 Reach P1

Seven piezometers exhibited high *K*, encompassing a total of 20 piezometers. The median q_z in the downward direction was -0.01 to -1.40 m/day for six of the piezometers. The piezometer with the largest median q_z in the downward direction was "TOM 25cm." Only one piezometer had a median q_z in the upward direction, which was "BR 75cm" with a q_z of 1.28 m/day (Table 35).

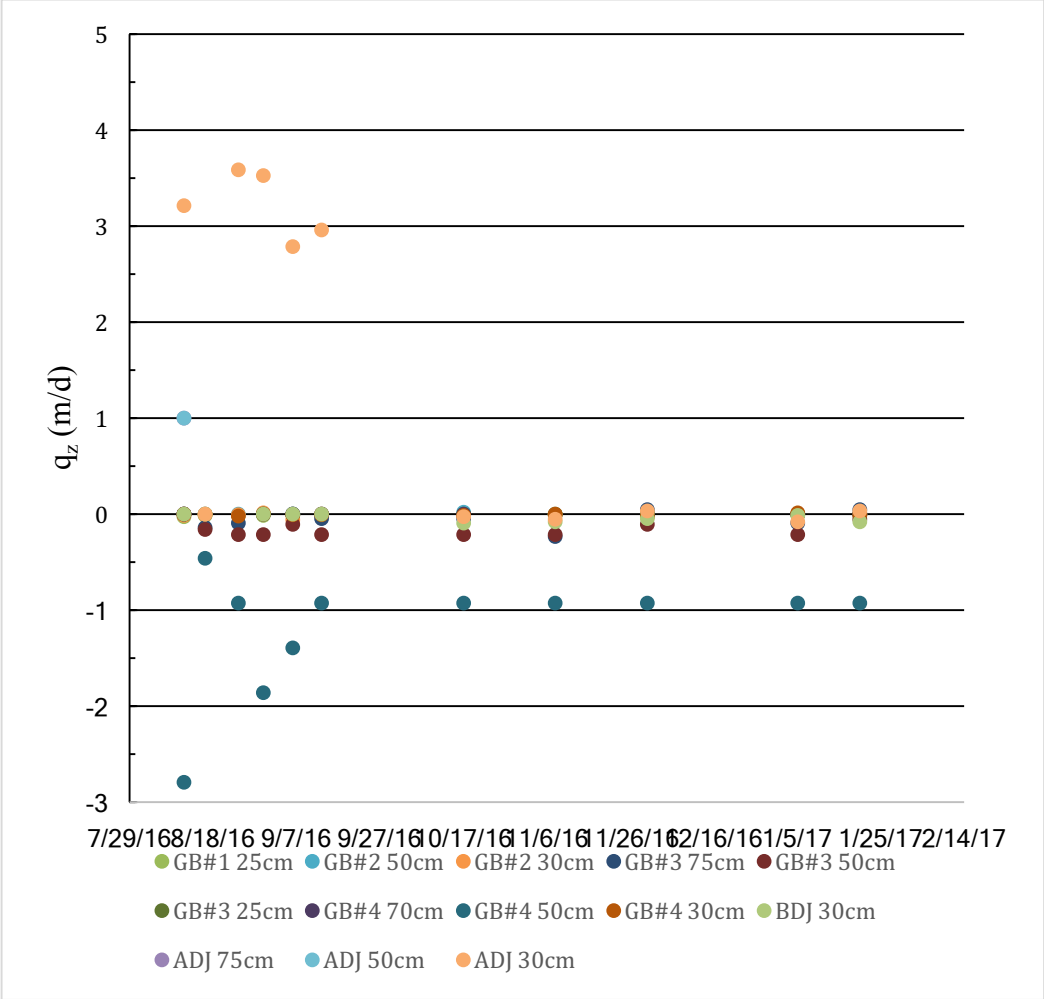

Figure 25. Reach R2 q_z from 8/11/16 to 1/20/17.

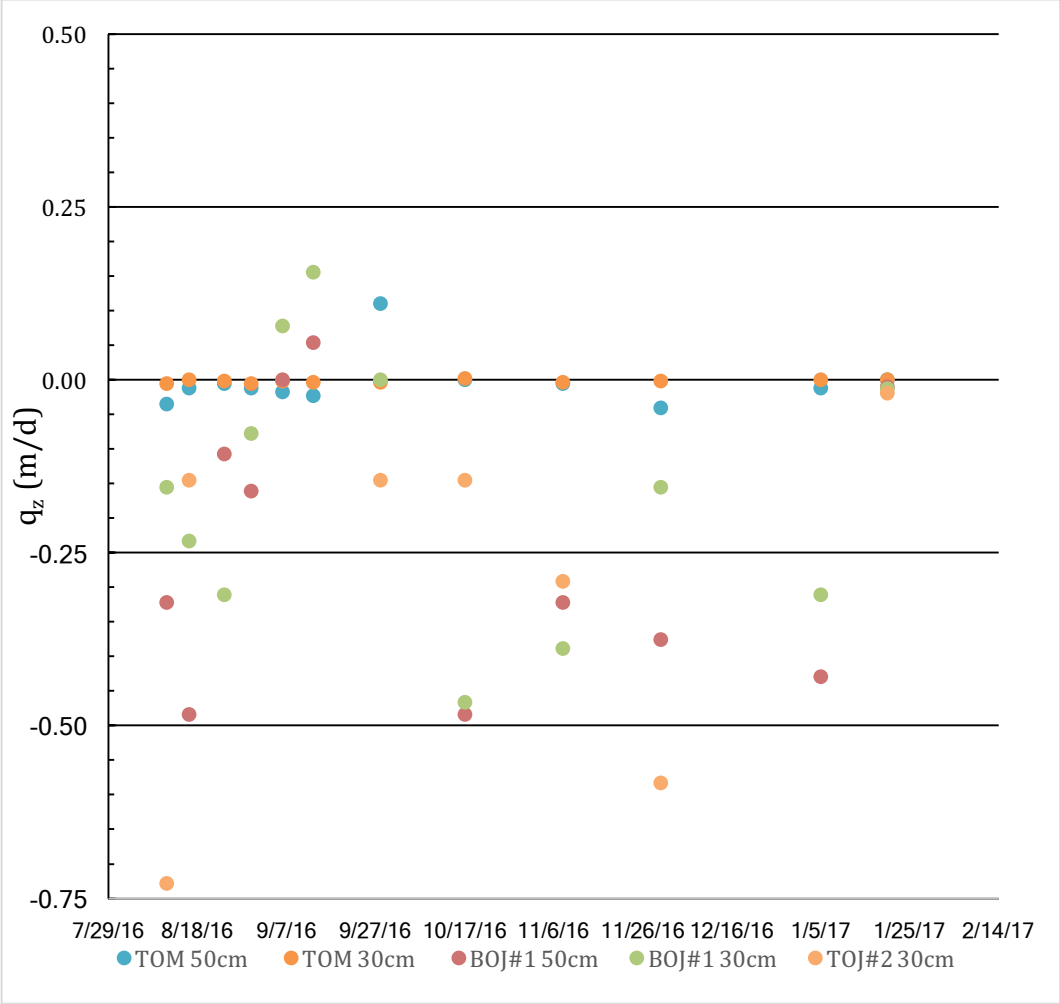

Figure 26. Reach A1 q_z from 8/11/16 to 1/20/17.

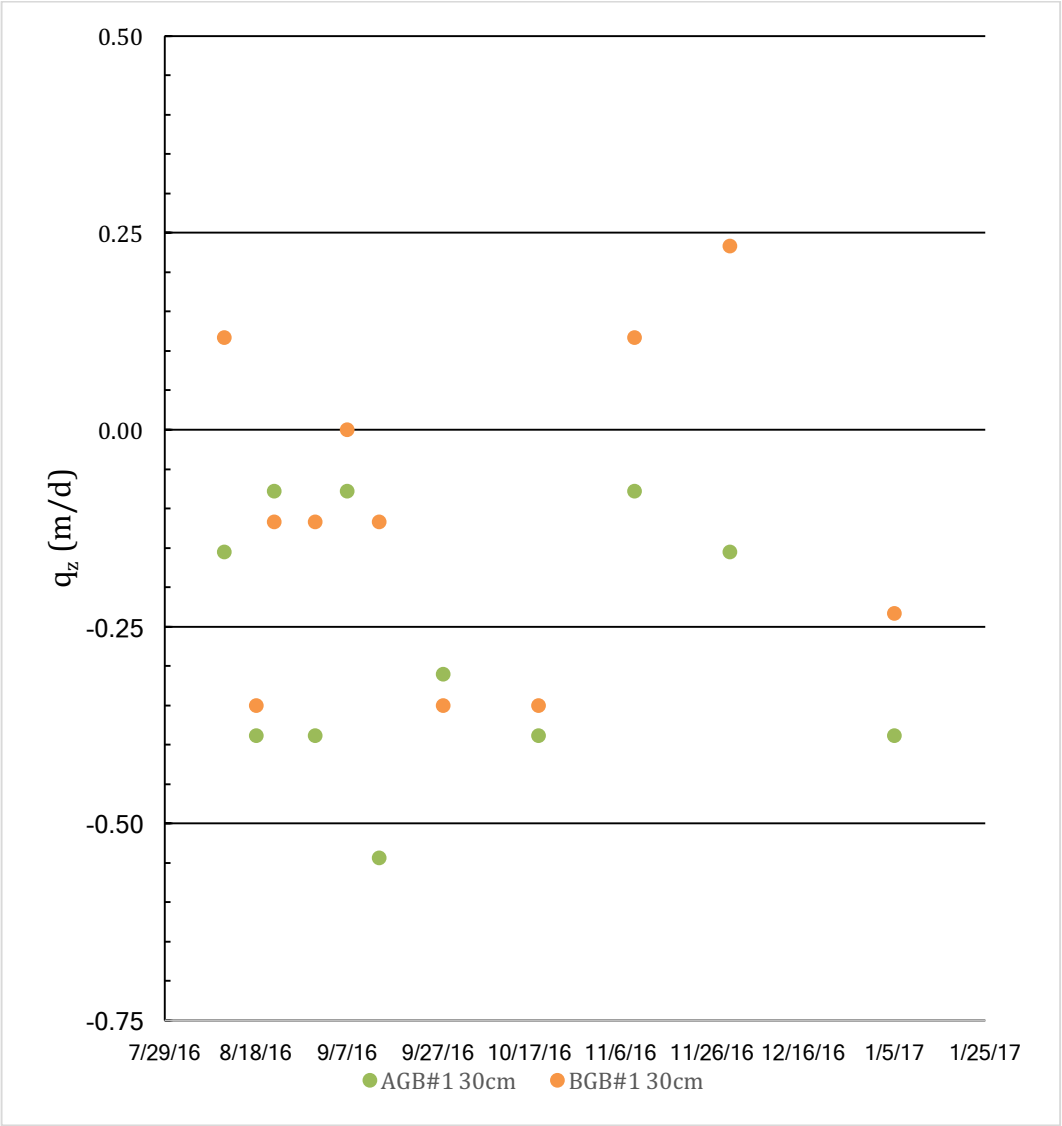

Figure 27. Reach C1 q_z from 8/11/16 to 1/5/17.

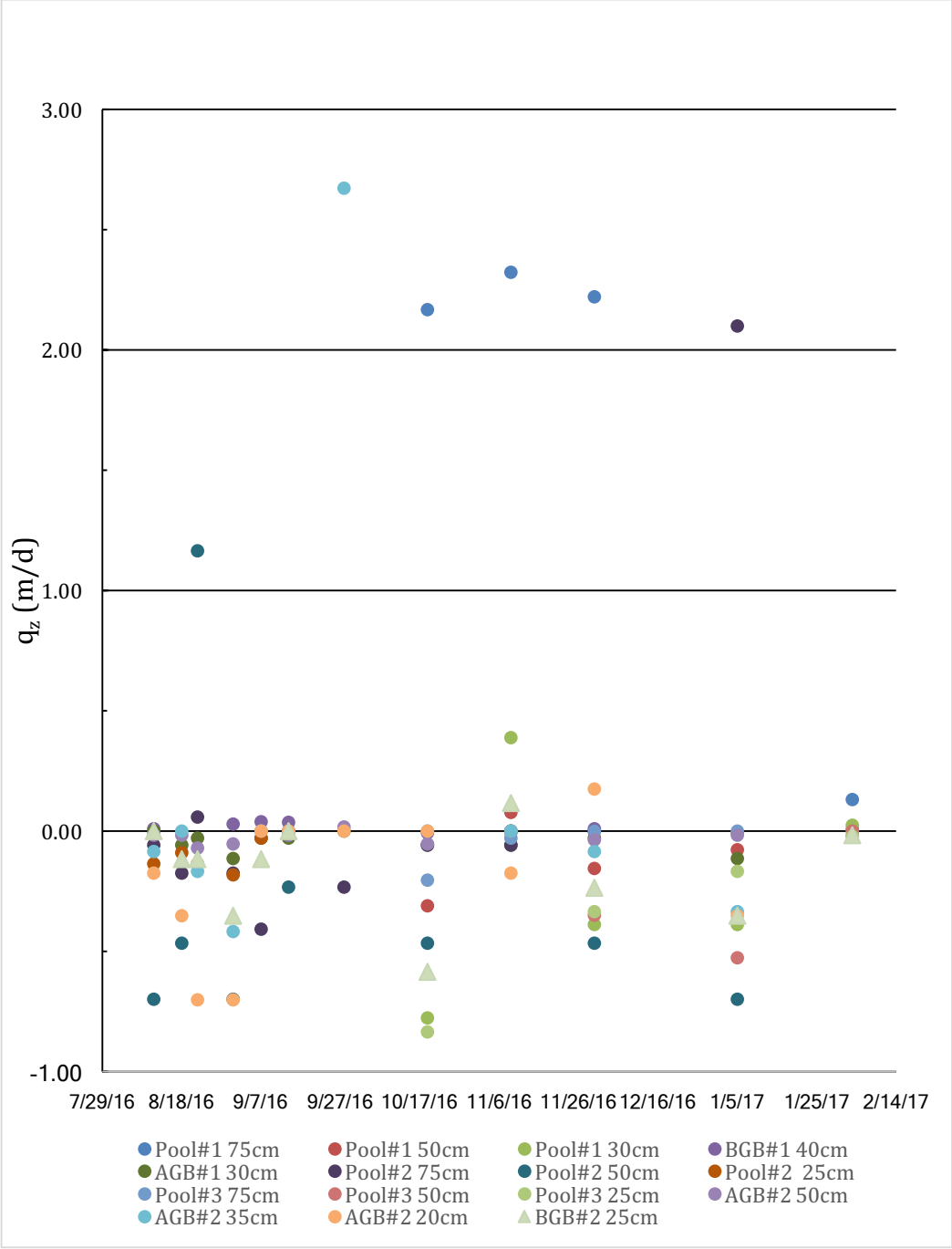

Figure 28. Reach D1 q_z from 8/11/16 to 2/3/17.

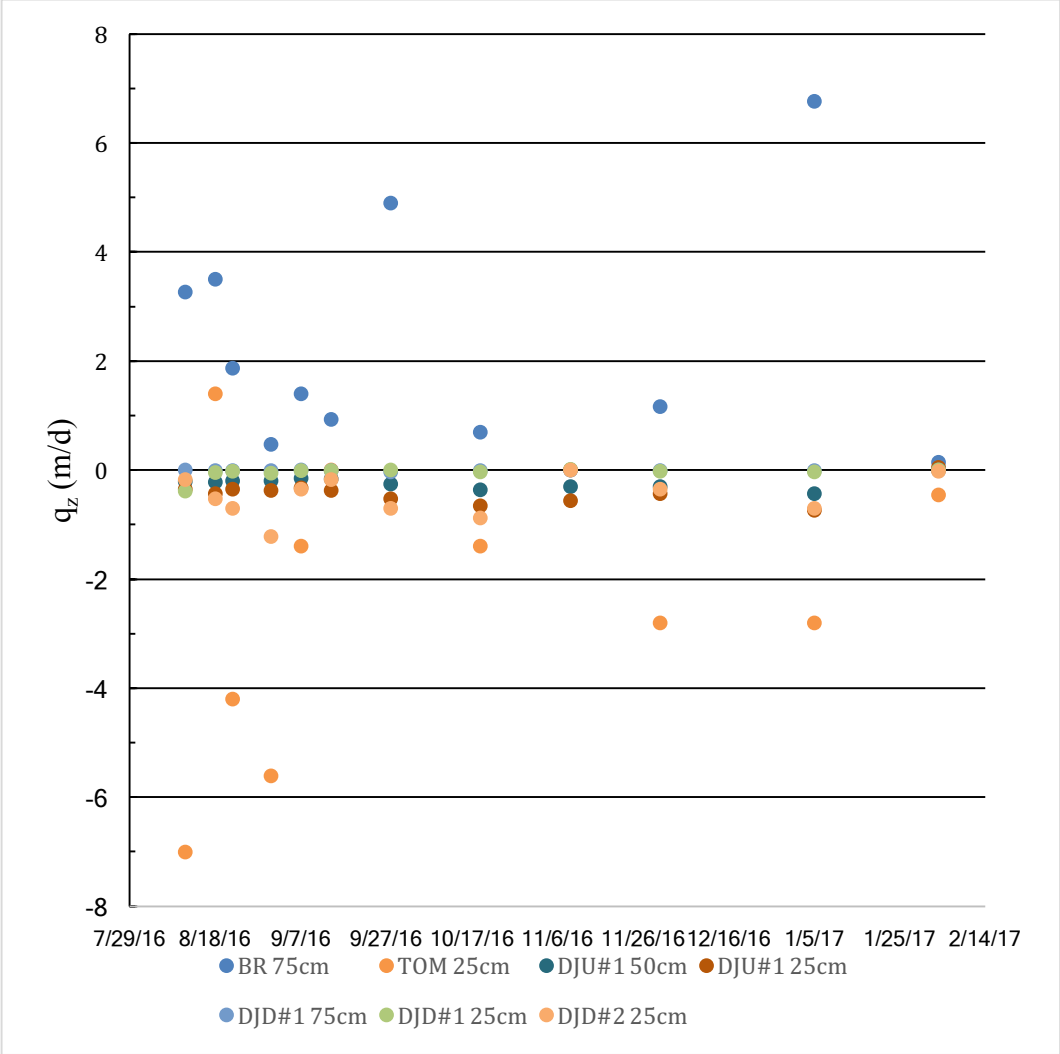

Figure 29. Reach P1 q_z from 8/11/16 to 2/3/17.

Table 26. Reach R2 q_z median, average, maximum, minimum and range values.

R2	8/11/16	8/16/16	8/24/16	8/30/16	9/6/16	9/13/16	10/17/16	11/8/16	11/30/16	1/5/17	1/20/17
	q_z (m/day)	q_z (m/day)	q_z (m/day)	q_z (m/day)	q_z (m/day)	q_z (m/day)	q_z (m/day)	q_z (m/day)	q_z (m/day)	q_z (m/day)	q_z (m/day)
Reach-wide Median	0.00	-0.01	-0.02	0.00	0.00	-0.01	-0.02	-0.03	-0.01	-0.01	0.00
Reach-wide Average	0.04	-0.11	0.29	0.16	0.12	0.17	-0.13	-0.16	-0.11	-0.14	-0.10
Reach-wide Max	3.21	0.00	3.58	3.53	2.79	2.96	0.02	0.00	0.05	0.01	0.05
Reach-wide Min	-2.80	-0.47	-0.93	-1.86	-1.40	-0.93	-0.93	-0.93	-0.93	-0.93	-0.93
Reach-wide Range	6.01	0.47	4.52	5.39	4.19	3.89	0.95	0.93	0.98	0.94	0.98

Table 27. Reach A1 q_z median, average, maximum, minimum and range of values.

A1	8/11/16	8/16/16	8/24/16	8/30/16	9/6/16	9/13/16	9/28/16	10/17/16	11/8/16	11/30/16	1/5/17	1/20/17
	q_z (m/day)	q_z (m/day)	q_z (m/day)	q_z (m/day)	q_z (m/day)	q_z (m/day)	q_z (m/day)	q_z (m/day)	q_z (m/day)	q_z (m/day)	q_z (m/day)	q_z (m/day)
Reach-wide Median	-0.16	-0.15	-0.11	-0.08	0.00	0.00	0.00	-0.15	-0.29	-0.16	-0.31	-0.01
Reach-wide Average	-0.25	-0.17	-0.41	-0.49	-0.34	-0.28	0.33	-0.22	-0.20	-0.23	-0.35	-0.01
Reach-wide Max	-0.01	0.00	0.00	-0.01	0.08	0.16	1.67	0.00	0.00	0.00	0.00	0.00
Reach-wide Min	-0.73	-0.48	-1.60	-2.19	-1.75	-1.60	-0.15	-0.48	-0.39	-0.58	-1.02	-0.02
Reach-wide Range	0.72	0.48	1.60	2.18	1.83	1.76	1.81	0.49	0.38	0.58	1.02	0.02

Table 28. Reach C1 q_z median, average, maximum, minimum and range values.

C1	8/11/16	8/18/16	8/22/16	8/31/16	9/7/16	9/14/16	9/28/16	10/19/16	11/9/16	11/30/16	1/5/17
	q_z (m/day)	q_z (m/day)	q_z (m/day)	q_z (m/day)	q_z (m/day)	q_z (m/day)	q_z (m/day)	q_z (m/day)	q_z (m/day)	q_z (m/day)	q_z (m/day)
Reach-wide Median	-0.02	-0.37	-0.10	-0.25	-0.04	-0.33	-0.33	-0.37	0.02	0.04	-0.31
Reach-wide Average	-0.02	-0.37	-0.10	-0.25	-0.04	-0.33	-0.33	-0.37	0.02	0.04	-0.31
Reach-wide Max	0.12	-0.35	-0.08	-0.12	0.00	-0.12	-0.31	-0.35	0.12	0.23	-0.23
Reach-wide Min	-0.16	-0.39	-0.12	-0.39	-0.08	-0.54	-0.35	-0.39	-0.08	-0.16	-0.39
Reach-wide Range	0.27	0.04	0.04	0.27	0.08	0.43	0.04	0.04	0.19	0.39	0.15

Table 29. Reach D1 q_z median, average, maximum, minimum and range values.

D1	8/11/16	8/18/16	8/22/16	8/31/16	9/7/16	9/14/16	9/28/16	10/19/16	11/9/16	11/30/16	1/5/17	2/3/17
	q_z (m/day)	q_z (m/day)	q_z (m/day)	q_z (m/day)	q_z (m/day)	q_z (m/day)	q_z (m/day)	q_z (m/day)	q_z (m/day)	q_z (m/day)	q_z (m/day)	q_z (m/day)
Reach-wide Median	-0.04	-0.12	-0.07	-0.26	-0.01	0.00	0.00	-0.14	0.00	-0.08	-0.17	-0.01
Reach-wide Average	-0.13	-0.17	0.02	-0.31	-0.33	-0.03	0.14	-0.17	0.17	0.01	0.18	0.00
Reach-wide Max	0.01	0.00	1.16	0.03	0.04	0.04	2.67	2.17	2.32	2.22	3.82	0.13
Reach-wide Min	-0.70	-0.47	-0.70	-0.70	-2.10	-0.23	-1.63	-1.22	-0.18	-0.47	-0.70	-0.04
Reach-wide Range	0.71	0.47	1.86	0.73	2.14	0.27	4.30	3.39	2.50	2.69	4.52	0.17

Table 30. Reach P1 q_z median, average, maximum, minimum and range values.

P1	8/11/16	8/18/16	8/22/16	8/31/16	9/7/16	9/14/16	9/28/16	10/19/16	11/9/16	11/30/16	1/5/17	2/3/17
	q_z (m/day)	q_z (m/day)	q_z (m/day)	q_z (m/day)	q_z (m/day)	q_z (m/day)	q_z (m/day)	q_z (m/day)	q_z (m/day)	q_z (m/day)	q_z (m/day)	q_z (m/day)
Reach-wide median	-0.21	-0.05	-0.20	-0.19	-0.15	-0.01	-0.14	-0.36	0.00	-0.31	-0.43	0.00
Reach-wide Average	-0.69	0.52	-0.52	-1.00	-0.12	0.03	0.56	-0.37	-0.12	-0.39	0.29	-0.04
Reach-wide Max	3.26	3.50	1.87	0.47	1.40	0.93	4.90	0.70	0.01	1.17	6.76	0.15
Reach-wide Min	-7.01	-0.52	-4.20	-5.60	-1.40	-0.37	-0.70	-1.40	-0.57	-2.80	-2.80	-0.46
Reach-wide Range	10.27	4.02	6.07	6.07	2.80	1.30	5.60	2.10	0.58	3.97	9.56	0.60

Table 31. Specific discharge (q_z) data for all piezometers with high K for reach R2. A blank cell means either that the piezometer data could not be collected or early data was not accurate due to slow recharge in the piezometer.

R2		8/11/16	8/16/16	8/24/16	8/30/16	9/6/16	9/13/16	10/17/16	11/8/16	11/30/16	1/5/17	1/20/17	Median for all dates
Nest	Depth (cm)	q_z (m/day)	q_z (m/day)	q_z (m/day)	q_z (m/day)	q_z (m/day)	q_z (m/day)	q_z (m/day)	q_z (m/day)	q_z (m/day)	q_z (m/day)	q_z (m/day)	q_z (m/day)
Gravel Bed #1	30	-0.03	-0.01	-0.02	-0.01	-0.01	-0.01	-0.01	-0.01	0.01	0.00	-0.02	-0.01
Gravel Bed #2	50	0.00		0.00	0.00	0.00	-0.01	0.02	-0.01	-0.01	-0.01	0.00	0.00
Gravel Bed #2	30	-0.01	-0.01	-0.01	0.01	-0.06	0.00	-0.01	-0.01	0.00	-0.01	0.00	-0.01
Gravel Bed #3	75	0.00	-0.14	-0.09	0.00	0.00	-0.05	-0.05	-0.23	0.05	-0.09	0.05	-0.05
Gravel Bed #3	50	0.00	-0.16	-0.21	-0.21	-0.11	-0.21	-0.21	-0.21	-0.11	-0.21	-0.05	-0.21
Gravel Bed #3	30				0.00	0.00	0.00	0.00	0.00	0.00	0.00	0.00	0.00
Gravel Bed #4	50	-2.80	-0.47	-0.93	-1.86	-1.40	-0.93	-0.93	-0.93	-0.93	-0.93	-0.93	-0.93
Gravel Bed #4	30	0.00	0.00	-0.02		-0.01	-0.01	-0.02	0.00	-0.03	0.01	-0.01	-0.01
BDJ	30	0.00	0.00		0.00	0.00	0.00	-0.10	-0.08	-0.05	-0.02	-0.08	-0.01
ADJ	30	3.21		3.58	3.53	2.79	2.96	-0.03	-0.06	0.03	-0.09	0.03	1.41

Table 32. Specific discharge (q_z) data for all piezometers with high K for reach A1. A blank cell means either that the piezometer data could not be collected or early data was not accurate due to slow recharge in the piezometer.

A1		8/11/16	8/16/16	8/24/16	8/30/16	9/6/16	9/13/16	9/28/16	10/17/16	11/8/16	11/30/16	1/5/17	1/20/17	Median for all dates
Nest	Depth (cm)	q_z (m/day)	q_z (m/day)	q_z (m/day)	q_z (m/day)	q_z (m/day)	q_z (m/day)	q_z (m/day)	q_z (m/day)	q_z (m/day)	q_z (m/day)	q_z (m/day)	q_z (m/day)	q_z (m/day)
TOM	50	-0.03	-0.01	-0.01	-0.01	-0.02	-0.02	0.11	0.00	-0.01	-0.04	-0.01	0.00	-0.01
TOM	30	-0.01	0.00	0.00	-0.01	0.00	0.00	0.00	0.00	0.00	0.00	0.00	0.00	0.00
BDJ#2	50	-0.32	-0.48	-0.11	-0.16	0.00	0.05	1.67	-0.48	-0.32	-0.38	-0.43	-0.01	-0.24
BDJ#2	30	-0.16	-0.23	-0.31	-0.08	0.08	0.16	0.00	-0.47	-0.39	-0.16	-0.31	-0.01	-0.16
ADJ#2	30	-0.73	-0.15	-1.60	-2.19	-1.75	-1.60	-0.15	-0.15	-0.29	-0.58	-1.02	-0.02	-0.66

Table 33. Specific discharge (q_z) data for all piezometers with high K for reach C1. A blank cell means either that the piezometer data could not be collected or early data was not accurate due to slow recharge in the piezometer.

C1		8/11/16	8/18/16	8/22/16	8/31/16	9/7/16	9/14/16	9/28/16	10/19/16	11/9/16	11/30/16	1/5/17	Median for all dates
Nest	Depth (cm)	q_z (m/day)	q_z (m/day)	q_z (m/day)	q_z (m/day)	q_z (m/day)	q_z (m/day)	q_z (m/day)	q_z (m/day)	q_z (m/day)	q_z (m/day)	q_z (m/day)	q_z (m/day)
AGB	30	-0.16	-0.39	-0.08	-0.39	-0.08	-0.54	-0.31	-0.39	-0.08	-0.16	-0.39	-0.31
BGB	30	0.12	-0.35	-0.12	-0.12	0.00	-0.12	-0.35	-0.35	0.12	0.23	-0.23	-0.12

Table 34. Specific discharge (q_z) data for all piezometers with high K for reach D1. A blank cell means either that the piezometer data could not be collected or early data was not accurate due to slow recharge in the piezometer.

D1		8/11/16	8/18/16	8/22/16	8/31/16	9/7/16	9/14/16	9/28/16	10/19/16	11/9/16	11/30/16	1/5/17	2/3/17	Median for all dates
Nest	Depth (cm)	q_z (m/day)	q_z (m/day)	q_z (m/day)	q_z (m/day)	q_z (m/day)	q_z (m/day)	q_z (m/day)	q_z (m/day)	q_z (m/day)	q_z (m/day)	q_z (m/day)	q_z (m/day)	q_z (m/day)
Pool #1	75								2.17	2.32	2.22	3.82	0.13	2.22
Pool #1	50								-0.31	0.08	-0.15	-0.08	0.01	-0.08
Pool #1	30								-0.78	0.39	-0.39	-0.39	0.03	-0.39
BGB# 1	40	0.01			0.03	0.04	0.04		-0.01	0.00	0.01	-0.01	0.00	0.01
AGB# 1	30	0.00	-0.06	-0.03	-0.11	-0.03	-0.03	0.00	-0.06	-0.06	-0.03	-0.11	0.00	-0.03
Pool #2	75	-0.06	-0.17	0.06	-0.17	-0.41	0.00	-0.23	-0.06	-0.06	0.00	2.10	-0.01	-0.06
Pool #2	50	-0.70	-0.47	1.16	-0.70	-2.10	-0.23	-1.63	-0.47	0.00	-0.47	-0.70	-0.04	-0.47
Pool #3	75								-0.20	-0.03	0.00	0.00	-0.02	-0.02
Pool #3	50								-1.22	0.00	-0.35	-0.52	0.00	-0.35
Pool #3	30								-0.83	0.00	-0.33	-0.17	-0.02	-0.17
AGB# 2	50	-0.02	-0.02	-0.07	-0.05	0.00	-0.02	0.02	-0.05	0.00	-0.03	-0.02	0.00	-0.02
AGB# 2	35	-0.08	0.00	-0.17	-0.42	0.00	0.00	2.67	0.00	0.00	-0.08	-0.33	-0.01	0.00
AGB# 2	20	-0.18	-0.35	-0.70	-0.70	0.00	0.00	0.00	0.00	-0.18	0.18	-0.35	-0.01	-0.09
BGB# 2	25	0.00	-0.12	-0.12	-0.35	-0.12	0.00		-0.58	0.12	-0.23	-0.35	-0.02	-0.12

Table 35. Specific discharge (q_z) data for all piezometers with high K for reach P1. A blank cell means either that the piezometer data could not be collected or early data was not accurate due to slow recharge in the piezometer.

P1		8/11/16	8/18/16	8/22/16	8/31/16	9/7/16	9/14/16	9/28/16	10/19/16	11/9/16	11/30/16	1/5/17	2/3/17	Median for all dates
Nest	Depth (cm)	q_z (m/day)	q_z (m/day)	q_z (m/day)	q_z (m/day)	q_z (m/day)	q_z (m/day)	q_z (m/day)	q_z (m/day)	q_z (m/day)	q_z (m/day)	q_z (m/day)	q_z (m/day)	q_z (m/day)
BR	75	3.26	3.50	1.87	0.47	1.40	0.93	4.90	0.70	0.00	1.17	6.76	0.15	1.28
TOM	25	-7.01	1.40	-4.20	-5.60	-1.40	0.00		-1.40	0.00	-2.80	-2.80	-0.46	-1.40
ADJ#1	50	-0.21	-0.22	-0.20	-0.19	-0.15	-0.16	-0.25	-0.36	-0.30	-0.31	-0.43	-0.01	-0.21
ADJ#1	25	-0.35	-0.44	-0.35	-0.37	-0.33	-0.37	-0.52	-0.65	-0.57	-0.44	-0.74	0.05	-0.40
BDJ#1	75	0.01	-0.01	-0.01	-0.01	0.00	-0.01	-0.04	0.00	0.00	-0.01	-0.01	0.00	-0.01
BDJ#1	25	-0.38	-0.05	-0.02	-0.06	-0.01	-0.01	0.00	-0.03	0.01	-0.02	-0.03	0.00	-0.02
DJD#2	25	-0.17	-0.52	-0.70	-1.22	-0.35	-0.17	-0.70	-0.87	0.00	-0.35	-0.70	-0.02	-0.44

4.5 Horizontal hydraulic gradient

Δh is the difference in hydraulic head from well to piezometer nest. Groundwater flows from high hydraulic head to low hydraulic head and therefore in the direction of -Δh. Δx is the distance in the lateral direction between well and piezometer nest. *dh/dx* is the total rate of change of total head along the direction of flow (Hiscock and Bense, 2014). When *dh/dx* is measured from the riparian well to the stream, positive *dh/dx* indicates that water is moving toward the stream (gaining). A negative value indicates water is moving away from the stream (losing).

4.5.1 Reach R2

Upland to the piezometers had an average *dh/dx* of 0.02. Riparian to the piezometers had an average of 0.03. The horizontal component of flow is from upland to the stream (gaining).

4.5.2 Reach A1

Upland to the piezometers had an average *dh/dx* of 0.02. Riparian to the piezometers had an average *dh/dx* of 0.07. The horizontal component of flow is moving from upland to the stream (gaining).

4.5.3 Reach C1

Upland well to the piezometers had an average *dh/dx* of -0.01. Riparian well to the piezometers had an average *dh/dx* of -0.06. The horizontal component of flow is moving from the piezometers to the riparian and upland wells.

4.5.4 Reach D1

Upland well to the piezometers had an average *dh/dx* of -0.01. Riparian well to the piezometers had an average *dh/dx* of -0.01. The horizontal component of flow is moving from the stream to the riparian (losing).

4.5.5 Reach P1

The *dh/dx* for the upland well toward the riparian well was -0.02. Upland well to the piezometers had an average *dh/dx* of -0.02. Riparian well to the piezometers had an average *dh/dx* of -0.01. The horizontal component of flow is moving from the stream to the riparian (losing).

4.6 Horizontal component of specific discharge

4.6.1 Reach R2

The upland well q_x to the riparian well was 0.39 m/day. The upland well average q_x to the piezometers was 0.24 m/day. The riparian well average q_x to the piezometers was 1.34 m/day (Table 20).

4.6.2 Reach A1

The upland well q_x to the riparian well was 0.06 m/day. The upland well average q_x to the piezometers was 0.08 m/day. The riparian well average q_x to the piezometers was 0.12 m/day (Table 21)

4.6.3 Reach C1

The upland well q_x to the riparian well was 1.75 m/day. The upland well average q_x to the piezometers was -0.07 m/day. The riparian well average q_x to the piezometers was -0.06 (Table 22).

4.6.4 Reach D1

Slug testing was not possible at D1 upland well, so there is no q_x data for the upland well. The riparian well average q_x to the piezometer was -0.03 (Table 23).

4.6.5 Reach P1

The upland well q_x to the riparian well was -0.11 m/day. The upland well average q_x to the piezometers was -0.44 m/day. The riparian well average q_x to the piezometers was -0.27 m/day (Table 24).

4.7 Student's T-test for difference of mean VHG between geomorphic features and reaches

4.7.1 Geomorphic features

The Student's T-test was performed for all geomorphic features in the stream except "Between Gravel Bed". "Between Gravel Bed" was not used because it is between a hypothesized apparent upwelling and apparent downwelling feature and was never given a

directional flow hypothesis. In summary, there was not a clear difference of VHG between hypothesized spots of apparent upwelling and apparent downwelling. For example, the geomorphic feature “Above Debris Jam” was hypothesized of being a location of apparent downwelling. The other geomorphic feature “Below Debris Jam” was hypothesized of being a location of apparent upwelling. The Student’s T-test resulted in a p-value greater than 0.05 meaning there is not a statistically significant difference between these reaches even though they are hypothesized as being complete opposite in flow direction. Some geomorphic features with hypothesized apparent downwelling locations were found to be statistically significant like “Top of Meander” and “Pool” but there is not enough clarity among of the VHG averages for the geomorphic features to be significantly different.

Table 36. P-value of student's T-test of all geomorphic features. The red shaded cells indicate geomorphic features hypothesized for hot spots of apparent downwelling. Green shaded cells indicated geomorphic features hypothesized to be hot spots of apparent upwelling. Yellow shaded cells indicate the *p*-value being lower than 0.05 indicating statistical significance for difference of means.

	TOP OF MEANDER	POOL	BOTTOM OF MEANDER	BELOW GRAVEL BED	BELOW DEBRIS JAM	BELOW BEDROCK	ABOVE GRAVEL BED
POOL	0.02						
BOTTOM OF MEANDER	0.74	0.01					
BELOW GRAVEL BED	0.04	0.25	0.01				
BELOW DEBRIS JAM	0.22	0.00	0.09	0.00			
BELOW BEDROCK	0.06	0.79	0.02	0.21	0.00		
ABOVE GRAVEL BED	0.57	0.00	0.85	0.00	0.02	0.00	
ABOVE DEBRIS JAM	0.94	0.07	0.87	0.15	0.17	0.15	0.77

4.7.2 All reaches

Table 37. P-value of student's T-test for difference of mean among all reaches.

Study Reach	R2	A1	D1	P1
A1	0.68			
D1	0.33	0.00		
P1	0.15	0.08	0.00	
C1	0.70	0.14	0.52	0.03

4.8 Water chemistry

Not all chemical analyses yielded values for each analyte for all reaches. Some chemicals were not detected for all reaches, for example nitrite.

4.8.1 Reach R2

Study reach R2's piezometer, surface water and groundwater chemical analyses are in Table 38 with average concentrations in Table 42. Piezometer water had an average alkalinity concentration of 1.18 meq/L. Piezometer water had an average δ^2H and $\delta^{18}O$ of -30.01‰ and -5.31‰ respectively).

Stream water had an alkalinity concentration of 1.68 meq/L. Stream water had a δ^2H of -29.19 ‰ and $\delta^{18}O$ of -5.19 ‰. Groundwater samples had an average alkalinity concentration of 1.10 meq/L. Groundwater δ^2H and $\delta^{18}O$ had an average for groundwater at -30.00 ‰ and -5.26 ‰ respectively. Stream water had a δ^2H of -29.19 ‰ and $\delta^{18}O$ of -5.19 ‰.

4.8.2 Reach A1

Study reach A1's piezometer, surface water and groundwater chemical analyses are in Table 39 with average concentrations in Table 42. Piezometer water had an average alkalinity concentration of 0.83 meq/L. Piezometer water had δ^2H and $\delta^{18}O$ an average of -28.34 ‰ and -5.14 ‰ respectively (Table 39).

Stream water had an alkalinity concentration of 0.78 meq/L. Stream water had δ^2H and $\delta^{18}O$ concentrations of -32.06 ‰ and -6.54 ‰. Groundwater samples had an average alkalinity concentration of 0.51 meq/L. Groundwater samples had an average δ^2H and $\delta^{18}O$ of -28.94 ‰ and -5.12 ‰.

4.8.3 Reach D1

Study reach D1's piezometer, surface water and groundwater chemical analyses are in

Table 40 with average concentrations in Table 42. Piezometer water had an average alkalinity concentration of 1.00 meq/L. δ^2H and $\delta^{18}O$ had average of -30.55 ‰ and -5.37 ‰ respectively.

Stream water had an alkalinity concentration of 0.96 meq/L. δ^2H and $\delta^{18}O$ were -28.44 ‰ and -6.05 ‰ respectively for stream water. Groundwater samples had an average alkalinity concentration of 0.50 meq/L. δ^2H and $\delta^{18}O$ had an averaged value of -29.62‰ and -5.37‰ respectively for groundwater samples.

4.8.4 Reach P1

Study reach P1's piezometer, stream water and groundwater chemical analyses are in Table 41 with average concentrations in Table 42. Piezometer water had an average alkalinity concentration of 0.95 meq/L. Piezometer water had an average δ^2H and $\delta^{18}O$ of -27.30 ‰ and -4.85 ‰ respectively.

Stream water had an alkalinity concentration of 0.81 meq/L. Stream water had a δ^2H and $\delta^{18}O$ of -26.85 ‰ and -5.32 ‰ respectively. Groundwater samples had an average alkalinity concentration of 0.61 meq/L. Groundwater samples had an average δ^2H and $\delta^{18}O$ of -26.06 ‰ and -4.46 ‰ respectively.

Table 38. Results of chemical analysis for reach R2, sampled on 1/20/17.

Sample	Sample Type	Fluoride (meq/L)	Chloride (meq/L)	Nitrite as N (meq/L)	Nitrate as N (meq/L)	Phosphate (meq/L)	Sulfate (meq/L)	Potassium (meq/L)	Sodium (meq/L)	Magnesium (meq/L)	Calcium (meq/L)	Alkalinity (meq/L)	δ^2H (‰)	$\delta^{18}O$ (‰)
ADJ 30cm	Piezometer	0.004	0.154	0.000	0.002	0.000	0.091	0.056	0.421	0.225	0.405	0.780	-27.88	-4.70
ADJ 50cm	Piezometer	0.006	0.166	0.000	0.002	0.000	0.033	0.013	0.258	0.090	0.228	1.360	-27.13	-4.59
BDJ 30cm	Piezometer												-29.46	-5.06
BDJ 50cm	Piezometer	0.003	0.092	0.000	0.003	0.000	0.080	0.027	0.462	0.066	0.208	0.750		
BDJ 75cm	Piezometer	0.004	0.108	0.000	0.002	0.000	0.099	0.042	0.309	0.235	0.453			
GB1 30cm	Piezometer	0.009	0.298	0.000	0.003	0.000	0.096	0.012	0.359	0.059	0.085	0.880	-27.47	-4.61
GB1 50cm	Piezometer	0.008	0.096	0.000	0.004	0.000	0.039	0.009	0.308	0.079	0.173	1.140	-27.68	-4.98
GB1 75cm	Piezometer	0.007	0.092	0.000	0.002	0.000	0.033	0.009	0.371	0.112	0.246	1.510	-29.66	-5.75
GB2 30cm	Piezometer	0.004	0.088	0.000	0.002	0.000	0.048	0.014	0.230	0.056	0.100		-27.38	-4.79
GB2 50cm	Piezometer	0.005	0.100	0.000	0.002	0.000	0.041	0.054	0.355	0.486	0.846	1.700	-41.88	-6.51
GB2 75cm	Piezometer	0.006	0.088	0.000	0.003	0.000	0.056	0.037	0.172	0.086	0.185	1.450		
GB3 30cm	Piezometer	0.005	0.120	0.000	0.001	0.000	0.042	0.099	0.356	0.345	0.748	1.480	-29.65	-5.18
GB3 50cm	Piezometer	0.004	0.220	0.000	0.002	0.000	0.076	0.047	0.427	0.270	0.451	0.800	-30.16	-5.35
GB3 75cm	Piezometer	0.005	0.106	0.000	0.001	0.000	0.056	0.048	0.331	0.348	0.655	1.360	-30.95	-6.03
GB4 30cm	Piezometer	0.005	0.101	0.000	0.002	0.000	0.070	0.027	0.343	0.465	0.748	1.420	-30.61	-5.34
GB4 50cm	Piezometer	0.005	0.087	0.000	0.003	0.001	0.066	0.029	0.296	0.402	0.679	1.160	-30.44	-5.30
GB4 75cm	Piezometer	0.004	0.063	0.000	0.003	0.001	2.170	0.103	0.090	0.220	0.450	0.710	-29.82	-6.14
GW RIP 20JAN17	Well	0.004	0.080	0.000	0.003	0.000	0.189	0.011	0.232	0.375	0.489	0.710	-31.37	-5.20
GW Up 20JAN17	Well	0.004	0.106	0.000	0.001	0.002	0.051	0.045	0.326	0.653	0.837	1.480	-28.64	-5.33
SW 20Jan17	Stream	0.004	0.122	0.000	0.002	0.000	0.096	0.038	0.361	0.317	0.521	1.680	-29.19	-5.19

Table 39. Summary of chemical analysis for Reach A1, sampled on 1/20/17.

Sample	Sample Type	Fluoride (meq/L)	Chloride (meq/L)	Nitrite as N (meq/L)	Nitrate as N (meq/L)	Phosphate (meq/L)	Sulfate (meq/L)	Sodium (meq/L)	Potassium (meq/L)	Magnesium (meq/L)	Calcium (meq/L)	Alkalinity (meq/L)	δ^2H (‰)	$\delta^{18}O$ (‰)
ADJ2 30cm	Piezometer	0.005	0.155	0.001	0.012	0.000	0.109	0.350	0.029	0.061	0.087	0.870	-29.26	-5.48
ADJ2 50cm	Piezometer	0.004	0.160	0.000	0.008	0.002	0.112	0.349	0.076	0.237	0.424	0.740		
ADJ2 75cm	Piezometer	0.004	0.153	0.000	0.004	0.000	0.166	0.223	0.047	0.044	0.067	0.740	-28.15	-4.60
BDJ1 75cm	Piezometer	0.010	0.076	0.000	0.003	0.000	0.028	0.325	0.009	0.070	0.110		-26.48	-4.95
BDJ2 30cm	Piezometer	0.004	0.164	0.000	0.011	0.000	0.122	0.338	0.057	0.100	0.203	0.720	-29.48	-5.51
BDJ2 50cm	Piezometer	0.004	0.153	0.000	0.002	0.000	0.090	0.366	0.083	0.215	0.480	0.730		
BDJ2 75cm	Piezometer	0.006	0.095	0.000	0.004	0.000	0.049	0.308	0.026	0.089	0.193	1.290		
BOM 30cm	Piezometer	0.009	0.194	0.000	0.002	0.000	0.124	0.360	0.034	0.137	0.204			
TOM 30cm	Piezometer	0.007	0.157	0.001	0.007	0.000	0.092	0.333	0.075	0.202	0.354	0.740		
TOM 50cm	Piezometer	0.006	0.167	0.000	0.015	0.000	0.118	0.368	0.050	0.315	0.519			
GW RIP 1-20-17	Well	0.003	0.056	0.000	0.004	0.000	0.164	0.082	0.004	0.111	0.146	0.110	-26.13	-4.92
GW UP 1-20-17	Well	0.005	0.100	0.000	0.001	0.011	0.069	0.526	0.009	0.234	0.396	0.900	-31.75	-5.32
SW 1-20-17	Stream	0.005	0.167	0.000	0.014	0.000	0.117	0.371	0.041	0.330	0.526	0.780	-32.06	-6.54

Table 40. Summary of chemical analysis for Reach D1, sampled on 2/3/17.

Sample	Sample Type	Fluoride (meq/L)	Chloride (meq/L)	Nitrite as N (meq/L)	Nitrate as N (meq/L)	Phosphate (meq/L)	Sulfate (meq/L)	Sodium (meq/L)	Potassium (meq/L)	Magnesium (meq/L)	Calcium (meq/L)	Alkalinity (meq/L)	δ^2H (‰)	δ18O (‰)
ABG1 30cm	Piezometer	0.004	0.111	0.000	0.004	0.000	0.107	0.320	0.035	0.116	0.174	1.140	-29.16	-4.46
AGB1 45cm	Piezometer	0.003	0.072	0.000	0.003	0.000	0.295	0.352	0.044	0.481	0.971	1.090	-28.34	-5.02
AGB1 60cm	Piezometer	0.004	0.068	0.000	0.001	0.000	0.216	0.224	0.067	0.450	0.954	1.070	-29.64	-5.06
AGB2 20cm	Piezometer	0.004	0.082	0.000	0.006	0.001	0.065	0.356	0.059	0.432	0.780	1.500	-33.39	-5.84
AGB2 35cm	Piezometer	0.004	0.079	0.000	0.008	0.005	0.064	0.321	0.024	0.086	0.152	0.990	-31.88	-5.42
AGB2 50cm	Piezometer	0.004	0.083	0.000	0.005	0.000	0.071	0.250	0.024	0.068	0.121	0.720	-33.86	-6.11
BGB1 20cm	Piezometer	0.005	0.144	0.000	0.008	0.000	0.118	0.401	0.087	0.343	0.594	0.960		
BGB1 30cm	Piezometer	0.005	0.116	0.000	0.006	0.000	0.177	0.329	0.070	0.439	0.722	0.860	-28.66	-4.78
BGB1 40cm	Piezometer	0.005	0.122	0.000	0.006	0.000	0.240	0.365	0.053	0.085	0.142	1.150		
BGB2 25cm	Piezometer	0.004	0.114	0.000	0.006	0.001	0.099	0.321	0.024	0.086	0.152	0.790	-27.93	-4.83
BGB2 50cm	Piezometer	0.004	0.075	0.000	0.007	0.000	0.110	0.305	0.021	0.074	0.133	1.310	-28.62	-5.23
BGB2 75cm	Piezometer	0.004	0.073	0.000	0.008	0.000	0.105	0.257	0.037	0.073	0.194	0.740	-30.93	-5.42
Pool1 30cm	Piezometer	0.004	0.090	0.000	0.002	0.000	0.073	0.437	0.023	0.098	0.199	1.240	-31.22	-5.23
Pool1 50cm	Piezometer	0.004	0.082	0.000	0.003	0.000	0.071	0.369	0.030	0.070	0.149	1.160	-28.72	-5.40
Pool1 75cm	Piezometer	0.004	0.066	0.000	0.005	0.003	0.058	0.112	0.060	0.058	0.147	0.400	-37.96	-6.28
Pool2 25cm	Piezometer	0.003	0.076	0.000	0.002	0.000	0.143	0.459	0.055	0.098	0.187	1.480	-29.80	-5.15
Pool2 50cm	Piezometer	0.004	0.077	0.000	0.004	0.007	0.078	0.465	0.034	0.097	0.476	1.160	-30.82	-5.65
Pool2 75cm	Piezometer	0.004	0.083	0.000	0.003	0.000	0.094	0.435	0.022	0.095	0.227	1.150	-29.28	-5.94
Pool3 30cm	Piezometer	0.004	0.080	0.000	0.002	0.001	0.031	0.358	0.024	0.090	0.184	1.140	-31.89	-4.97
Pool3 50cm	Piezometer	0.004	0.074	0.000	0.004	0.001	0.067	0.413	0.017	0.088	0.164	1.030	-31.05	-4.98
Pool3 75cm	Piezometer	0.004	0.077	0.000	0.003	0.000	0.071	0.415	0.018	0.070	0.130	1.070	-31.35	-5.54
GW Rip 3Feb17	Well	0.005	0.096	0.000	0.001	0.003	0.217	0.539	0.040	0.274	0.531	0.690	-28.90	-5.14
GW Up 3Feb17	Well	0.004	0.072	0.000	0.001	0.000	0.147	0.131	0.032	0.209	0.382	0.310	-30.34	-5.60
SW 3Feb17	Stream	0.004	0.144	0.000	0.006	0.000	0.116	0.432	0.057	0.448	0.736	0.960	-28.44	-6.05

Table 41. Summary of chemical analysis for Reach P1, sampled on 2/3/17.

Sample	Sample Type	Fluoride (meq/L)	Chloride (meq/L)	Nitrite as N (meq/L)	Nitrate as N (meq/L)	Phosphate (meq/L)	Sulfate (meq/L)	Sodium (meq/L)	Potassium (meq/L)	Magnesium (meq/L)	Calcium (meq/L)	Alkalinity (meq/L)	δ^2H (‰)	$\delta^{18}O$ (‰)
BOM 25cm	Piezometer	0.004	0.085	0.000	0.002	0.000	0.073	0.234	0.024	0.063	0.110	0.720	-28.02	-3.98
BOM 50cm	Piezometer	0.004	0.059	0.000	0.004	0.000	0.041	0.153	0.017	0.050	0.148	0.790	-26.92	-6.18
BOM 75cm	Piezometer	0.004	0.082	0.000	0.001	0.000	0.071	0.233	0.041	0.286	0.489	0.730	-28.16	-4.69
BR 25cm	Piezometer	0.004	0.080	0.000	0.002	0.000	0.065	0.213	0.040	0.237	0.426	0.760	-29.34	-4.83
BR 50cm	Piezometer	0.004	0.061	0.001	0.005	0.000	0.047	0.193	0.039	0.062	0.182	1.310	-32.12	-5.89
BR 75cm	Piezometer	0.005	0.076	0.000	0.004	0.000	0.263	0.301	0.033	0.097	0.133	0.870	-30.26	-4.69
BDJ1 25cm	Piezometer	0.003	0.086	0.000	0.004	0.000	0.234	0.195	0.032	0.060	0.119	0.550	-27.57	-4.12
BDJ1 50cm	Piezometer	0.004	0.079	0.000	0.002	0.000	0.104	0.222	0.016	0.068	0.108	0.910	-24.87	-4.12
BDJ1 75cm	Piezometer	0.004	0.082	0.000	0.002	0.000	0.184	0.275	0.021	0.083	0.201	1.180	-24.85	-3.74
BDJ2 25cm	Piezometer	0.004	0.079	0.000	0.002	0.000	0.063	0.223	0.035	0.263	0.480	0.690	-27.38	-4.27
BDJ2 75cm	Piezometer	0.004	0.078	0.000	0.003	0.000	0.043	0.248	0.008	0.081	0.189			
ADJ1 25cm	Piezometer	0.005	0.093	0.000	0.004	0.002	0.065	0.318	0.037	0.418	0.974	1.340	-24.02	-6.19
ADJ1 50cm	Piezometer	0.004	0.079	0.000	0.002	0.000	0.043	0.269	0.031	0.399	0.740	0.970	-25.55	-5.19
ADJ1 75cm	Piezometer	0.005	0.086	0.000	0.002	0.001	0.063	0.352	0.153	0.546	0.980	1.470	-23.70	-3.89
ADJ2 50cm	Piezometer	0.004	0.060	0.000	0.007	0.000	0.068	0.239	0.083	0.054	0.125	0.840	-28.49	-5.79
TOM 25cm	Piezometer	0.004	0.074	0.000	0.002	0.000	0.061	0.183	0.031	0.220	0.438	0.550	-26.23	-4.61
TOM 50cm	Piezometer	0.004	0.058	0.000	0.009	0.000	0.036	0.185	0.038	0.489	1.075	1.540	-32.11	-6.04
TOM 75cm	Piezometer	0.005	0.076	0.000	0.004	0.000	0.056	0.384	0.038	0.536	1.154	1.680	-27.47	-4.50
GW RIP 3Feb17	Well	0.004	0.074	0.000	0.002	0.000	0.250	0.262	0.050	0.334	0.559	0.750	-24.65	-4.31
GW UP 3Feb17	Well	0.004	0.071	0.000	0.000	0.000	0.149	0.384	0.010	0.216	0.289	0.460	-27.47	-4.62
STRM 3Feb17	Stream	0.004	0.086	0.000	0.001	0.000	0.070	0.249	0.039	0.274	0.516	0.810	-26.85	-5.32

Table 42. Summary of all reaches' averages for piezometers and wells.

Sample	Average	Fluoride (meq/L)	Chloride (meq/L)	Nitrite as N (meq/L)	Nitrate as N (meq/L)	Phosphate (meq/L)	Sulfate (meq/L)	Sodium (meq/L)	Potassium (meq/L)	Magnesium (meq/L)	Calcium (meq/L)	Alkalinity (meq/L)	δ^2H (‰)	$\delta^{18}O$ (‰)
A1	Piezometer	0.006	0.147	0.000	0.007	0.000	0.101	0.332	0.049	0.147	0.264	0.833	-28.34	-5.14
A1	Wells	0.004	0.078	0.000	0.003	0.006	0.117	0.304	0.007	0.172	0.271	0.505	-28.94	-5.12
A1	Stream	0.005	0.167	0.000	0.014	0.000	0.117	0.371	0.041	0.330	0.526	0.780	-32.06	-6.54
R2	Piezometer	0.005	0.124	0.000	0.002	0.000	0.194	0.039	0.318	0.222	0.416	1.179	-30.01	-5.31
R2	Wells	0.004	0.093	0.000	0.002	0.001	0.120	0.028	0.279	0.514	0.663	1.095	-30.00	-5.26
R2	Stream	0.004	0.122	0.000	0.002	0.000	0.096	0.038	0.361	0.317	0.521	1.680	-29.19	-5.19
D1	Piezometer	0.004	0.088	0.000	0.005	0.001	0.112	0.346	0.039	0.167	0.331	1.055	-30.76	-5.33
D1	Wells	0.004	0.084	0.000	0.001	0.002	0.182	0.335	0.036	0.241	0.456	0.500	-29.62	-5.37
D1	Stream	0.004	0.144	0.000	0.006	0.000	0.116	0.432	0.057	0.448	0.736	0.960	-28.44	-6.05
P1	Piezometer	0.004	0.076	0.000	0.003	0.000	0.088	0.246	0.040	0.223	0.448	0.994	-27.47	-4.87
P1	Wells	0.004	0.073	0.000	0.001	0.000	0.200	0.323	0.030	0.275	0.424	0.605	-26.06	-4.46
P1	Stream	0.004	0.086	0.000	0.001	0.000	0.070	0.249	0.039	0.274	0.516	0.810	-26.85	-5.32

4.8.5 Hydrochemical facies (water types)

Piper diagrams are used to classify water samples into hydrochemical facies or water types. The piper diagram consists of the dominant cation and anion from each piezometer sample. The combination of dominant cation and anion creates a hydrochemical facies.

4.8.5.1 Reach A1

Both the surface water and upland well samples reflected a Mixed Cation - HCO_3^- type (Figure 41, Table 43). The riparian well sample was a Mixed Cation - SO_4^{2-} type. The piezometers show a mix of two hydrochemical facies, Mixed Cation - HCO_3^- type (three piezometers) and Na^+- HCO_3^- type (four piezometers).

4.8.5.2 Reach R2

The surface water and both well samples show a hydrochemical facies of Mixed Cation – HCO_3^- (Figure 42, Table 44). Mixed Cation - HCO_3^- and Na^+- HCO_3^- were the dominant hydrochemical facies in the piezometer samples (nine piezometers). One piezometer (GB4 75cm) showed Mixed Cation – SO_4^{2-} type.

4.8.5.3 Reach D1

Both the surface water and riparian well samples had the hydrochemical facies Mixed Cation – HCO_3^- type and the upland well had the Ca^{2+} - HCO_3^- type (Figure 43, Table 45). The dominant water type for the piezometers was Na^+- HCO_3^-, with 11 piezometers. Five piezometers exhibited the Mixed Cation – HCO_3^- water type. Only one piezometer showed Ca^{2+} - HCO_3^- water type (AGB#1 60cm).

4.8.5.4 Reach P1

The surface water sample shows a hydrochemical facies of Mixed Cation – HCO_3^- type and both well samples show Ca^{2+} - HCO_3^- type (Figure 44, Table 46). The piezometers showed hydrochemical facies of Mixed Cation – HCO_3^- (three piezometers), Ca^{2+} - HCO_3^- (13 piezometers) and Na^+- HCO_3^- type (one piezometer). The only piezometer with Na^+- HCO_3^- water type was “ADJ#2 50cm.”

Table 43. Summary of hydrochemical facies for piezometer, well and stream samples in reach A1.

Sample	Sample Type	Depth (cm)	Hydrochemical facies
Stream	Stream		Mixed Cation - HCO_3^-
Riparian	Well		Mixed Cation - SO_4^{2-}
Upland	Well		Mixed Cation - HCO_3^-
ADJ#2	Piezometer	30	Na^+- HCO_3^-
ADJ#2	Piezometer	50	Mixed Cation - HCO_3^-
ADJ#2	Piezometer	75	Na^+- HCO_3^-
BDJ#2	Piezometer	30	Na^+- HCO_3^-
BDJ#2	Piezometer	50	Mixed Cation - HCO_3^-
BDJ#2	Piezometer	75	Na^+- HCO_3^-
TOM	Piezometer	30	Mixed Cation - HCO_3^-

Table 44. Summary of hydrochemical facies for piezometer, well and stream samples in reach R2.

Sample	Sample Type	Depth (cm)	Hydrochemical facies
Stream	Stream		Mixed Cation – HCO_3^-
Riparian	Well		Mixed Cation – HCO_3^-
Upland	Well		Mixed Cation – HCO_3^-
GB#1	Piezometer	30	Na^+- HCO_3^-
GB#1	Piezometer	50	Na^+- HCO_3^-
GB#1	Piezometer	75	Na^+- HCO_3^-
GB#2	Piezometer	50	Mixed Cation – HCO_3^-
GB#2	Piezometer	75	Mixed Cation – HCO_3^-
GB#3	Piezometer	30	Mixed Cation – HCO_3^-
GB#3	Piezometer	50	Mixed Cation – HCO_3^-
GB#3	Piezometer	75	Mixed Cation – HCO_3^-
GB#4	Piezometer	30	Mixed Cation – HCO_3^-
GB#4	Piezometer	50	Mixed Cation – HCO_3^-
GB#4	Piezometer	75	Mixed Cation – SO_4^{2-}
ADJ	Piezometer	30	Mixed Cation – HCO_3^-
ADJ	Piezometer	50	Mixed Cation – HCO_3^-
BDJ	Piezometer	50	Na^+- HCO_3^-

Table 45. Summary of hydrochemical facies for piezometer, well and stream samples in reach D1.

Sample	Sample Type	Depth (cm)	Hydrochemical facies
Stream	Stream		Mixed Cation – HCO_3^-
Riparian	Well		Mixed Cation – HCO_3^-
Upland	Well		Ca^{2+} - HCO_3^-
AGB#1	Piezometer	30	Na^+- HCO_3^-
AGB#1	Piezometer	45	Na^+- HCO_3^-
AGB#1	Piezometer	60	Ca^{2+} - HCO_3^-
AGB#2	Piezometer	20	Mixed Cation – HCO_3^-
AGB#2	Piezometer	35	Na^+- HCO_3^-
AGB#2	Piezometer	50	Na^+- HCO_3^-
BGB#1	Piezometer	20	Mixed Cation – HCO_3^-
BGB#1	Piezometer	30	Mixed Cation – HCO_3^-
BGB#1	Piezometer	40	Na^+- HCO_3^-
Pool#1	Piezometer	30	Na^+- HCO_3^-
Pool#1	Piezometer	50	Na^+- HCO_3^-
Pool#1	Piezometer	75	Mixed Cation – HCO_3^-
Pool#2	Piezometer	30	Na^+- HCO_3^-
Pool#2	Piezometer	50	Na^+- HCO_3^-
Pool#2	Piezometer	75	Mixed Cation – HCO_3^-
Pool#3	Piezometer	30	Mg^{2+} - HCO_3^-
Pool#3	Piezometer	50	Na^+- HCO_3^-
Pool#3	Piezometer	75	Na^+- HCO_3^-

Table 46. Summary of hydrochemical facies for piezometer, well and stream samples in reach P1.

Sample	Sample Type	Depth (cm)	Hydrochemical facies
Stream	Stream		Mixed Cation – HCO_3^-
Riparian	Well		Ca^{2+} - HCO_3^-
Upland	Well		Ca^{2+} - HCO_3^-
BOM	Piezometer	25	Mixed Cation – HCO_3^-
BOM	Piezometer	50	Ca^{2+} - HCO_3^-
BOM	Piezometer	75	Ca^{2+} - HCO_3^-
BR	Piezometer	25	Ca^{2+} - HCO_3^-
BR	Piezometer	50	Ca^{2+} - HCO_3^-
BR	Piezometer	75	Mixed Cation – HCO_3^-
BDJ#1	Piezometer	25	Mixed Cation – HCO_3^-
BDJ#1	Piezometer	50	Ca^{2+} - HCO_3^-
BDJ#1	Piezometer	75	Ca^{2+} - HCO_3^-
BDJ#2	Piezometer	25	Ca^{2+} - HCO_3^-
ADJ#1	Piezometer	25	Ca^{2+} - HCO_3^-
ADJ#1	Piezometer	50	Ca^{2+} - HCO_3^-
ADJ#1	Piezometer	75	Ca^{2+} - HCO_3^-
ADJ#2	Piezometer	50	Na^{+}- HCO_3^-
TOM	Piezometer	25	Ca^{2+} - HCO_3^-
TOM	Piezometer	50	Ca^{2+} - HCO_3^-
TOM	Piezometer	75	Ca^{2+} - HCO_3^-

4.8.6 Water isotopes

At study reach R2 had a piezometer average of -29.95 ‰ δ^2H and -5.36 ‰ $\delta^{18}O$. The piezometer δ^2H ranged from -27.31‰ to -41.88 ‰ and $\delta^{18}O$ ranged from -4.59 ‰ to -6.51 ‰. The stream, upland and riparian well samples had -29.19 ‰, -28.64 ‰ and -31.37 ‰ respectively. $\delta^{18}O$ for the stream, upland and riparian well samples were -5.19 ‰, -5.33 ‰ and -5.20 ‰ respectively (Figure 30).

At study reach A1 had a piezometer average of -28.27 ‰ δ^2H and -5.17 ‰ $\delta^{18}O$. The piezometer δ^2H ranged from -26.48 ‰ to -29.48 ‰ and $\delta^{18}O$ ranged from -4.60 ‰ to -5.51 ‰ $\delta^{18}O$. The stream, upland and riparian well samples had -32.06 ‰, -31.75 ‰, and -26.13 ‰ respectively. The $\delta^{18}O$ for the stream, upland and riparian were -6.54 ‰, -5.32 ‰ and -4.92 ‰ respectively (Figure 31).

At study reach D1 had a piezometer average of -30.51 ‰ δ^2H and -5.31 ‰ $\delta^{18}O$. The piezometer δ^2H ranged from -27.93 ‰ to -33.86 ‰ and $\delta^{18}O$ ranged from -4.46 ‰ to -6.28 ‰. The δ^2H for the stream, upland and riparian were -28.44 ‰, -30.34 ‰, and -28.69 ‰ respectively. The $\delta^{18}O$ for the stream, upland and riparian were -6.05 ‰, -5.60 ‰, and -5.15 ‰ (Figure 32).

At study reach P1 had a piezometer average δ^2H of -27.47 ‰ and an average $\delta^{18}O$ of -4.83 ‰. The piezometer δ^2H ranged from -23.70 ‰ to -32.12 ‰ and $\delta^{18}O$ ranged from -3.89 ‰ to -6.19 ‰. The stream, upland and riparian δ^2H were -26.85 ‰, -27.47 ‰ and -24.78 ‰ respectively. The $\delta^{18}O$ for stream, upland and riparian were -5.32 ‰, -4.62 ‰, and -4.38 ‰ respectively (Figure 33).

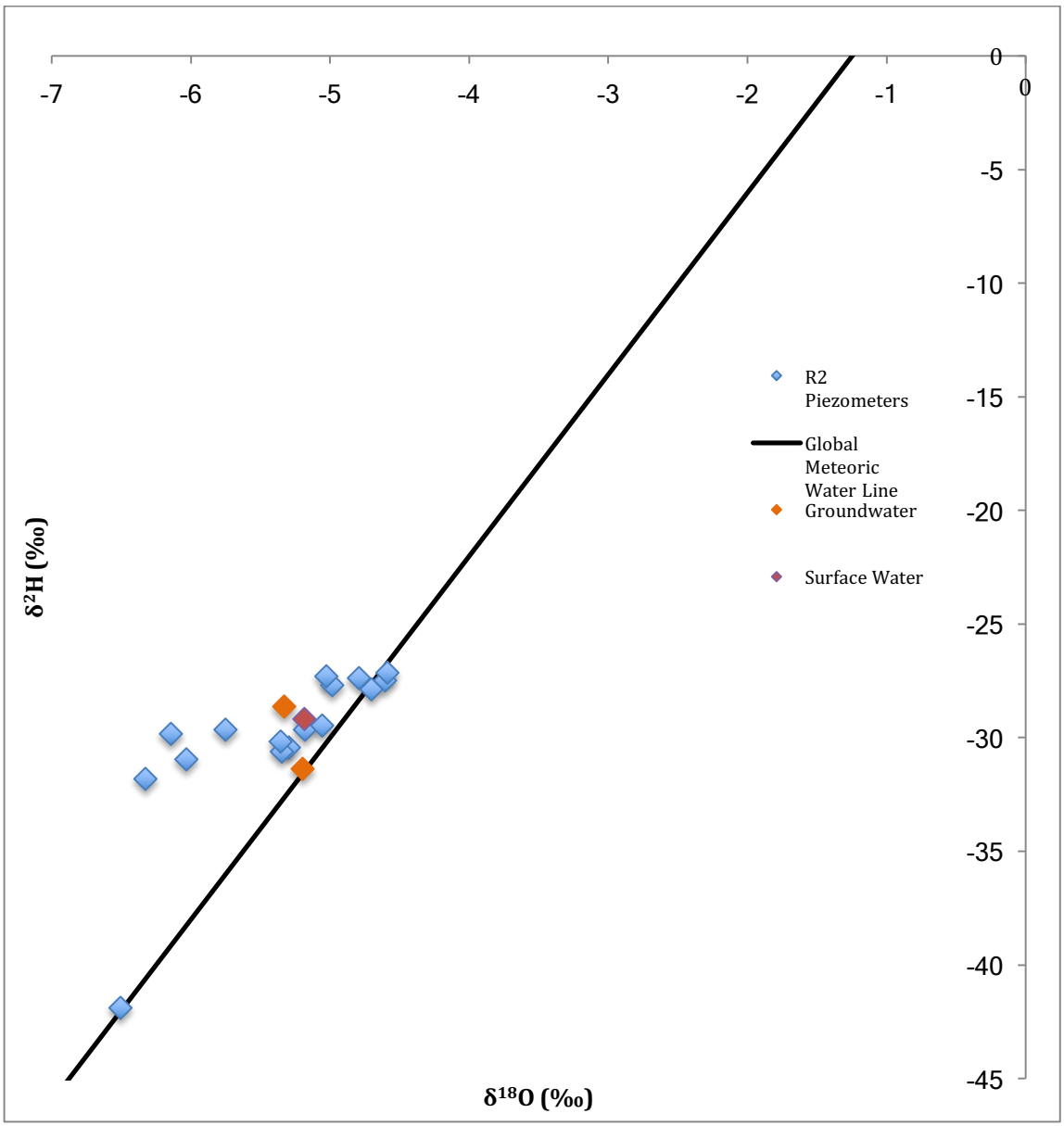

Figure 30. Reach R2 stable isotopes plotted with $\delta^{18}O$ on the x-axis and $\delta^{2}H$ on the y-axis. Piezometer samples are in blue, groundwater samples in orange, and surface water in red. Note that groundwater and surface water are not isotopically distinctive.

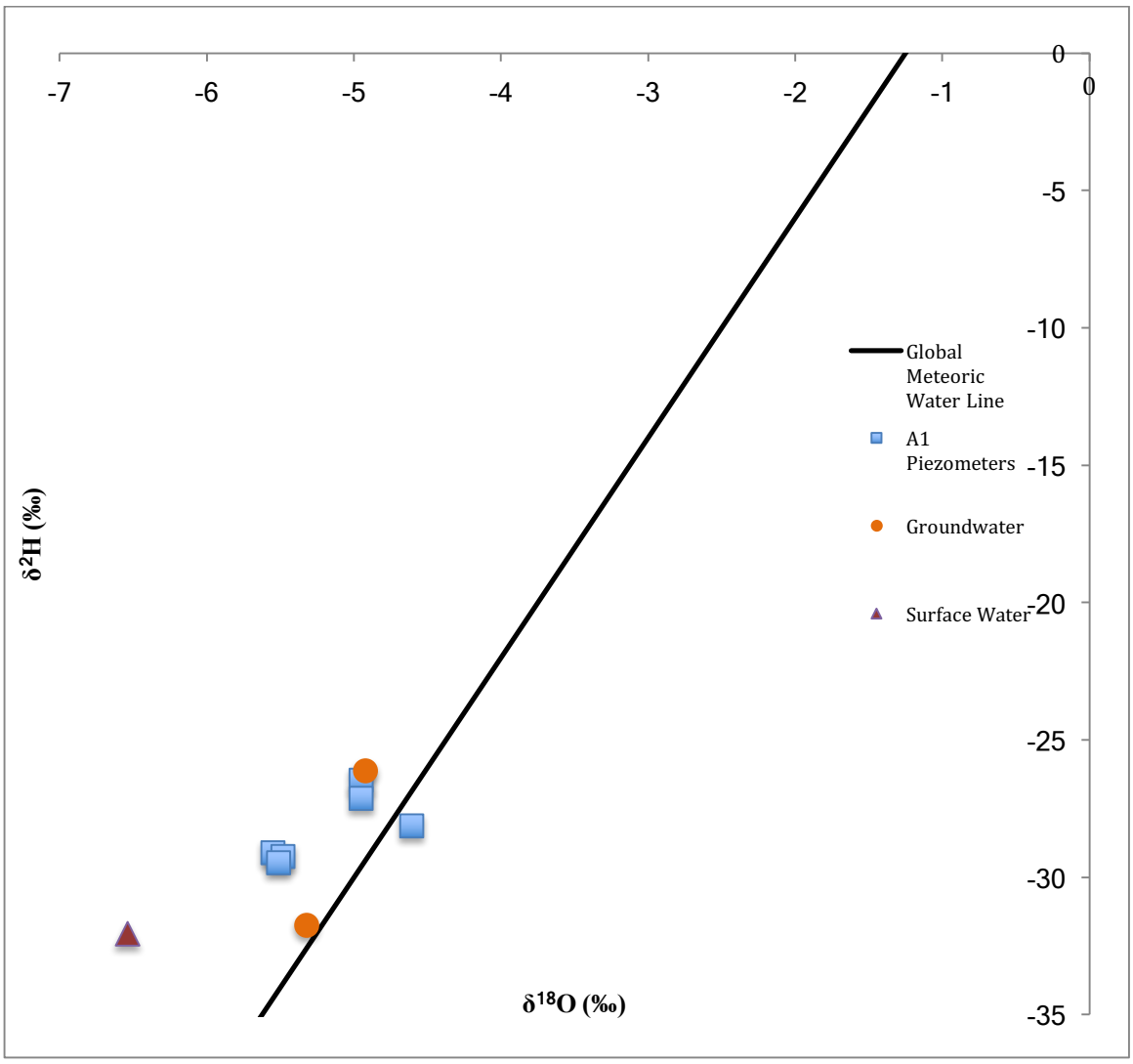

Figure 31. Reach A1 stable isotopes plotted with $\delta^{18}O$ on the x-axis and $\delta^{2}H$ on the y-axis. Piezometer samples are in blue, groundwater samples orange, and surface water in red. Note that groundwater and surface water are not isotopically distinctive.

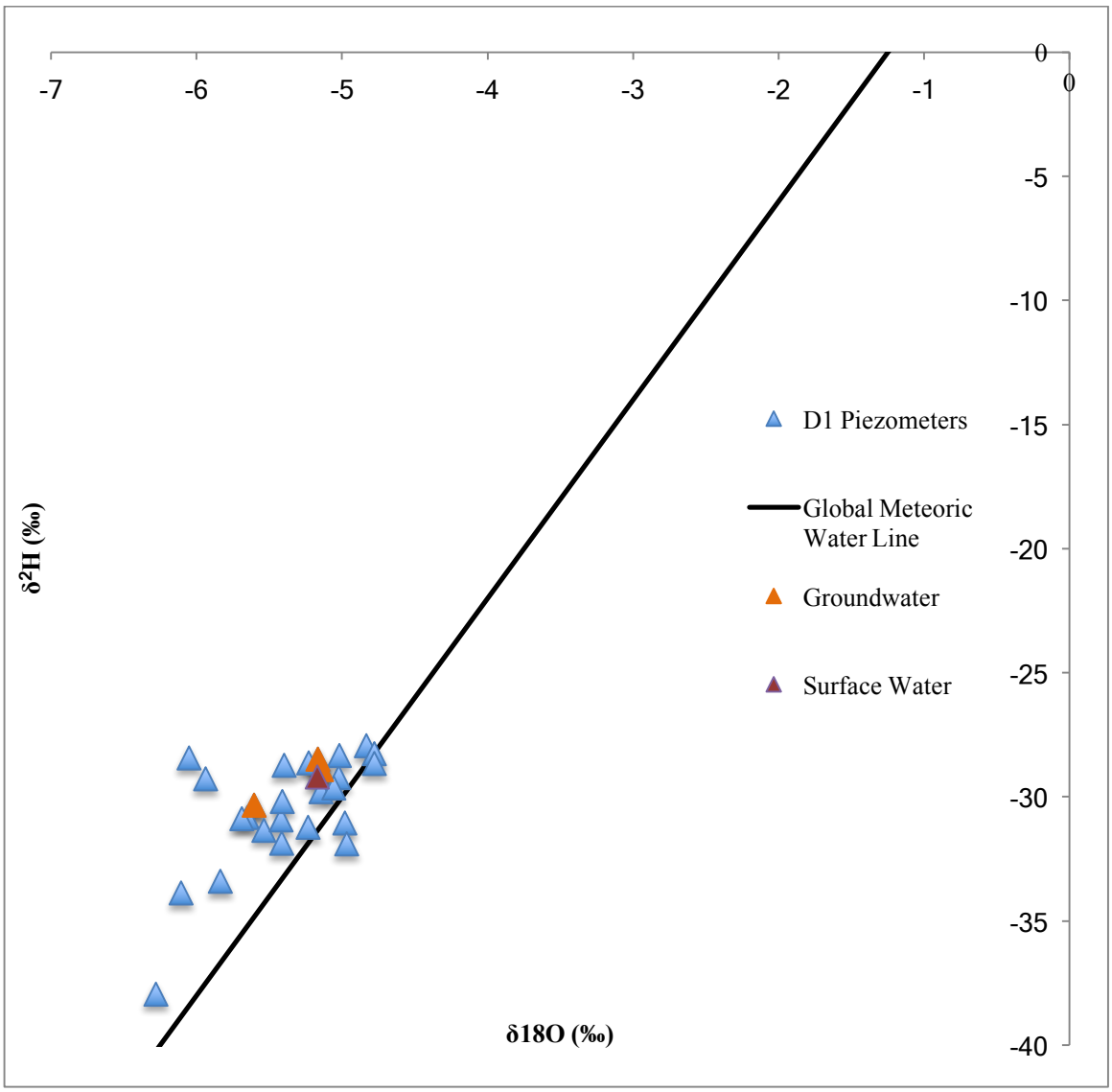

Figure 32. Reach D1 stable isotopes plotted with $\delta^{18}O$ on the x-axis and $\delta^{2}H$ on the y-axis. Piezometer samples are in blue, groundwater samples orange, and surface water in red. Note that groundwater and surface water are not isotopically distinctive.

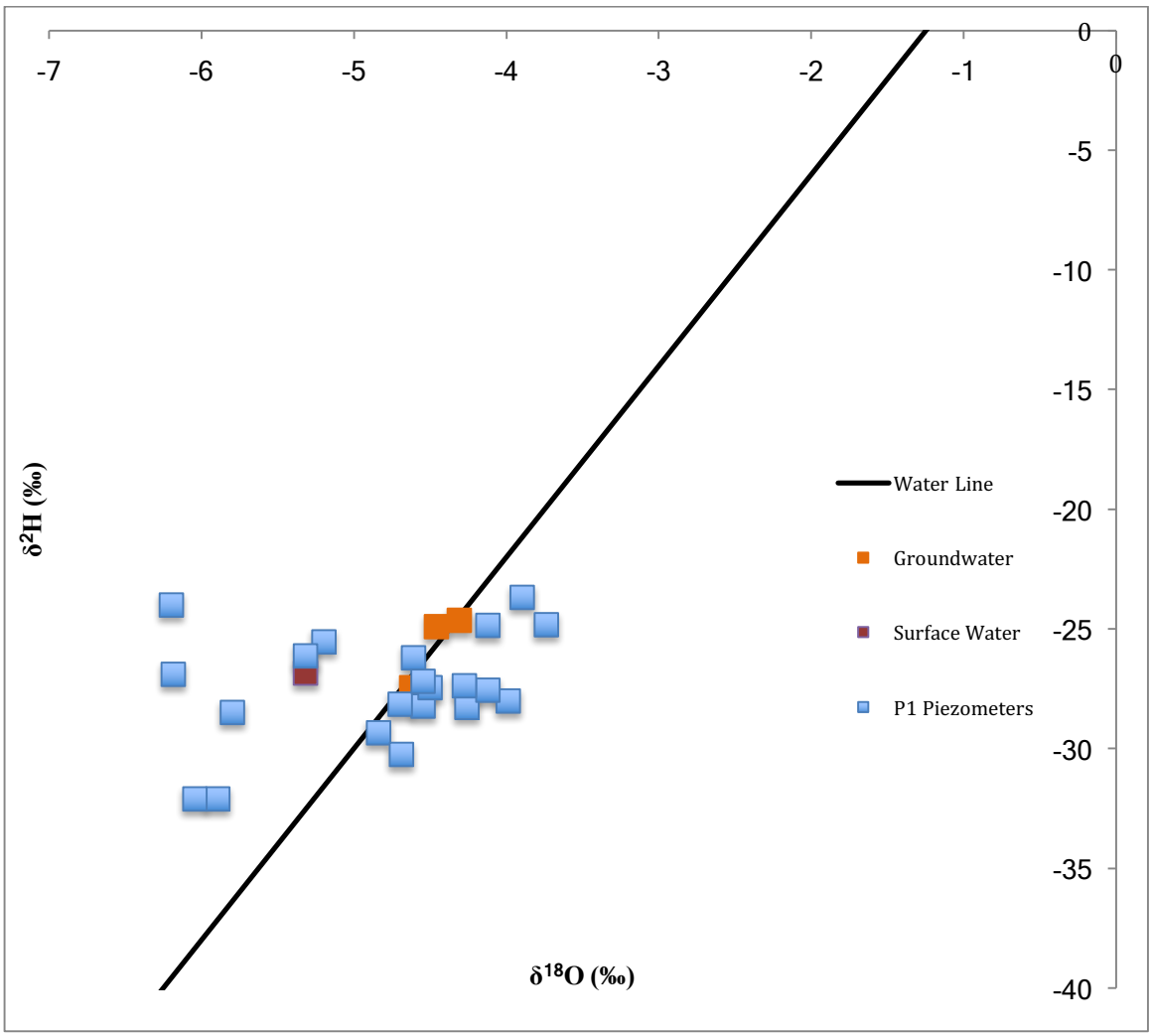

Figure 33. Reach P1 stable isotopes plotted with $\delta^{18}O$ on the x-axis and $\delta^{2}H$ on the y-axis. Piezometer samples are in blue, groundwater samples orange, and surface water in red. Note that groundwater and surface water are not isotopically distinctive.

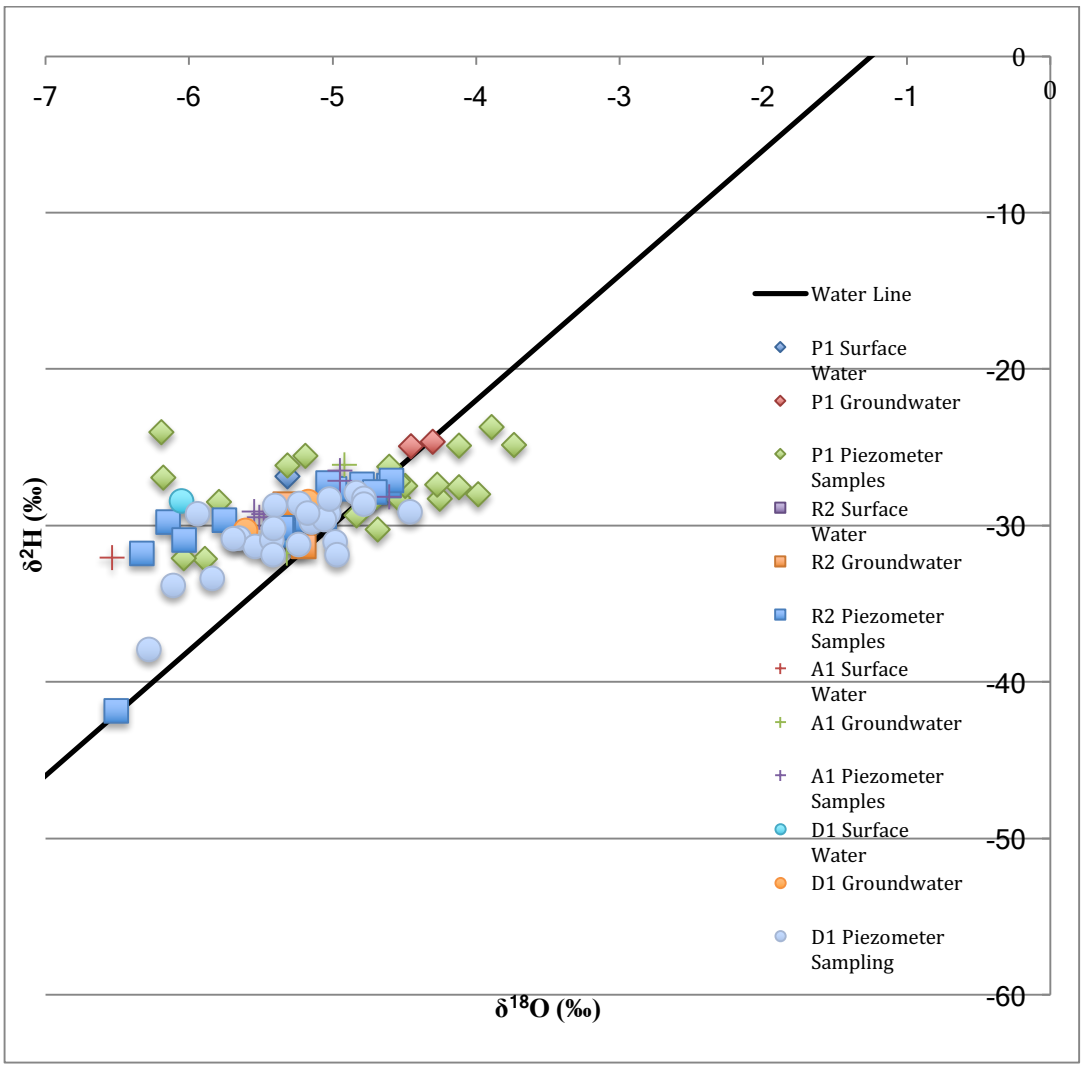

Figure 34. Stable isotopes (all reaches) plotted with $\delta^{18}O$ on the x-axis and $\delta^{2}H$ on the y-axis.

5 Discussion

5.1 VHG by reach

The five reaches showed variation in the extent and direction of VHG. All five reaches had a majority of piezometers showing apparent downwelling. R2 had the most apparent downwelling piezometers with 14 out of 18. C1 had the fewest apparent downwelling piezometers with six out of 10. Reach R2 had the lowest range of median hyporheic flux (-0.03 to 0.00) while C1 had the largest (-0.37 to 0.04). Two study reaches, C1 and P1, were the only reaches that had a date of median reach-wide apparent upwelling VHG.

VHGs fluctuated with time for all piezometers. There were some dates that resulted in changes in a piezometer's vertical flow. Some piezometers had apparent downwelling change to apparent upwelling and vice versa on some dates. A possible implication for change of direction could be influenced by previous rain events. On the falling limb of the hydrograph there is apparent upwelling at certain piezometers for some dates, for example 9/28/16 and 1/5/17. The stream water level falls at a faster pace than the water level in the subsurface, after a rain event. As stated before, groundwater flows from high hydraulic head to hydraulic low head. At the point of the falling limb on the hydrograph, the stream water level is lower than the water table. This results in upward-directed VHG. This was seen on 9/28/16 for some piezometers at study reaches P1, A1 and D1.

Five study reaches were compared against one another using Student's t-test (Table 37). From this analysis, it is evident that the mean of A1 is statistically different from D1, D1 statistically different from A1 and P1 and P1 statistically different from C1 and A1. R2 was found to not be statistically different from any of the reaches. However overall, no reach was consistently distinctive from all others.

5.2 VHG by geomorphic feature

Each geomorphic feature category had a hypothesized vertical hydraulic gradient direction (green shaded cells represent apparent upwelling; red shaded cells represent apparent

downwelling). Some of the categories are consistent with the stated hypotheses. For example, "ABOVE GRAVEL BED" and "BELOW GRAVEL BED" have a *p*-value of < 0.05 meaning that the mean VHGs are statistically different. It was hypothesized that apparent downwelling would take place at the above gravel bed while apparent upwelling would be shown at the below gravel bar feature (Table 36). However, multiple feature categories are inconsistent with this hypothesis. For example, "TOP OF MEANDER" vs. "BOTTOM OF MEANDER" had a *p*-value of > 0.05 so their means are not statistically different. It was hypothesized that these geomorphic features would exhibit opposite vertical flux movements but overall the student's t-test is inconsistent with the hypothesized relationships.

5.3 VHGs in relation to *K*

Darcy's law dictates the direction and velocity of groundwater flow. Darcy's law is hydraulic conductivity multiplied by the hydraulic gradient and cross-sectional area. To have significant flow, it must have both high *K* and high VHG. Piezometers that show high VHG but low *K* could be an indication of perched water that is not flowing vertically (that is, surface and subsurface waters are not well connected). Other piezometers that exhibit low VHG but high *K* could mean rapid horizontal movement but little vertical movement (that is, underflow but not rapid vertical exchange with the channel). Hyporheic exchange is more heavily reliant on vertical movement than horizontal. High VHG and high *K* are the strongest indicators of hyporheic exchange. Figure 35 depicts all piezometers with high *K* rates in comparison with their respective VHGs. The piezometers that fall left of the yellow line and between the red lines are inferred to not have hyporheic hot spot potential due to having both low VHG and *K*. A hotspot of hyporheic exchange favors a combination of high VHG and a high *K*, indicating active flow toward or from the stream. The piezometers with a VHG of < -0.02 and a *K* >0.10 m/day are hot spots for apparent downwelling hyporheic flow. There are 15 piezometers with that combination of VHG and *K*, and 10 are the shallowest piezometer in the nest. Five of the 15 piezometers were deeper

than the shallow piezometer in the nest but were overlain by piezometers with low K. This shows a lack of connection to the stream despite having high *K* and high VHG.

From the available slug test information, the majority of piezometer nests only had one piezometer with a high *K*. Only two nests had all three piezometers that had high *K* values. These nests were D1 Pool #3 (30cm, 50cm and 75cm) and D1 Pool#2 (30cm, 50cm and 75cm). Nests D1 Pool#2 and Pool#3 were in close proximity to one another. With these nests having high *K* values, there is a connection at all depths where hyporheic exchange can take place.

The other nests that had the shallow and intermediate piezometers hydrologically connected (measureable *K* values) were nest A1 BDJ#2 (30cm and 50cm), D1 Pool #1 (30cm and 50cm), and P1 ADJ#1 (25cm, 50cm). These piezometers show the layer of sand and gravel in the shallowest layer in the subsurface and show connection with the stream. These piezometers with high *K* indicate that the hyporheic zone is shallow within these nests. Hyporheic exchange can happen in the shallower sediments but not deeper due to impermeable sediment.

Piezometer nests that had two or more piezometers with high *K* but are not connected hydrologically were P1 BDJ#1 (25cm and 75cm), P1 BDJ#2 (25cm and 75cm), D1 Pool#1 (30cm and 75cm). These piezometers show that a clay lens or impermeable media is in the intermediate piezometer that blocks direct vertical hyporheic exchange at that location. At these nest locations, there is little or no vertical exchange between the shallow and deep piezometers.

The rest of the piezometer nests either had only one piezometer with a high *K* or none, implying that these nests are have limited hyporheic exchange potential based on their hydraulic conductivity. The majority of piezometer nests in Reedy Creek exhibit limited hyporheic exchange potential.

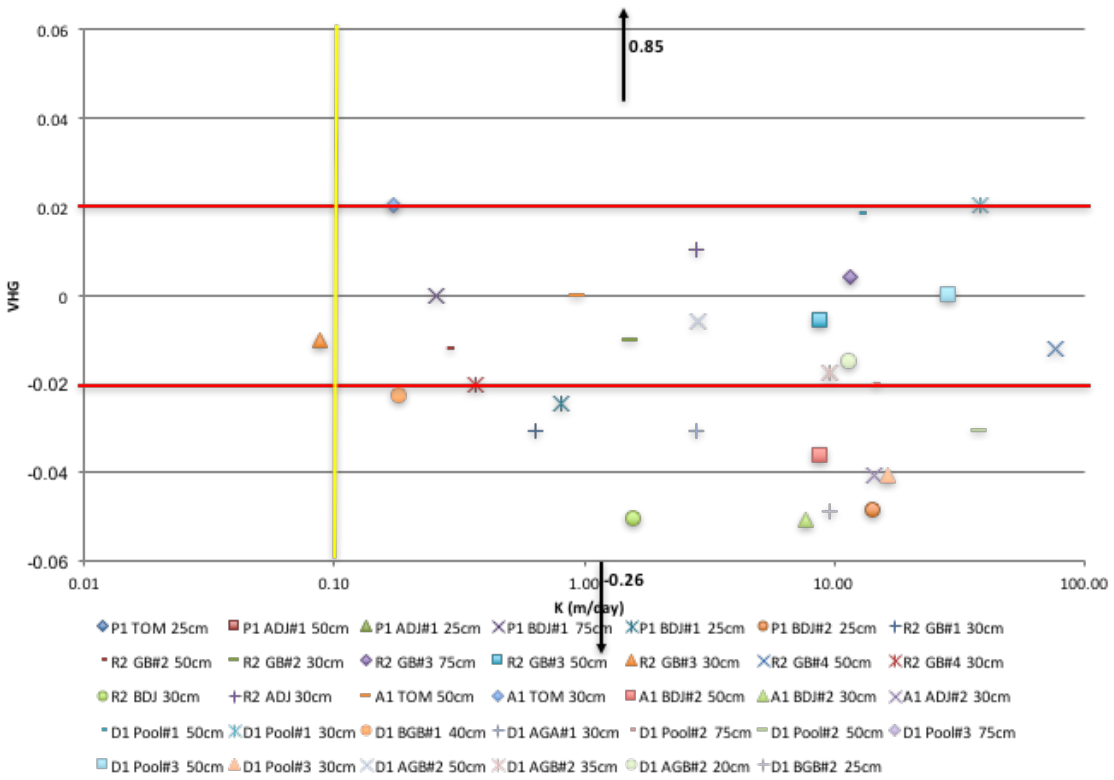

Figure 35. Hydraulic conductivity (*K*) vs VHG for all piezometers with having quantified slug test results. Points between the red lines and to the left of yellow line are inferred to not be hot spots for hyporheic exchange. Between red lines = -0.02> VHG <0.02. Left of yellow line = <0.1m/day. The two black lines signify two different piezometers that were too large or negative to fit on the graph. The top arrow is “P1 ADJ#1 25cm”, the bottom arrow is “P1 ADJ#1 50cm."

5.4 Horizontal hydraulic gradient

Topography has a large influence on groundwater flow so it was expected to see all five reaches flow toward the stream (Daniel and Dahlen 2002). Unexpectedly, the horizontal flow direction is not solely dictated by topography. Reaches R2 and A1 show groundwater flow directions matching topography, flowing from the riparian wells toward the stream (Table 20, Table 21). Reach R2 had an average *dh/dx* of 0.03 for the riparian well to the piezometer. Reach A1 had an average *dh/dx* of 0.06 for the riparian well to the piezometers. Reaches C1, D1 and P1 show different apparent flowpaths in the horizontal direction, having the bulk of piezometers flow from the stream toward the wells (Table 22, Table 23, Table 24). Based upon calculated *dh/dx*, the horizontal hydraulic gradient is negative for most of the piezometers in reaches C1, D1 and P1, indicating horizontal flow from the stream. This was an unexpected result but is consistent with the downward vertical VHGs in these study reaches. Another reason could be that the stream is perched on the subsurface flow system due to the low permeability of the clay rich saprolite.

Reach C1 had an average *dh/dx* of -0.06 for the riparian well to the piezometers. Reach P1 had an average *dh/dx* of -0.01 from the riparian to the piezometers. Reach D1 had an average *dh/dx* of -0.01 from the riparian to the piezometers. The riparian well at reach P1 had a negative horizontal hydraulic gradient for all piezometers implying flow from the stream to the well. Groundwater moves from high hydraulic head to low hydraulic head. This would signify that the water level is lower at the riparian well than the stream. Reaches C1 and D1's groundwater movement however, does not mirror topography. At both reaches, the riparian well exhibits negative horizontal hydraulic gradients toward the piezometers, implying flow from the stream toward the well. Understanding that groundwater is controlled by changes in the hydraulic gradient and that groundwater does not necessarily flow with topography is important for determining the contribution groundwater makes to surface waters in the Piedmont of North Carolina.

Reaches C1, D1 and P1were inconsistent with the expectation that horizontal flow would be toward the stream. Since the horizontal hydraulic gradient was negative for the riparian well to the piezometer this implies a horizontal flow away from the stream. Potential reasons for C1, D1 and P1 not being net gaining is that the hydraulic head measurements were taken the days of being surveyed. If the time of measuring did not have typical season precipitation this would affect groundwater levels and reverse horizontal flow. Other possible implications could be these streams are perched on top of the groundwater system due to low *K* sediments. The P, C and D streams pass over impermeable bedrock features just before reaching the lowland area found at the three reaches. It is possible these study reaches are spots where water flows into the subsurface being prevented by bedrock upstream. The longitudinal diagrams show a mostly horizontal subsurface flow that is parallel to the stream. Due to low *K* sediments, horizontal flow seems to dominate the flow in these study reaches instead of vertical flow (Figure 36, Figure 37, Figure 38, Figure 39, Figure 40).

5.5 Vertical and horizontal specific discharge

Vertical and horizontal specific discharge calculations were made from equations derived from Darcy's Law (equation 5, equation 6) to determine the rate of groundwater flow in both directions. By observing both vertical and horizontal specific components of discharge, the dominant flow could be assessed. For three of the five reaches the horizontal component of flow dominated, $q_x > q_z$. The q_x were from the wells to the piezometers and the q_z were from each piezometer. A1, D1 and R2 have a larger horizontal specific discharge than vertical (Table 20, Table 21, Table 23). C1 and P1 are dominated by the vertical component of flow, $q_z > q_x$ (Table 22, Table 24). Both P1 monitoring wells are in relatively flat land, which yielded a lower hydraulic gradient and a lower horizontal specific discharge. C1 also is at a plateau but there is more room for error in C1. C1 only had two piezometers suitable for slug testing leaving a small amount of data for *K* and q_x. Reaches A1, D1 and R2 have their monitoring wells at the foothills and in the upland which yielded a larger *dh* which results in a larger *dh/dx*. From upland to

piezometer horizontal flow. Specific discharge also indicated that at all reaches the q_x is higher from the riparian well than the upland well toward the stream. This is a result of the average hydraulic gradient from the riparian well to the piezometers being greater than the average hydraulic gradient from the upland well to the piezometers. Due to the large amount of stream incision, the stream is lowered and creates a greater hydraulic gradient from the riparian well to the stream.

5.6 Longitudinal subsurface diagrams

Longitudinal subsurface diagrams were created to relate the sub-streambed hydraulic heads in relation to stream morphology and to relate the piezometer nests to each other. The longitudinal diagrams show distance down each transect (x-axis) at each study reach in relation to the transect of monitoring wells intersecting the channel. The elevation (y-axis) is in meters above mean sea level. It was hypothesized that there would be strong areas of apparent upwelling and apparent downwelling due to the different geomorphic features in the stream. Among piezometers, there are different hydraulic head measurements among the nests themselves. Along the stream however, there is a broader picture with more underflow than hot spots of vertical flow which may occur due to the streambed's particle size. Most of the reaches have a shallow layer of sand and gravel but have a thick underlying layer of impermeable sediment. The sediment's small particle size (low permeability and low *K*) reduces the *q* of flow in both vertical and horizontal directions. This is true looking at the longitudinal diagrams where the flow is dominated horizontally and not vertically (Figure 36, Figure 37, Figure 38, Figure 39, Figure 40).

The study reach A1's longitudinal diagram shows that the hydraulic head in the deep piezometer is higher than the intermediate and shallow piezometers. When comparing these piezometers there is an upward vertical VHG trend. This is interesting since most flows are showing a downward VHG when comparing the piezometer water to the stream. Study reach A1 has the clearest indication of groundwater discharge to the stream. It has the largest hydraulic gradient from riparian well to stream and has the most consistent flow lines on the longitudinal

diagram This may be showing that upward flow would be happening but it is expected that due to the low permeability of the clay rich saprolite vertical flow may not be active (Figure 37).

Among the reaches the dominant lateral flow was parallel to the stream (underflow). Both upward and downward vertical flow was found within the reaches, however some reach exhibited greater VHGs than other reaches. Reach C1's longitudinal diagram shows only horizontal flow and little to zero vertical flow (Figure 40).

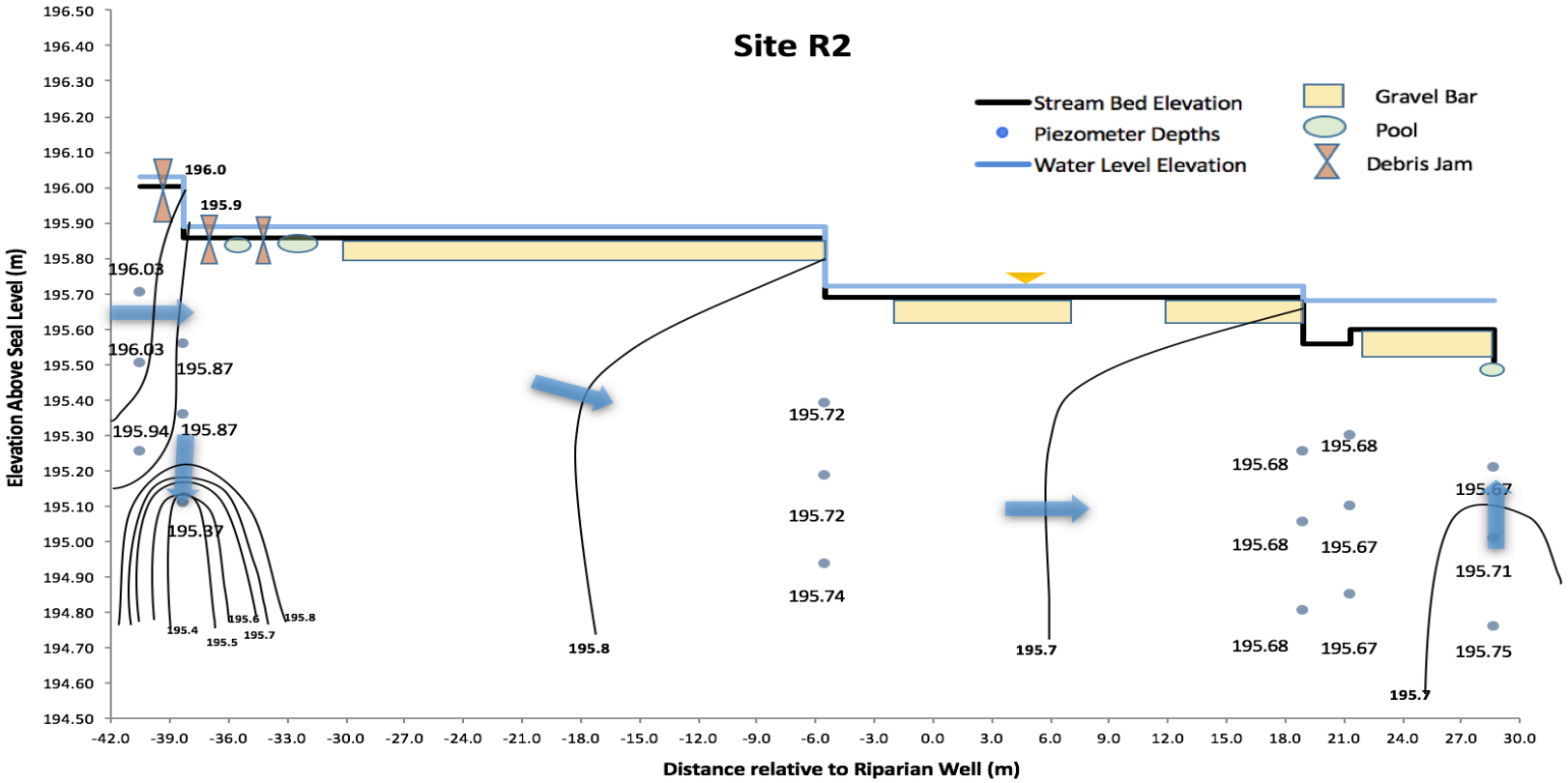

Figure 36. Longitudinal diagram showing reach R2 on 1/20/17. The x-axis shows the along-stream distance in relation to the riparian well transect in meters. The y-axis shows the elevation above mean sea level in meters. This diagram shows both the stream and streambed elevations. Major geomorphic features are shown on the streambed with distance relative to riparian well. Blue arrow represents subsurface flow direction assuming that a hydraulic connection exists between piezometers.

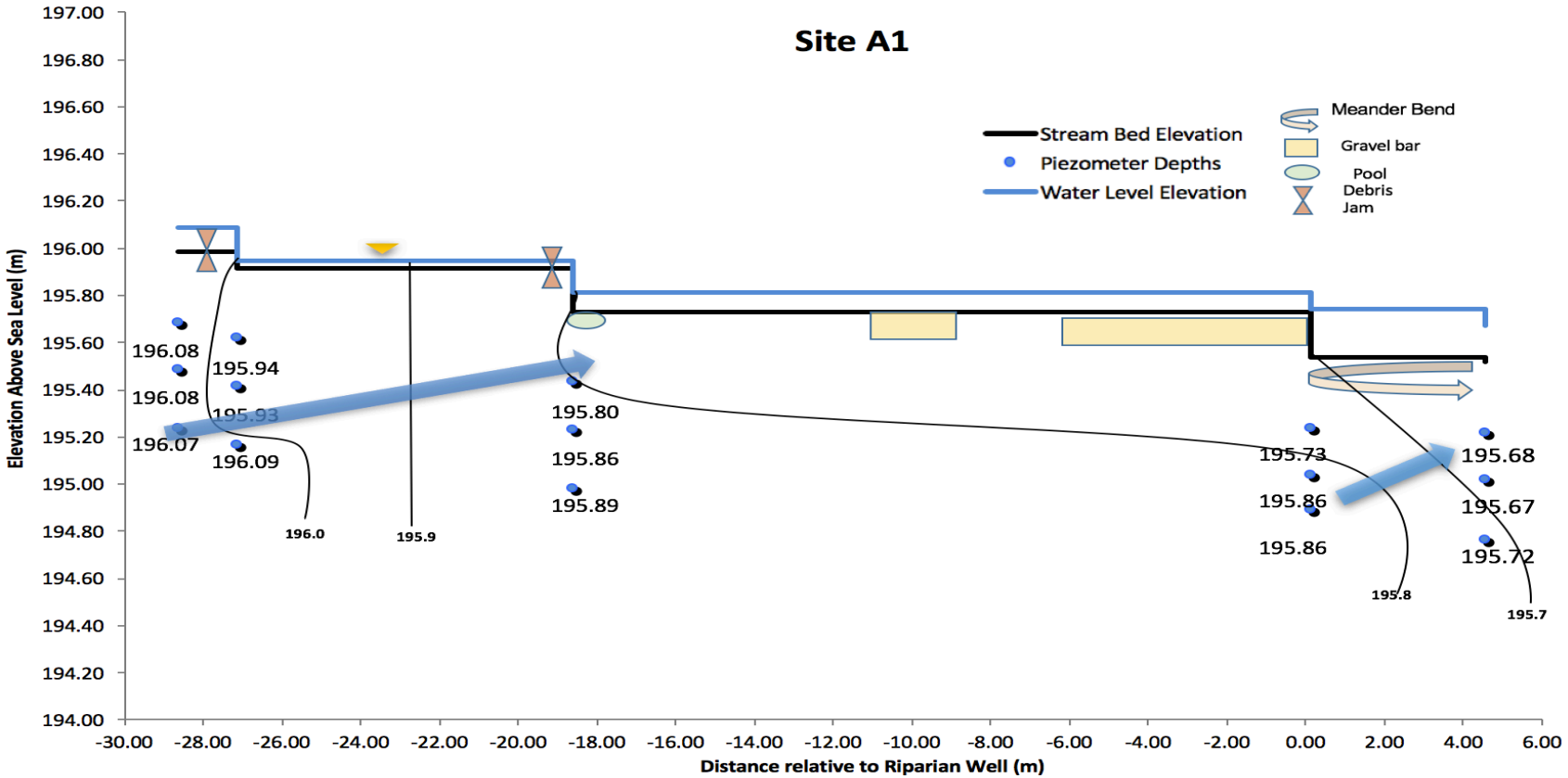

Figure 37. Longitudinal diagram of reach A1 on 1/20/17. The x-axis shows the distance in relation to the riparian well in meters. The y-axis shows the elevation above mean sea level in meters. This diagram shows both the stream and streambed elevations. Major geomorphic features are shown on the streambed with distance relative to riparian well. Blue arrow represents subsurface flow direction assuming that a hydraulic connection exists between piezometers.

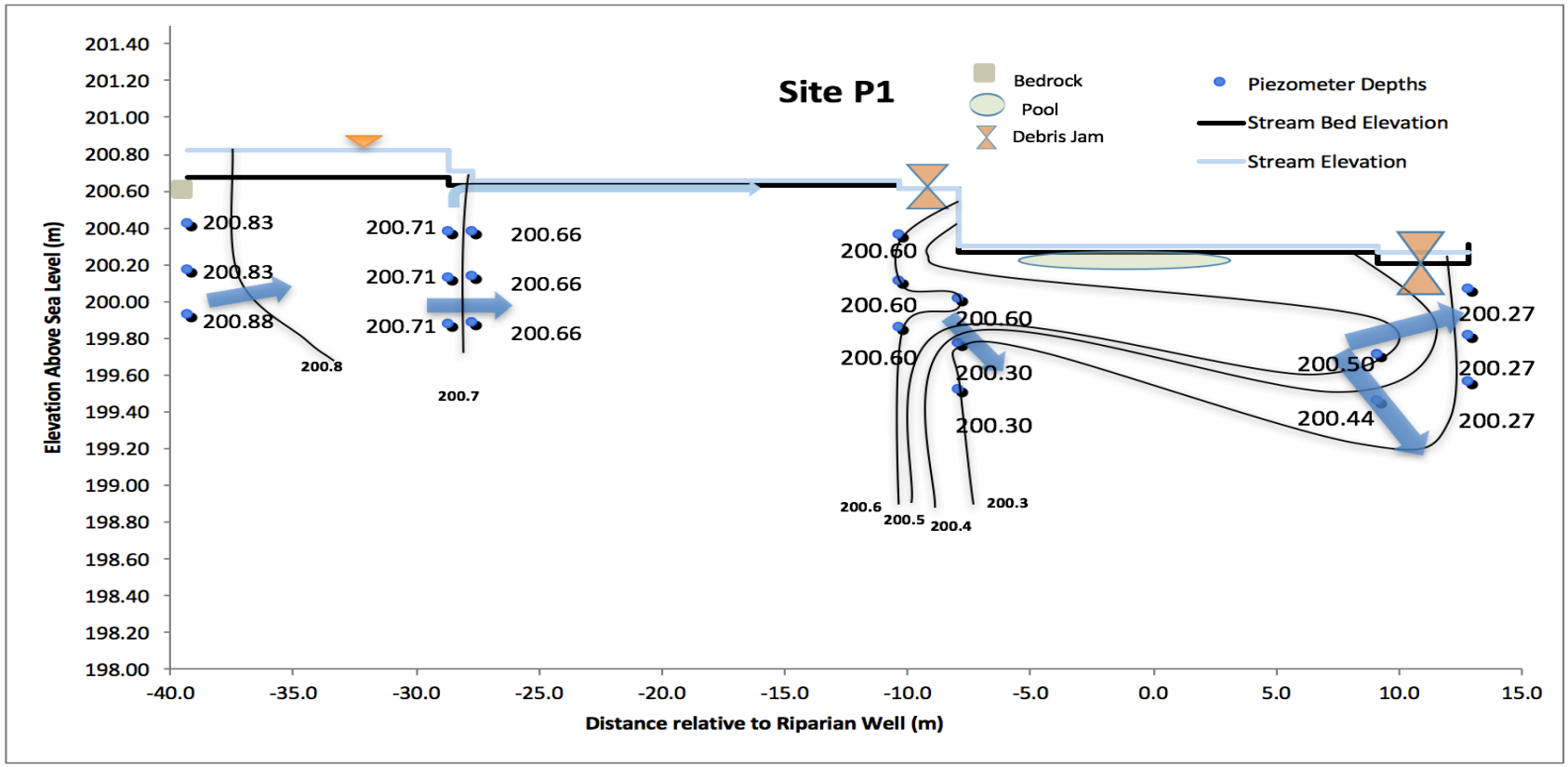

Figure 38. Longitudinal diagram of reach P1 on 2/3/17. The x-axis shows the distance in relation to the riparian well in meters. The y-axis shows the elevation above mean sea level in meters. This diagram shows both the stream and streambed elevations. Major geomorphic features are shown on the streambed with distance relative to riparian well. Blue arrow represents subsurface flow direction assuming that a hydraulic connection exists between piezometers.

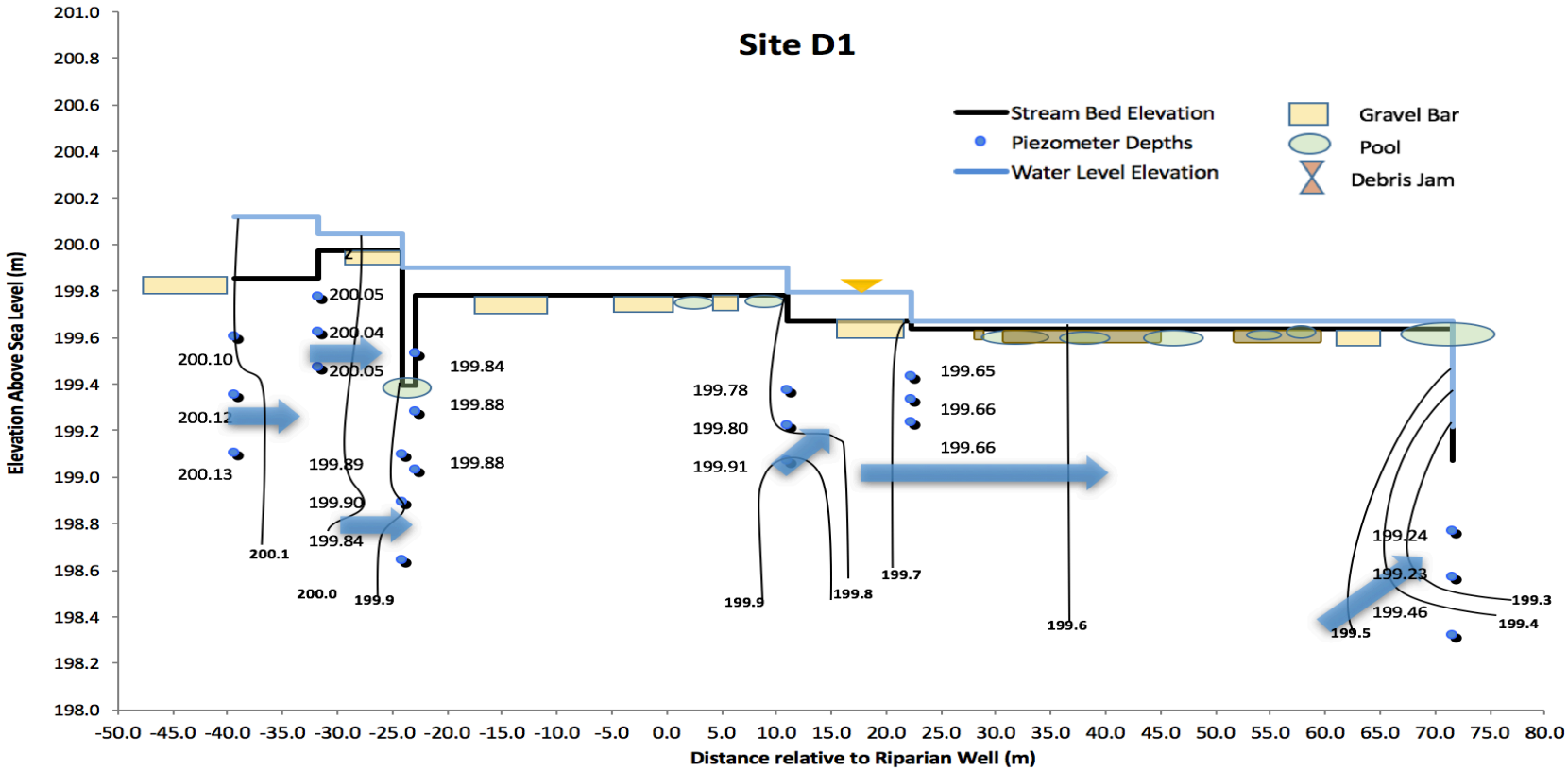

Figure 39. Longitudinal diagram of reach D1 on 2/3/17. The x-axis shows the distance in relation to the riparian well in meters. The y-axis shows the elevation above mean sea level in meters. This diagram shows both the stream and streambed elevations. Major geomorphic features are shown on the streambed with distance relative to riparian well. Blue arrow represents subsurface flow direction assuming that a hydraulic connection exists between piezometers.

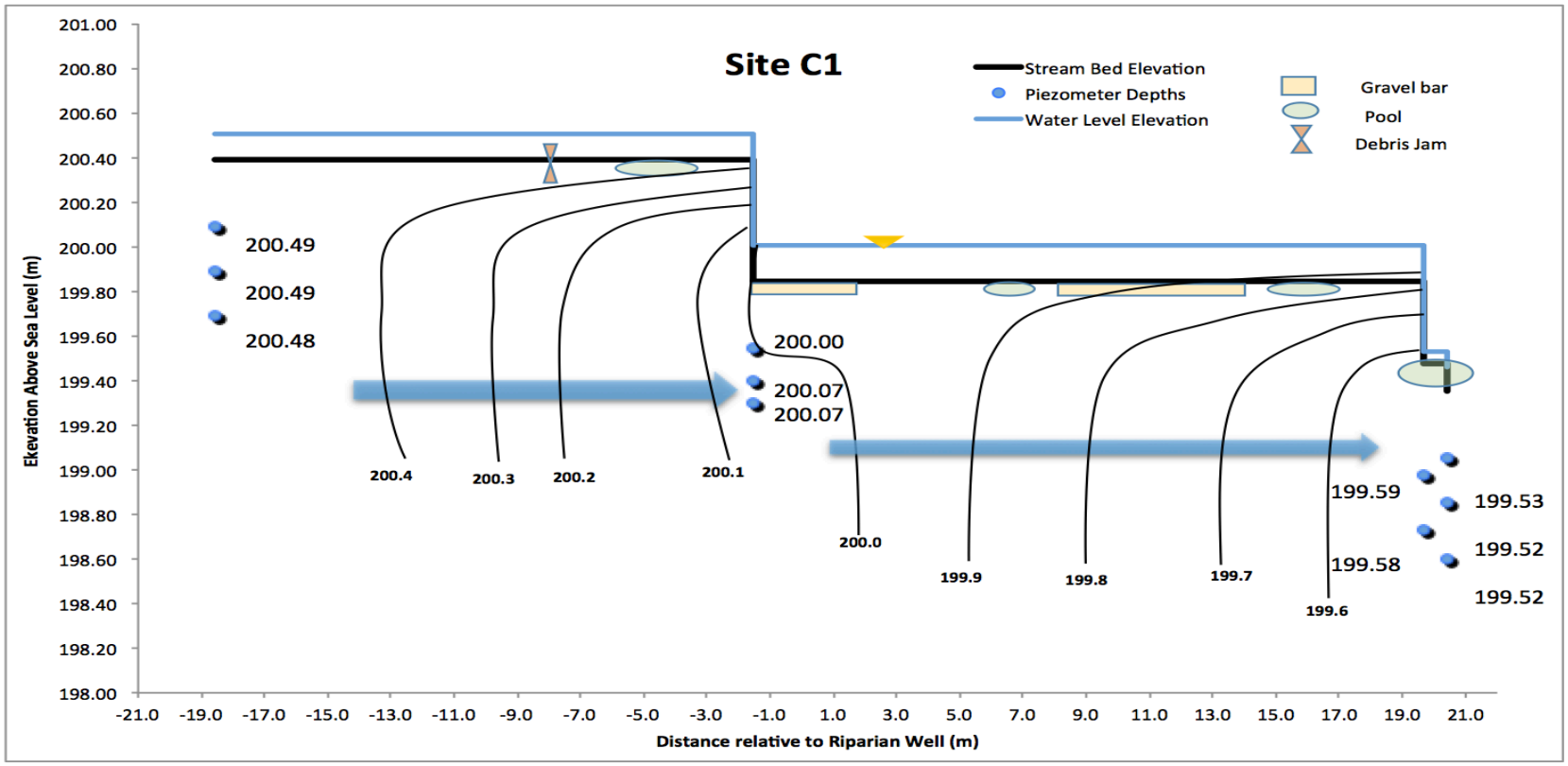

Figure 40. Longitudinal diagram of reach C1 on 1/5/17. The x-axis shows the distance in relation to the riparian well in meters. The y-axis shows the elevation above mean sea level in meters. This diagram shows both the stream and streambed elevations. Major geomorphic features are shown on the streambed with distance relative to riparian well. Blue arrow represents subsurface flow direction assuming that a hydraulic connection exists between piezometers.

5.7 Water chemistry

The objective of the chemical and isotopic analyses was to differentiate the stream samples from the groundwater samples. If there was a strong distinction between the stream and groundwater samples, the piezometer samples could be compared to quantify groundwater surface water mixing.

5.7.1 Intra-reach variability of water chemistry

5.7.1.1 R2

Only a few analyses for reach R2 show a significant difference between groundwater and stream water on 1/20/17. Nitrate concentrations were the same for stream, wells and piezometers (0.002 meq/L). Magnesium concentrations were highest in the well samples (0.51 meq/L) compared to both stream (0.32 meq/L) and piezometer (0.22 meq/L). Alkalinity concentrations are highest in the stream (1.68 meq/L) in comparison to the wells (1.10 meq/L) and piezometers (1.18 meq/L). Both well and stream water were assigned to the water type mixed cation - HCO_3^-. Out of 14 piezometers, 13 piezometers showed the water type mixed cation - HCO_3^- . Study reach R2 shows no chemical distinction among the water types for the well and stream water (Figure 42).

5.7.1.2 A1

Only a few analyses for study reach A1 show a significant difference between groundwater and stream water on 1/20/17. Nitrate concentrations were the highest in the stream (0.014 meq/L). The wells had the lowest average nitrate concentration (0.003 meq/L). The piezometers' nitrate concentrations were between the wells and stream (0.007 meq/L). Fluoride was detected in the piezometer samples but not in the wells or stream sample. Groundwater and surface water's magnesium and calcium concentrations were approximately double the amount in the stream than both the piezometers and well samples.

The upland well and surface water were mixed cation - HCO_3^- water type. The riparian well exhibited a Mixed Cation - SO_4^{2-} water type. Three of the seven piezometers had the water

type Mixed Cation - HCO_3^-. Zero piezometers had the water type mixed cation - SO_4^{2-}. Since both the upland well and surface water have the same water type it is not clear if the piezometer had groundwater or surface water (Figure 41).

5.7.1.3 D1

Only a few analyses for study reach D1 show a significant difference between groundwater and stream water on 2/3/17. The major differences in chemical analyses were in nitrate, magnesium, calcium and alkalinity. Nitrate concentrations were highest in the stream (0.006 meq/L). The piezometers had the second highest nitrate concentrations (0.005 meq/L) followed by the wells (0.001 meq/L). The stream had the highest magnesium concentration of 0.45 meq/L. The wells were 0.24 meq/L and piezometers were 0.17 meq/L. The highest calcium concentration was the stream (0.74 meq/L) followed by the wells (0.46 meq/L) and then piezometers (0.33 meq/L). The piezometers had the highest alkalinity concentration (1.05 meq/L) followed by the stream (0.96 meq/L) and then the wells (0.50 meq/L). The riparian well and surface water samples at D1 had the water type mixed cation + HCO_3^-. The upland well had the Ca^{2+} - HCO_3^- water type. Five piezometers out of eighteen had the water type Mixed Cation - HCO_3^-. One piezometer had the water type Ca^{2+} - HCO_3^-. Both the riparian well and surface water share the same water type making the piezometers with the same indistinguishable (Figure 43).

5.7.1.4 P1

Only a few analyses for study reach P1 show a significant difference between groundwater and stream water on 2/3/17. For reach P1 the major differences in chemical analyses were in sulfate and alkalinity. The highest concentration of sulfate was the well samples (0.20 meq/L) followed by the piezometer samples (0.09 meq/L) and then the surface water sample (0.07 meq/L). The highest alkalinity concentration was the piezometer samples (0.99 meq/L) followed by the stream (0.81 meq/L) and then the wells (0.61 meq/L). Both well samples have a water type of the Ca^{2+} - HCO_3^- at reach P1. The stream sample had a water type of mixed cation - HCO_3^-. Thirteen piezometers had the water type Ca^{2+} - HCO_3^- and three had the water type Mixed

Cation - HCO_3^-. With the stream and groundwater having distinct water types it can be seen that thirteen piezometers have a high chance of being predominantly groundwater and three being predominantly surface water (Figure 44). Groundwater and surface water mixing could not be distinguished in study reach P1 due to the similarities in both samples.

For all study reaches, the groundwater and surface water were chemically similar. The chemical analyses performed on them could not find a large enough difference between the groundwater and surface water. Groundwater surface water mixing could not be quantified in the study reaches.

5.7.2 Inter-reach variability

Among the reaches sampled, the chemical analyses were similar. Reach R2 shows the largest variation among the five study reaches. Only reach R2 had a large concentration of phosphate found in the wells and piezometers. R2 also had the largest average concentration of potassium in the wells and piezometers. Sodium was a magnitude lower in concentration in reach R2 than the rest of the reaches. Study Reach R2 is a mixture of the upstream watersheds and is the confluence of D, P and C study reaches.

Nitrate concentrations were found in all study reaches. Study reach A1 had the greatest nitrate concentrations for stream, well, and piezometer samples. It was expected that study reach A1 to have the greatest nitrate due to the legacy sediments from historic agricultural use. Study reach D1 had the second highest nitrate concentration for the stream and piezometer samples. Study reach D1 is part of the "development" sub-watershed and is understandable why it had higher nitrate than P1 and C1. The "development" sub-watershed is expected to have high nutrient runoff from urban uses like application of fertilizer.

Alkalinity concentrations exhibited one of the largest variation among the reaches. R2 had the highest alkalinity concentrations among piezometers (1.18 meq/L). A1 had the lowest alkalinity concentration with 0.83 meq/L. Among steam samples R2 had the highest alkalinity concentration (1.68 meq/L) while A1 had the lowest (0.78 meq/L). Groundwater samples showed

R2 having the highest alkalinity concentration (1.10 meq/L) and D1 the lowest with (0.50 meq/L).

The four Piper diagrams showed differences among the study reaches. Chemical data showed that R2 well and stream water were dominated by the mixed cation + HCO_3^- hydrochemical facies. Piezometer water was dominated by mixed cation + HCO_3^- (ten piezometers), then Na^+ - HCO_3^-(four piezometers) and then mixed cation - SO_4^{2+}(one piezometer). Cation exchange is happening within study reach R2. The dominant hydrochemical facies is mixed cation - HCO_3^- and some piezometers have Na^+ - HCO_3^- hydrochemical facies. This shows potential cation exchange from Na^+ dominated to a more mixed cation solution. One piezometer exhibited the hydrochemical facies mixed cation - SO_4^{2+}, which has potential for sulfide oxidation to take place.

Study reach A1's riparian well sample had mixed cation – SO_4^{2-} hydrochemical facies and the upland and surface water sample had mixed cation – HCO_3^-. This can be seen as a water-rock interaction with oxidation of iron sulfides. A1 had the fewest water samples with four piezometers showing Na^+ - HCO_3^- and three piezometers with mixed cation – HCO_3^-. Reach A1 shows potential for cation exchange with a high amount of Na^+ - HCO_3^- water type.

Study reach D1's riparian well sample and surface water sample showed mixed cation - HCO_3^- while the upland well sample showed Ca^{2+}-HCO_3^-. Unlike the groundwater or surface water samples the dominant hydrochemical facies among the piezometers was Na^+ - HCO_3^-, (11 piezometers). With Na^+ - HCO_3^- being the dominant water type, D1 had high potential for cation exchange. Five piezometer mixed cation – HCO_3^- and one showed Mg^{2+} - HCO_3^-.

Study reach P1 showed the dominant hydrochemical facies as Ca^{2+} - HCO_3^-. Both well samples and 13 piezometer samples were Ca^{2+} - HCO_3^-. Four piezometer samples and the surface water sample showed mixed cation – HCO_3^- and one showed Na – HCO_3^-. With Ca^{2+} - HCO_3^- being the dominant water type, reach P1 shows large potential for calcium dissolution in subsurface.

In summary, across all sampled reaches, the water type mixed cation - HCO_3^- is dominant for surface water and groundwater. The mixed cation - HCO_3^- water type is also the dominant water type with 24 total piezometers. The water type with the second most piezometers is Na^+ - HCO_3^- with 20 total piezometers. The only reach with had distinguishable water types for groundwater and surface water was reach P1. The stream had the mixed cation + HCO_3^- water type and groundwater had Ca^{2+} - HCO_3^-.

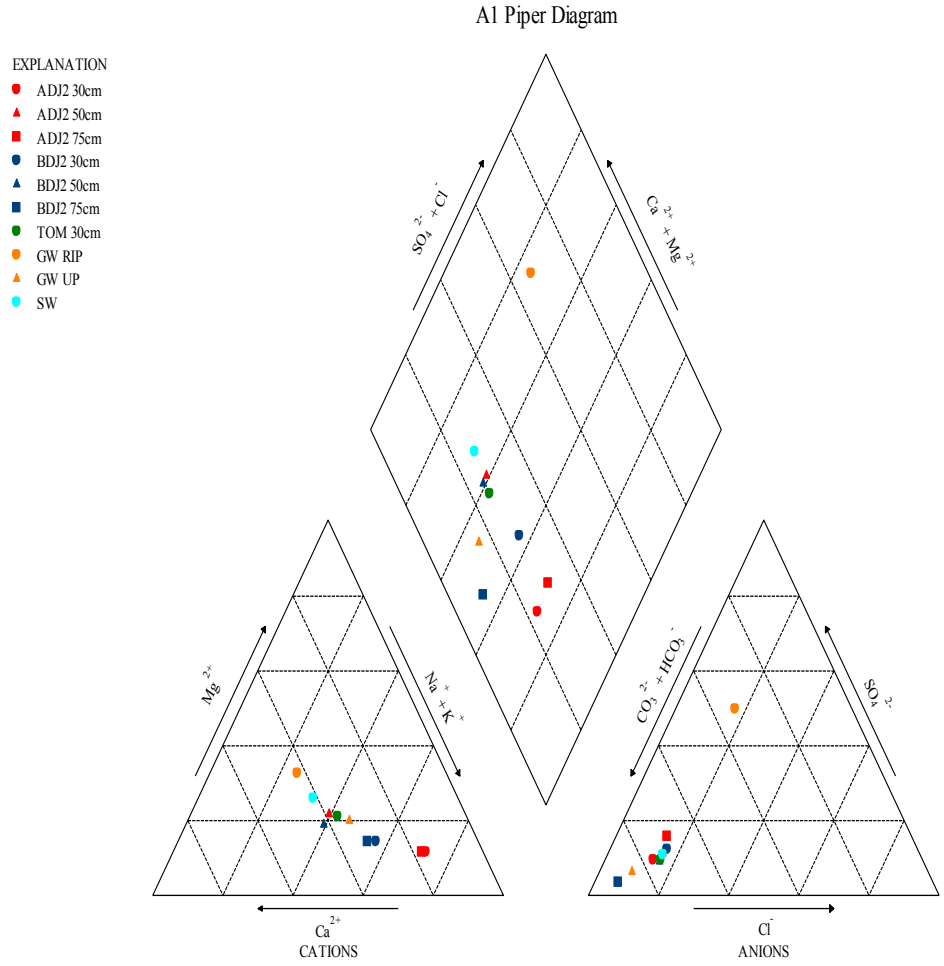

Figure 41. Piper diagram showing the major cations and anions of reach A1 samples.

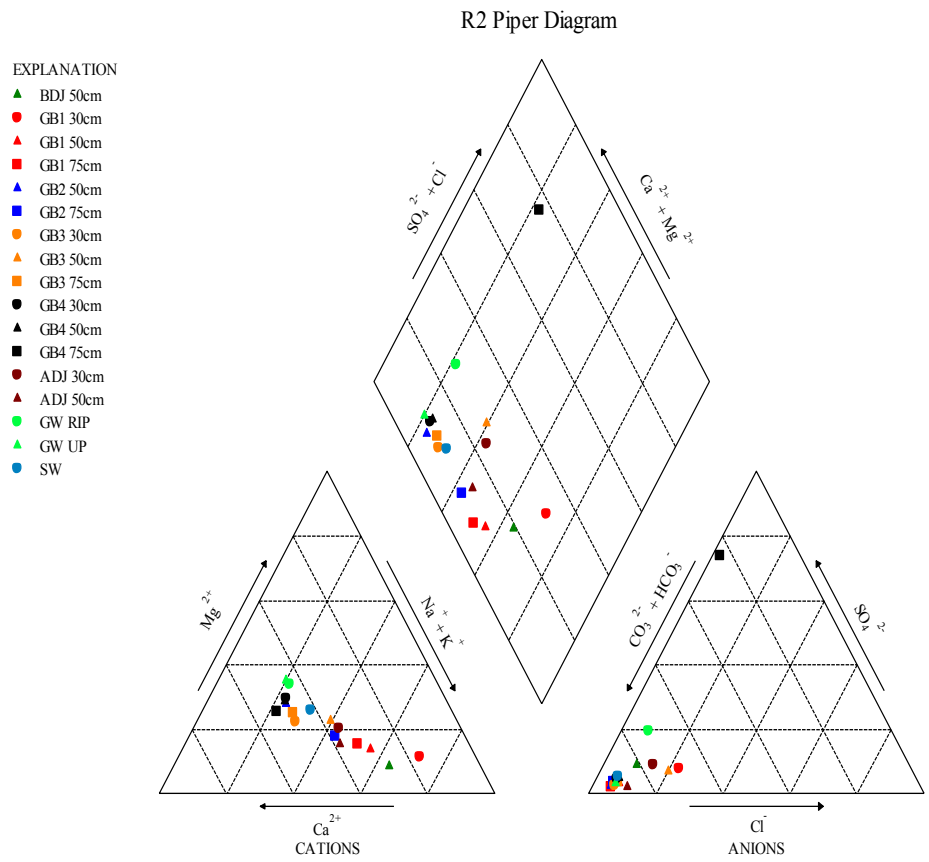

Figure 42. Piper diagram showing the major cations and anions of reach R2 samples.

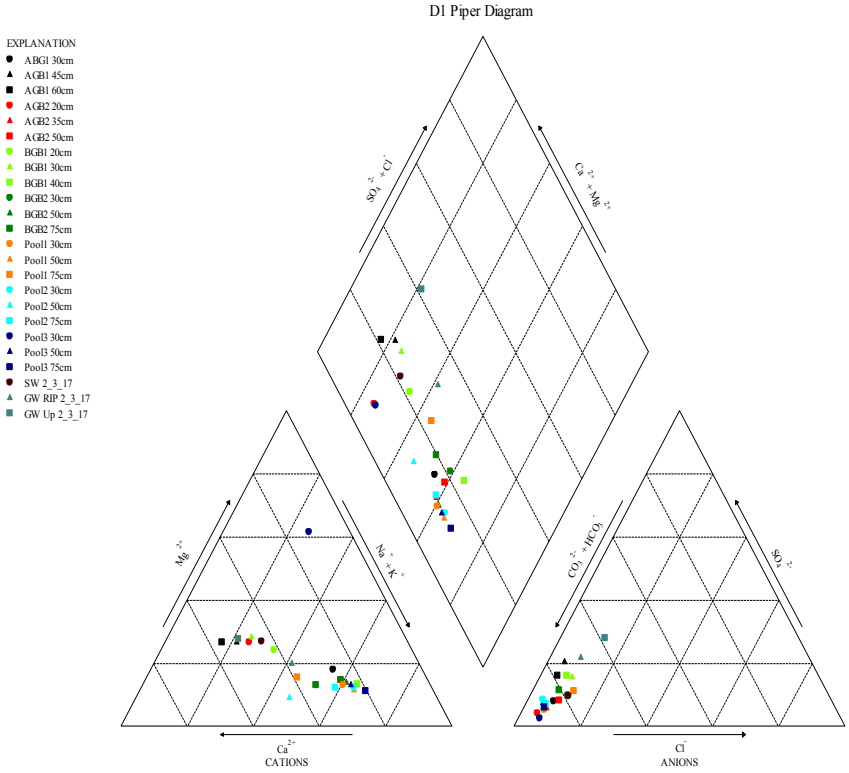

Figure 43. Piper diagram showing the major cations and anions of reach D1 samples.

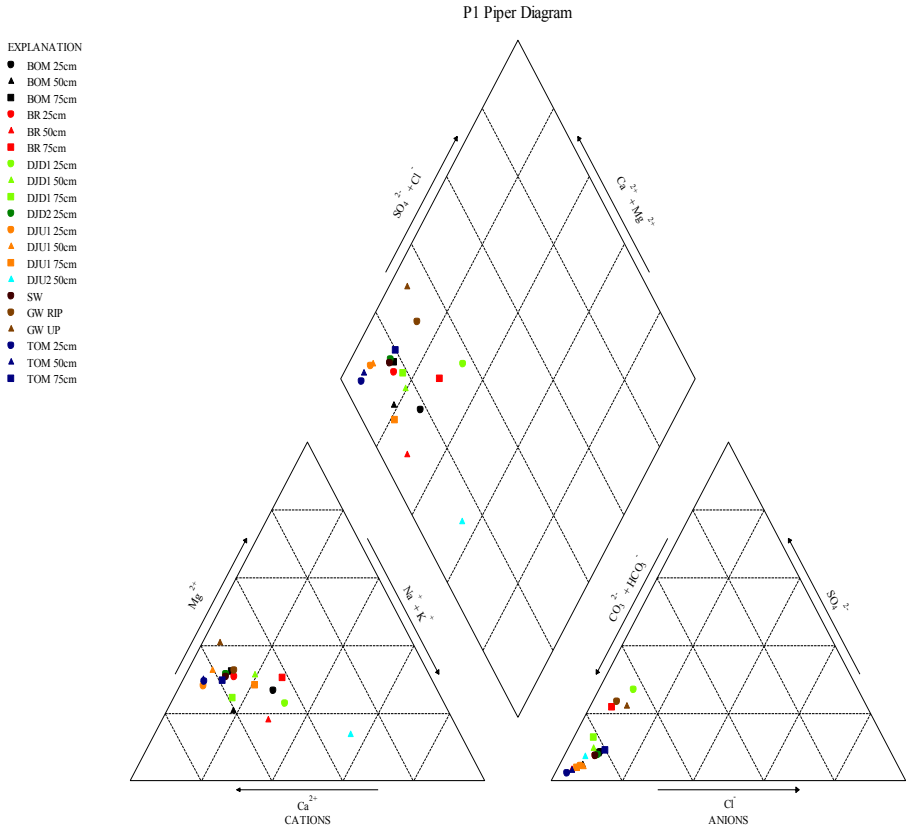

Figure 44. Piper diagram showing the major cations and anions of reach P1 samples.

5.8 Isotopes

5.8.1 Intra-reach variability

At study reach R2 had the majority of piezometer samples fell to the left the global meteoric water line. Both well samples and stream sample also fell to the left of the global meteoric water line. The well and stream water samples are not distinctive enough. With both groundwater and surface water signatures similar, groundwater and surface water mixing within the piezometers could not be determined using a single sampling event of water isotopes (Figure 30).

At study reach A1 the majority of the piezometer samples fell to the left of the global meteoric water line. The stream and well samples fell to the left of the global meteoric water line. The well and stream water samples are not distinctive enough. With both groundwater and surface water signatures similar, groundwater and surface water mixing within the piezometers could not be determined using a single sampling event of water isotopes (Figure 31).

At study reach D1 had the majority of the piezometer samples fell to the left of the global meteoric water line. Both well samples and stream sample fell to the left of the global meteoric water line. The well and stream water samples are not distinctive enough. With both groundwater and surface water signatures similar, groundwater and surface water mixing within the piezometers could not be determined using a single sampling event of water isotopes (Figure 32).

At study reach P1 had the majority of piezometer samples near and to the right of the global meteoric water line. This indicates an evaporation trend within the reach. Groundwater samples fell on the global meteoric water line. The stream sample was to the left of the global meteoric water line. Groundwater and surface water mixing within the piezometers could not be determined using a single sampling event of water isotopes (Figure 33).

5.8.2 Inter-reach variability

Study reaches P1 and D1 were sampled the same day; D1 shows results along the global meteoric water line while P1 shows an evaporation trend. Reaches A1 and R2 were sampled the

same day and both results align with the Global Meteoric Water Line. Among the study reaches, one reach exhibited an evaporation trend (P1). There are multiple possible implications for an evaporation trend in P1. Study reach P1 is within the "Pond Influence" sub-watershed and is a reach that is drained from a pond further upstream. Due to the lack of canopy cover and slow movement of a pond, the water would be under direct sunlight for a considerable amount of time. This longer residence time may affect its seasonal storage contributing to this evaporation trend. Within the reach itself, P1 also had the lowest amount of canopy cover in relation to the other study reaches. Lower canopy would allow more direct sunlight and increase evaporation.

Among all sampled reaches the groundwater and stream water samples were not isotopically distinct enough to determine groundwater and surface water mixing from one sampling date.

6 Conclusions

The objective of this study was to observe and evaluate the amount of hyporheic exchange at different geomorphic features within Reedy Creek in its "Pre-Restoration Phase." Over 85 piezometers were installed at five different reaches. The extent of hyporheic flux varied from piezometer to piezometer. VHGs did not occur at specific geomorphic features as hypothesized. For example, "Bottom of Meander" was hypothesized to be a hot spot for apparent upwelling. "Bottom of Meander" did experience apparent upwelling but had a stronger apparent downwelling VHG.

All the study reaches within the study area exhibited apparent downwelling as the dominant apparent vertical flow direction within the piezometers. This was unexpected due to the hypothesis of all the study reaches having flow toward the stream and having net apparent upwelling. The VHGs and horizontal hydraulic gradient lead to a few possibilities. There simply could be many locations of apparent downwelling within all the study reaches. The surface water is perched over the subsurface water heads due to the low permeability of the bed sediments. The

last possibility, the water is equilibrated with a point further downstream. If the sites do have many locations of apparent downwelling this would be beneficial for denitrification.

The hyporheic potential for Reedy Creek is contingent on the permeability of its sediments. Slug testing data showed that half of the piezometers installed were in impermeable sediment. Of those piezometers that were in impermeable sediment the majority of them were in the deeper sediments. The majority of hyporheic potential is within the shallow sediments within the stream beds. Of all the piezometer nests within Reedy Creek there are only two that have all three piezometers connected. This impermeable sediment restricts hyporheic potential in all five of the study reaches. Other studies within the Piedmont have found vertical trends similar to Reedy Creek. Permeability was greatest in the shallow sediments but decreased with increased depth (Smock et al., 1992; Ryan and Boufadel, 2007). Just like in Reedy Creek it was found that some sediments >30-40cm deep were found to be impermeable and restricted hyporheic flow (Smock et al., 1992).

The five reaches' VHGs did not vary as much as the geomorphic features. The reaches with the largest apparent downwelling was P1 (-0.01 to -0.06). The smallest amount of apparent downwelling was both R2 (-0.01 to -0.02) and D1 (-0.01 to -0.02). Only two of the reaches had reach-wide median apparent upwelling VHGs. Reach C1 had the largest reach-wide median apparent upwelling (0.01 to 0.08) and P1 had the lowest (<0.01). Vertical specific discharge rates from other papers found the vertical flux to be ~0.30m/day (Daniluk et al., 2013; Zimmer and Lautz, 2015; Battin et al., 2003). The vertical specific discharges within Reedy Creek were similar to 30m/day.

Some restoration practices that may increase the study area's hyporheic function are to coarsen the stream bed sediments and to add geomorphic features. The study area has very low permeability in >30cm sediments. Adding coarser sediments increases permeability and promotes hyporheic flux. Geomorphic features placed in the stream can create beneficial head gradients and induce hyporheic flux.

AWKNOWLEDGMENTS

Thanks to the Charlotte-Mecklenburg Stormwater Services for research funding. Thanks to Cody Starnes, Ella Wickliff and Nick Allison for survey assistance and data analysis. Thanks to Taylor Kiker, Geoffrey Fey, Rebecca Black and Noah Richardson for field assistance. Thanks to Jon Watkins for lab and chemical analysis assistance. Thanks to my committee, Dr. Sandra Clinton, Dr. Martha Cary Eppes and Dr. David Vinson for guidance and oversight.

References Cited

Alvarez, L., Bricio, C., Blesa, A., Hidalgo, A., and Berenguer, J. (2013). Transferable denitrification capability of thermus thermophilus. *Applied and Environmental Microbiology, 80*(1), 19-28.

Baker, M. A., C. N. Dahm, H. M. Valett, J. A. Morrice, K. S. Henry, M. E. Campana, and G. J. Wroblicky. (1994). Spatial and temporal variation in methane distribution at the ground water-surface water interface in headwater catchments. *In Proceedings of the Second International Conference on Ground Water Ecology*. (J.A.Stanford and J. M. Valett, eds.), pp. 29-37. American Water Resources Association, Herndon, MD.

Battin, T. J., Kaplan, L. A., Newbold, J. D., & Hendricks, S. P. (2003). A mixing model analysis of stream solute dynamics and the contribution of a hyporheic zone to ecosystem function. *Freshwater Biology, 48*(6), 995-1014.

Bell, C. D., McMillan, S. K., Clinton, S. M., & Jefferson, A. J. (2016). Hydrologic response to stormwater control measures in urban watersheds. *Journal of Hydrology, 541*, 1488-1500.

Bencala, K.E. (1993). A perspective on stream-catchment connections. *Journal of the North American Benthological Society 12*, 44–47.

Bencala, K. E., Gooseff, M. N., and Kimball, B. A. (2011). Rethinking hyporheic flow and transient storage to advance understanding of stream-catchment connections. *Water Resources Research*, 46. doi:10.1029/2019WR010066

Bernhardt, E. S., and Palmer, M. A. (2007). Restoring streams in an urbanizing world. *Freshwater Biology, 52*(4), 738-751.

Boulton, A. J., Findlay, S., Marmonier, P., Stanley, E. H., and Valett, H. M. (1998). The functional significance of the hyporheic zone in streams and rivers. *Annual Review of Ecology and Systematics, 29*(1), 59-81.

Boulton, A. J. (2000). River ecosystem health down under: Assessing ecological condition in riverine groundwater zones in Australia. *Ecosystem Health, 6*(2), 108-118.

Boulton, A. J. (2007). Hyporheic rehabilitation in rivers: Restoring vertical connectivity. *Freshwater Biology, 52*(4), 632-650.

Charlton, R. (2008). *Fundamentals of Fluvial Geomorphology*. London: Routledge.

Cordy, G.E., (2001). A primer on water quality. U.S. Geological Survey Fact Sheet FS-027-01.

Daniel, C. C., and Dahlen, R. P. (2002). Preliminary hydrogeologic assessment and study plan for a regional ground-water resource investigation of the Blue Ridge and Piedmont provinces of North Carolina. USGS *Water-Resources Investigation,* Report 02 – 4105.

Daniluk, T. L., Lautz, L. K., Gordon, R. P., and Endreny, T. A. (2012). Surface water-groundwater interaction at restored streams and associated reference reaches. *Hydrological Processes, 27*(25), 3730-3746.

Dent, C. L., Schade, J. D., Grimm, N. B., and Fisher, S. G. (2000). Subsurface influences on surface biology. *Streams and Ground Waters,* 381-402.

Ensign, S. H., and Doyle, M. W. (2006). Nutrient spiraling in streams and river networks. *Journal of Geophysical Research. Biogeosciences, 111*(G4).

Feral, D., Camann, M.A., and Welsh, H.H., Jr. (2005). Dicamptodon tenebrosus larvae within hyporheic zones of intermittent streams in California. *Herpetol*. *Rev*. 36, 26.

Gagrani, V., Diemer, J. A., Karl, J. J., & Allan, C. J. (2013). Assessing the hydrologic and water quality benefits of a network of stormwater control measures in a SE U.S. Piedmont watershed. *JAWRA Journal of the American Water Resources Association, 50*(1), 128-142.

Groffman, P. M., Bain, D. J., Band, L. E., Belt, K. T., Brush, G. S., Grove, J. M., Pouyant, R. V, Yesilonis, I. C., Zipperer, W. C. (2003). Down by the riverside: Urban riparian ecology. *Frontiers in Ecology and the Environment, 1*(6), 315.

Hancock, P. J. (2002). Human impacts on the stream-groundwater exchange zone. *Environmental Management, 29*(6), 763-781.

Hester, E. T., and Doyle, M. W. (2008). In-stream geomorphic structures as drivers of hyporheic exchange. *Water Resources Research, 44*(3). doi:10.1029/2006wr005810

Hester, E. T., and Gooseff, M. N. (2010). Moving beyond the banks: Hyporheic restoration is fundamental to restoring ecological services and functions of streams. *Environmental Science and Technology*, *44*(5), 1521-1525.

Hester, E. T., & Gooseff, M. N. (2013). Hyporheic restoration in streams and rivers. *Stream Restoration in Dynamic Fluvial Systems Geophysical Monograph Series, 194,* 167-187.

Hough, P., and Robertson, M. (2008). Mitigation under section 404 of the Clean Water Act: Where it comes from, what it means. *Wetlands Ecology and Management, 17*(1), 15-33.

Hiscock, K. M., and Bense, V. F. (2014). *Hydrogeology: Principles and Practice* (2nd ed.) Oxford: Wiley-Blackwell.

Jackson, T. R., Haggerty, R., Apte, S. V., Coleman, A., and Drost, K. J. (2012). Defining and measuring the mean residence time of lateral surface transient storage zones in small streams. *Water Resources Research, 48*(10). doi:10.1029/2012wr012096

Lawrence, J. E., Skold, M. E., Hussain, F. A., Silverman, D. R., Resh, V. H., Sedlak, D. L., Richard, G.L, Mccray, J. E. (2013). Hyporheic zone in urban streams: A review and opportunities for enhancing water quality and improving aquatic habitat by active management. *Environmental Engineering Science, 30*(8), 480-501.

Marshall, M. C., and Hall, R. O. (2004). Hyporheic invertebrates affect N cycling and respiration in stream sediment microcosms. *Journal of the North American Benthological Society, 23*(3), 416-428.

Meyer, E. I., Niepagenkemper, O., Molls, F., and Spänhoff, B. (2008). An experimental assessment of the effectiveness of gravel cleaning operations in improving hyporheic

water quality in potential salmonid spawning areas. *River Research and Applications, 24*(2), 119-131.

McMillan, S., and Clinton S. (2013). Reedy Creek Restoration Study, proposal submitted to Charlotte Mecklenburg Stormwater Services.

Niezgoda, S. L., and Johnson, P. A. (2005). "Improving the urban stream restoration effort: Identifying critical form and processes relationships." *Environmental Management, 35*(5), 579-592.

O'Driscoll, M., Clinton, S., Jefferson, A., Manda, A., McMillan, S. (2010). Urbanization effects on watershed hydrology and in-stream processes in the southern United States. *Water 2*, 605–648.

Ryan, R. J., & Boufadel, M. C. (2007). Lateral and longitudinal variation of hyporheic exchange in a piedmont stream pool. *Environmental Science & Technology, 41*(12), 4221-4226.

Smock, L. A., Gladden, J. E., Riekenberg, J. L., Smith, L. C., & Black, C. R. (1992). Lotic macroinvertebrate production in three dimensions: Channel surface, hyporheic, and floodplain environments. *Ecology, 73*(3), 876-886.

Triska, F. J., Kennedy, V. C., Avanzino, R. J., Zellweger, G. W., and Bencala, K. E. (1989). Retention and transport of nutrients in a third-order stream in northwestern California: Hyporheic processes. *Ecology, 70*(6), 1893-1905.

Valett, H. M., Dahm, C. N., Campana, M. E., Morrice, J. A., Baker, M. A., and Fellows, C. S. (1997). Hydrologic influences on groundwater-surface water ecotones: Heterogeneity in nutrient composition and retention. *Journal of the North American Benthological Society, 16*(1), 239-247.

Vaux, W. G. (1968), Intragravel flow and interchange of water in a streambed, *U. S. Fish Wildlife Service Fishery Bulletin*, *66*(3), 479–489.

Walsh, C., Roy, A., Feminella, J., Cottingham, P., Groffman, P., and Morgan, R. (2005). The urban stream syndrome: Current knowledge and the search for a cure. *Journal of the North American Benthological Society*, 24(3), 706-723.

Ward, J. V., Bretschko, G., Brunke, M., Danielopol, D., Gibert, J., Gonser, T., and Hildrew, A. G. (1998). The boundaries of river systems: The metazoan perspective. *Freshwater Biology, 40*(3), 531-569.

Ward, A. S. (2015). The evolution and state of interdisciplinary hyporheic research. *Wiley Interdisciplinary Reviews: Water, 3*(1), 83-103.

White, A. F., Bullen, T. D., Schulz, M. S., Blum, A. E., Huntington, T. G., & Peters, N. E. (2001). Differential rates of feldspar weathering in granitic regoliths. *Geochimica et Cosmochimica Acta, 65*(6), 847-869.

Winter, T. C. (1999). Ground Water and Surface Water a Single Resource. *U.S. Geological Survey Circular, 1139*.

Wood, P. J., Boulton, A. J., Little, S., and Stubbington, R. (2010). Is the hyporheic zone a refugium for aquatic macroinvertebrates during severe low flow conditions? *Fundamental and Applied Limnology, 176*(4), 377-390.

Zimmer, M. A., & Lautz, L. K. (2015). Pre- and postrestoration assessment of stream water–groundwater interactions: Effects on hydrological and chemical heterogeneity in the hyporheic zone. *Freshwater Science, 34*(1), 287-300.